482021

ANALYSIS OF LIQUID ROCKET ENGINE COMBUSTION INSTABILITY

TECHNICAL REPORT NO. AFRPL-TR-65-254

January 1966

AIR FORCE ROCKET PROPULSION LABORATORY
RESEARCH AND TECHNOLOGY DIVISION
AIR FORCE SYSTEMS COMMAND
UNITED STATES AIR FORCE
EDWARDS, CALIFORNIA

Project No. 3058, Task No. 305802

Prepared under Contract No. AF 04(611) -10542

Propulsion Department
DYNAMIC SCIENCE CORPORATION
Monrovia, California

DISCLAIMER NOTICE

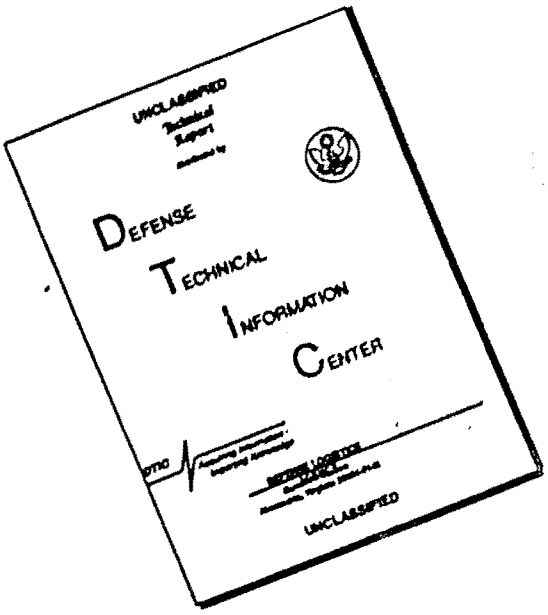

THIS DOCUMENT IS BEST QUALITY AVAILABLE. THE COPY FURNISHED TO DTIC CONTAINED A SIGNIFICANT NUMBER OF PAGES WHICH DO NOT REPRODUCE LEGIBLY.

ANALYSIS OF

LIQUID ROCKET ENGINE COMBUSTION INSTABILITY

Technical Report No. AFRPL-TR-65-254

Contract No. AF 04(611)-10542

For the

AIR FORCE ROCKET PROPULSION LABORATORY
RESEARCH AND TECHNOLOGY DIVISION
AIR FORCE SYSTEMS COMMAND
UNITED STATES AIR FORCE
EDWARDS, CALIFORNIA

Prepared by:
M. R. Beltran
B. P. Breen
R. J. Hoffman
T. C. Kosvic
C. F. Sanders
R. O. Wright

DYNAMIC SCIENCE CORPORATION
Monrovia, California

FOREWORD

This special report describes a nonlinear model which can be used to predict combustion instability zones in liquid rocket engines. The report was prepared by M. R. Beltran, B. P. Breen, R. J. Hoffman, T. C. Kosvic, C. F. Sanders, and R. O. Wright of the Propulsion Department of Dynamic Science Corporation, 1900 Walker Avenue, Monrovia, California. The work was funded on Air Force Contract No. AF 04(611)-10542 under Task No. 305802 of Project No. 3058, during the period January 1, 1965 through December 30, 1965. This contract was administered under the direction of R. R. Weiss and Lt. J. J. Stewart of the Rocket Propulsion Laboratory, Edwards Air Force Base, California.

Approved:

M R Beltran

M. R. Beltran, Director of Propulsion

Melvin Gerstein

Melvin Gerstein, Ph.D.
President

ABSTRACT

This report develops a nonlinear model which can be used to predict combustion instability zones in liquid rocket engines. The nonlinear model is developed by combining a nonlinear instability model with a steady-state vaporization model. Such an analysis determines the zones of an engine in which a tangential mode of high frequency instability is most easily initiated. A rocket engine can be analyzed by incrementally dividing the combustion chamber into annular nodes in the r and z directions. Steady-state properties at each annular node or position in the chamber are computed from the steady-state vaporization computer program. The steady-state program is capable of computing combustion profiles in thermally unstable propellants of the monomethylhydrazine/nitrogen tetroxide type. This model describes droplet vaporization with vapor phase decomposition. Using the computed steady-state properties and the stability limit curves from the instability computer program, stability at each node is determined. This process is repeated for each node to determine a stability map of the entire engine. Thus stability can be related to hardware design parameters, thereby enabling the influences of system design and stability rating devices to be determined.

This report has been divided into four main parts. Part one deals with the application of the steady-state and instability program to determine stability zones in a rocket engine. Part two covers the details of the steady-state model for monopropellant type fuels such as monomethylhydrazine. Part three deals with the nonlinear instability model used to generate the stability limit curves and finally, part four contains the details of the steady-state and instability programs and computer listings.

NOTICES

This report may be reproduced to satisfy the needs of U.S. Government Agencies. No other reproduction is authorized except with permission of United States Air Force, Rocket Propulsion Laboratory, Edwards Air Force Base, California. The distribution of this report is limited because general foreign dissemination is not desired.

Qualified users may obtain copies of this report from the Defense Documentation Center.

TABLE OF CONTENTS
SYMBOLS

		Page No.
I.	INTRODUCTION	1
II.	APPLICATION OF STEADY-STATE AND COMBUSTION INSTABILITY MODEL	4
	1. Introduction	4
	2. Nodal Method	7
	3. Conclusion	16
III.	STEADY-STATE DROPLET COMBUSTION IN THE MONOMETHYLHYDRAZINE-NITROGEN TETROXIDE SYSTEM	18
	1. Steady-State Vaporization with Vapor Phase Decomposition	18
	2. The Model	19
	3. The Stability Drop Size	39
IV.	COMBUSTION INSTABILITY MODEL	42
	1. Introduction	42
	2. Theory	43
APPENDIX I - STEADY-STATE PROGRAM		56
	1. Introduction	57
	2. Input Data	57
	3. Program Nomenclature	59
	4. Program Listing	67
APPENDIX II - COMBUSTION INSTABILITY PROGRAM DESCRIPTION		113
FIGURES		
	1. Transtage Rocket Engine Model	5
	2. Profile of Steady-State Droplet Relative Mach Number	9
	3. Profile of Drop Reynolds Number Re_d	10
	4. Profile of Steady-State Vaporization Rate	11
	5. Burning Rate Parameter Distribution in Combustion Chamber	13
	6. Stability Limit Curve	14
	7. Pulse Pressure Contour Lines Defining Unstable Zones	15
	8. Stability Map	17
	9. Nitrogen-Tetroxide Droplet Vaporization Model	24

TABLE OF CONTENTS (Continued) Page No.

10. Photograph of Experimental Burning Drop Showing Two Flame Fronts 26
11. Photograph of Experimental Burning Drop Showing Two Flame Fronts 27
12. Two-Regime Model of Decomposition-Front Position, Adiabatic Oxidation Temperature the same in both cases. 29
13. Film Thickness for Decomposition Flame 32
14. Evaporation Rate Constant for Decomposition 33
15. Combustion Rate, Initial Drop Size 49.4μ 34
16. Fuel Fraction Vaporized, Mass Median Drop Size 75μ 36
17. Experimental Performance of Hydrazine Propellant Combinations 37
18. Comparison of Experimental and Calculated Efficiencies Showing Hydrazine Efficiencies Computed by the Two-Flame Model 38
19. Schematic Diagram of Heat Transfer to Vapor Film and Liquid Drop 52
20. Input Listing 60
21. Input Listing 61
22. Flow Chart for Dynamic Science Corporation Steady-State Program 62
23. Printed Output 98
24. Printed Output 99
25. Printed Output 100
26. O/F Ratio of Combustion Gases 101
27. Fraction Vaporized 102
28. Gas Mach Number 103
29. Vaporization Rate 104
30. Fuel Relative Mach Number 105
31. Oxidizer Relative Mach Number 106
32. Fuel Drop Radii 107
33. Oxidizer Drop Radii 108
34. Fuel Drop Velocity 109
35. Oxidizer Drop Velocity 110
36. Chamber Temperature 111
37. Chamber Pressure 112
38. Flow Chart for the DSC Instability Program 118
39. Input Listing 119
40. ΔP Plot 120

TABLE OF CONTENTS (Continued)

		Page No.
41.	Maximum Pressure Node	121
42.	Pressure Wave Perturbation	122
43.	Pressure Wave Perturbation	123
44.	Pressure Wave Perturbation	124
45.	Pressure Wave Perturbation	125
46.	Pressure Wave Perturbation	126
47.	Pressure Wave Perturbation	127
48.	Pressure Wave Perturbation	128
49.	Pressure Wave Perturbation	129
REFERENCES		149
DISTRIBUTION		151
DOCUMENT CONTROL DATA		160

NOMENCLATURE

A	combustor contraction ratio, A_c/A_t
A_c	cross-sectional area of combustor
A_k	kinetic constant, equation III-31
A_p	amplitude of pressure disturbance
A_t	nozzle-throat area of combustor
A_v	amplitude of velocity disturbance
a	speed of sound in gases
B	reaction velocity constant, equation III-31 and laminar film thickness
C_d	drag coefficient
C_{dr}	concentration of liquid drops
C_p	specific heat at constant pressure
C_v	specific heat at constant volume
C^*	characteristic exhaust velocity
c	droplet concentration III-3
$\mathcal{F}$	local fuel fraction vaporized
$f(\gamma)$	function of gamma $\sqrt{\frac{2}{\gamma+1}^{\frac{\gamma+1}{\gamma-1}}}$
g	acceleration due to gravity
I	momentum flux
J_H	mechanical equivalent
J	viscous-dissipation parameter
k	thermal conductivity
L	burning-rate parameter
M	molecular weight
m	burning rate of propellant, fraction/inch and mass of drop
Nu_h	Nusselt number, heat transfer

Nu_m	Nusselt number, mass transfer
n	number of drops/second in each drop size group and exponent of reaction velocity equation, III-31
P	pressure
P_a	vapor pressure
P_r	Prandtl number
ΔP	maximum pressure minus minimum pressure in annulus
q	rate of heat transferred
q_r	heat of reaction
q_v	heat arriving at drop surface
R	universal gas constant
Re	Reynolds number
Re_d	Reynolds number of droplet based on the speed of sound
r	drop radius and radial direction
Δr	radial element thickness
r_{an}	radius of annular ring
r_t	decomposition flame radius
S	surface area
S_c	Schmidt number
T	temperature
$\bar{T}$	average film temperature $(T_g - T_\ell)/2$
t	time
U_ℓ	internal energy of liquid
u	gas velocity (only in Section III and Appendix I)
v	velocity and drop velocity (only in Section III and Appendix I)

Δv	absolutive value of velocity difference between gases and drops
Δv_z	absolutive value of velocity difference between gases and drops in axial direction
$\dot{W}$	propellant flow rate
w	vaporization rate of single drop (lbm/sec)
x	axial position ($x=0$ at injector)
z	axial direction and as defined by equation III-11
Δz	axial element thickness
α	correction factor for mass transfer, equation III-5
β	defined by III-35
γ	specific-heat ratio
∇	del operator
η_{C^*}	efficiency based on characteristic velocity
θ	angular direction and defined by equation III-29
λ	heat of vaporization (Section III and Appendix I) and thermal conductivity of gases
μ	viscosity
ξ	defined by equation III-37
ρ	density
τ	stress tensor
Φ	mixture ratio, O/F
ϕ	defined by equation III-36
X_s	defined by equation III-27
X^*	defined by equation III-28
ω	local instantaneous burning rate (lbm/sec in^3)

Subscripts

a	vapor
c	combusted or combustion chamber
d	droplet
f	fuel
g	product gas
i	index of summation
j	at injector
ℓ	liquid
m	vaporization mantle
o	oxidizer, stagnation, or steady-state
p	particle
s	stability quantity
v	vaporized

Superscripts:

'	reduced parameter, defined in equation
-	average

I. INTRODUCTION

The problem of unstable combustion in rockets represents one of the most serious obstacles to reliable performance. Despite the research which has been performed in an attempt to understand the mechanism of combustion instability, there has not been a satisfactory model relating stability to propellant properties and combustion chamber design. The research developed herein is directed at obtaining an understanding of the behavior of propellant sprays in a liquid propellant engine under oscillating flow conditions as a means of relating combustion stability to propellant properties and injector design.

A number of different types of instability are recognized which differ in observed characteristics and which depend on different mechanisms. The work discussed in this report is concerned only with liquid propellant rocket engines. Further, of the various types of instabilities observed in liquid propellant engines, this work is pertinent to the type usually defined as the high frequency instability. The principal characteristics of such an instability, in terms of the theoretical analysis, is that the processes involved in these instabilities are assumed to be isolated within the combustion chamber and are not coupled, nor do they interact with processes outside the combustion chamber.

The steady-state combustion process can be considered to consist of the following processes occurring in sequence or in parallel: (1) atomization; (2) vaporization; (3) mixing; and (4) chemical reaction. Certain assumptions and approximations must be made in order to treat the problem theoretically without introducing such a great complexity that useful solutions cannot be obtained. In order to define the theoretical approach and objectives of the study reported here, a qualitative discussion of the combustion process in the combustion chamber is useful.

For the steady-state combustion process as well as the unstable combustion, it is assumed that atomization of the propellant occurs very rapidly close to the injector face. This does not mean that atomization is ignored. On the contrary, it is assumed that the atomization process determines the size, position and velocity distribution of the drops which participate in the combustion process. Changes in conditions which affect atomization thus affect the droplet distribution. The description of the atomization process becomes, since it is omitted from the theory, an essential part of an experimental program. The experimental program determines the relationship between the injector variables and droplet distributions. The theory begins with a droplet distribution.

Droplet vaporization is treated in the theory as the rate controlling process. This implies that the rates of mixing and chemical reaction are extremely rapid compared to vaporization rates. On such a basis, vaporization represents a major part of the total process and only a small error is introduced by neglecting the time for mixing and chemical reaction. The work of Priem and co-workers (Ref. 1) indicates considerable justification for such an assumption for many propellant combinations. If the mixing and chemical reaction times are of the same order of magnitude as the vaporization times, or a more extreme case, if the vaporization time is short compared to the time required for the other processes, the model does not apply. The assumption of a combustion process controlled by vaporization rate thus becomes an essential part of the theoretical discussion which follows. The theory does not apply to propellant which evaporates so rapidly that the combustion process occurs essentially in the gas phase or, of course, for propellants injected as gases. It is important to remember, however, that only one component of a bi-propellant system need have a slow vaporization rate for the assumption to apply. For steady-state combustion it is assumed that a given drop distribution enters at the injector face, and that the vaporization process, including rapid mixing and reaction, occurs within the combustion chamber.

The previous discussion describes a model for steady-state combustion. Presumably, once initiated, such a system should continue burning in a stable manner. The problem of combustion instability becomes involved when a disturbance produces a change in distribution, pressure, temperature, velocity or some combination of these. While it is possible to visualize a combustion process which is unstable by itself (linear instability), the theory described here requires some initiating disturbance (nonlinear instability). Such a disturbance may be a starting transient, a transient variation in injection, or any change in the established steady-state conditions. The interaction between such a disturbance and the normal combustion process may lead to a decrease or increase in the intensity of the disturbance. A decrease in intensity would result in a return to stable operation, while an increase in intensity, if continued, could lead to a disturbance level which results in engine failure.

An initial disturbance may build up to intensity levels or originate at an intensity level which completely changes the combustion process. For example, large amplitude pressure waves could shatter droplets producing small droplets that change the model. The existence or development of a strong pressure wave could also lead to detonation combustion. The

theory developed in this report does not describe such phenomena. The work conducted by Dynamic Science Corporation is divided into two models: (1) linear model; and (2) nonlinear model. The linear model describes the amplification of an initially sm ll disturbance which could lead to other processes. In this sense the linear model is concerned with the initial phases in the transition from a small disturbance to instability. The linear model is described in detail in Reference 2, and will not be repeated in this report. The nonlinear model is concerned with the transition from a finite disturbance to a large amplitude disturbance.

Combustion instability zones in a liquid rocket engine are determined in this report by combining a nonlinear instability program with a steady-state vaporization program, providing an analytical framework for determining the relationship of design parameters to stability. The analysis determines the zones of an engine in which a tangential mode of high frequency instability is most easily initiated. The Dynamic Science Corporation instability program considers the nonlinear conservation equations with mass addition using a steady-state vaporization expression for the burning rate. From such a model, important nonlinear phenomena are predicted, i.e., (1) stability dependence on disturbance amplitude, (2) the limiting amplitude of pressure oscillations, and (3) nonsinusoidal waveforms. This model applies to a one-dimensional annulus of small length (Δz) and thickness (Δr).

Applying the results of this model, a rocket engine can be analyzed by incrementally dividing the combustion chamber into annular nodes in the r and z directions. Steady-state properties at each annular node or position in the chamber are computed from the steady-state vaporization computer program. These steady-state properties and the stability limit curves from the instability computer programs are used to determine the stability at each node. This process is repeated for each node to determine a stability map of the entire engine. Thus stability can be related to hardware design parameters, i.e., parameters related to injector design, chamber configuration, and propellants, thereby enabling the influences of system design and stability rating devices to be determined.

The following report has been divided into four main parts. Part one deals with the application of the steady-state and instability program to determine stability zones in a rocket engine. Part two covers the details of the steady-state model for monopropellant type fuels such as monomethylhydrazine. Part three deals with the nonlinear instability model used to generate the stability limit curves and finally, Part four contains the details of the steady-state and instability programs and computer listings.

II. APPLICATION OF STEADY-STATE AND COMBUSTION INSTABILITY MODEL

1. Introduction.

Dynamic Science Corporation has developed a nonlinear model for determining the zones of a liquid rocket engine in which a tangential mode of high frequency instability is most easily initiated. This model has been related to hardware design parameters, i.e., parameters related to injector design, chamber configuration, and propellants, thereby enabling the influences of system design and stability rating devices to be determined.

A method for determining the zones of a liquid rocket engine in which a tangential mode of high frequency is most easily initiated was developed by Beltran and Frankel (Ref. 3). This method uses the Priem-Guentert (Ref. 4) nonlinear model in conjunction with the Priem-Heidmann (Ref. 1) propellant vaporization model. A rocket engine is analyzed by incrementally dividing the combustion chamber into annular nodes in the r and z directions as illustrated in Figure 1.

From a nonlinear model important nonlinear phenomena are predicted, i.e., (1) stability dependence on disturbance wave shape, amplitude, type (velocity or pressure), and position; (2) the limiting amplitude of the unstable pressure oscillations; and (3) the shape of the unstable wave forms. Such information is not only of use from the preliminary design standpoint, but also as an invaluable tool in understanding how rocket engines should be disturbed during their development test program to determine the degree of stability of an engine. The Dynamic Science Corporation model enables the engine designer to determine the position to introduce the disturbance, a reasonable disturbance amplitude criteria, and the most effective wave profile (pressure and velocity disturbance). Since the injector design variables can be related to threshold disturbance amplitude parameters can be modified to increase stability of a given engine configuration or be used in the preliminary design of an engine.

While the Priem-Guentert instability model (Ref. 4) solved the nonlinear conservation equations with a steady-state vaporization expression for the burning rate, the results are only valid for a large droplet-gas relative velocity or droplet Reynolds number based on the speed of sound. The solution of the nonlinear model (Ref. 4) used an explicit first order finite difference scheme. Different integration techniques were attempted for the solution of the nonlinear model in

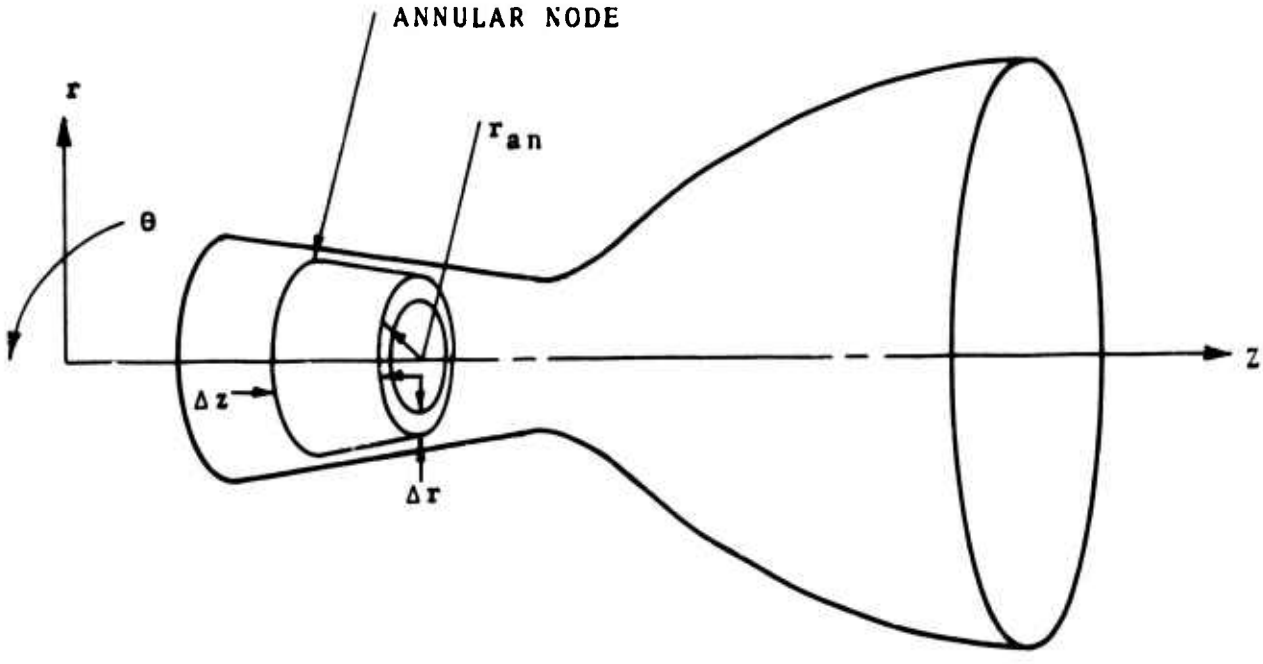

FIGURE I. Transtage Rocket Engine Model

Reference 5. Difficulties were encountered in attempting to reproduce the solutions of Reference 4. It was determinded that numerical instability was generating false indications of combustion instability in the nonlinear model for small values of the burning rate parameter L. Under NASA contract NAS 3-677 the Priem-Guentert results (Ref. 4) were recalculated by Beltran and Wright (Ref. 6) using predictor-corrector formulae. Stability limit curves were generated to determine the influences of droplet Reynolds number. Results from this program will be used for the following report.

The steady-state combustion model being used for this study is a steady-state, adiabatic, one-dimensional flow model treating propellant evaporation as the rate limiting step in the combustion process. The program treats storable propellants by using a two-flame model to account for propellant decomposition. Such a program is unique in that it can calculate steady-state combustion rates of hydrazine type propellants. Steady-state properties at each annular node or position in the chamber are computed from the propellant vaporization program. These steady-state properties and the curves from the instability program were used to determine the stability of the node. This process is repeated for each node to determine a stability map of the entire engine.

Major results of this analysis show that the amplitude and position of a pressure disturbance required to initiate instability can be determined, thereby defining a sensitive zone (and the best place to disturb the engine). This sensitive zone extends several inches from the injector face and occurs where the average droplets are moving the slowest relative to the gases.

Dynamic Science Corporation has shown that an annular combustor section will be more stable as the droplet Reynolds number approaches zero. Thus, a significant result of this work is that there are, for a vaporization controlled combustion process, three parameters affecting stability:

(a) Burning rate parameter - L

(b) Absolute value of relative velocity - Δv

(c) Reynolds number of drop based on speed of sound - Re_d

2. Nodal Method.

Combustion instability zones in a liquid rocket engine are determined by combining a nonlinear instability model with a steady-state vaporization program. The analysis determines the zones of an engine in which a tangential mode of high frequency instability is most easily initiated. In addition, it represents an a priori method for determining the relationship of design parameters to stability.

The instability model considers the nonlinear conservation equations with mass addition using a steady-state expression for the burning rate. This model applies to a one-dimensional annulus of small length (Δz) and thickness (Δr) shown in Figure 1. Applying the results of this model, a rocket engine can be analyzed by incrementally dividing the combustion chamber into annular nodes in the r and z directions. Steady-state properties at each annular node or position in the chamber are computed from a steady-state vaporization program. These steady-state properties and the curves from the instability model are used to determine the stability of the node. This process is repeated for each node to determine a stability map of the entire engine.

For a vaporization controlled combustion process, the significant parameters affecting stability are L, Δv, and Re_d. The burning rate parameter (L) is derived from Damkohler's similarity group based on the speed of sound $\left(\frac{r_a n \omega_o}{\rho_o \; a_o}\right)$.

The Reynolds number of the droplet based on the speed of sound $\left(\frac{r_d a_o \; \rho_o}{\mu_o}\right)$ is derived from the droplet vaporization equation.

For a steady-state combustion process, Δv, ω_o, ρ_o, r_d, μ_o, and a_o are functions of r, θ, and z. If one-dimensional flow is considered, these properties are only functions of z. Then L may be defined as:

$$\frac{r_a n \omega_o}{\rho_o \; a_o} = \frac{r_a n^m}{A} \left[\frac{2}{\gamma+1} \quad \frac{\gamma+1}{2(\gamma-1)}\right] = Lf(\gamma) \qquad \text{(II-1)}$$

where

$$L = \frac{r_a n^m}{A} \qquad \text{(II-2)}$$

Therefore, since m and A are functions of z only, L is a function of r and z. Since annuli are being considered in this model it is assumed that the contraction ratio of any annulus at z is equal to the contraction ratio of the chamber at z. The Reynolds number of the droplet is a function of z.

The steady-state vaporization program was used to compute $\Delta v(z)$, $Re_d(z)$ and $m(z)$. This program assumes that vaporization is the controlling combustion process, which is equivalent to assuming that mixing and reaction rates are fast compared to vaporization rates and that reacted products are formed at the same rate as the propellants are vaporized. This condition is satisfied in most high performance rocket engines where the propellant is injected uniformly over the entire injector face. Since it is also assumed that the combustion processes begin at the point where droplets are formed, a length required for atomization was added.

Example

To illustrate the nodal method, combustion of a monomethyl hydrazine spray in nitrogen tetroxide was considered. This method can be used on other propellant combinations as well. Calculations were based on a monodispersed spray with a drop radius of 0.003 inches (75 microns).
Typical transtage engine parameters were used: chamber diameter, 11.65 inches; chamber pressure, 100 psia; chamber contraction ratio, 2.43; initial drop velocity, 1000 inches per second; and initial drop temperature, 530°R.

Using the outlined chamber parameters Δv_z, Re_d, and m are computed as functions of z and plotted in Figures 2, 3 and 4 respectively. Using the vaporization program, only the relative velocity in the z direction is computed; however, in the injection zone there are large gradients and recirculation zones due to the viscous action between the sprays and combustion gases, so that velocity differences exist in the r and θ directions as well.
A level of turbulence equivalent to $\frac{v_z}{a_o}$ of 0.01 is reasonable in view of the measurements made by Hersh.(Ref.7) If it is assumed that the drops are unaffected by turbulent oscillations, which is justified with the drop size group considered, this velocity can be added to Δv_z thereby obtaining the total Δv. A mean drop size was selected to represent the average Δv since the smallest droplets will follow the gas velocity and the largest droplets will lag. The choice of a mean drop size serves to illustrate the method used; however, this does not imply necessarily that a mean drop is a good representation of the spray drop distribution. The method is quite flexible in

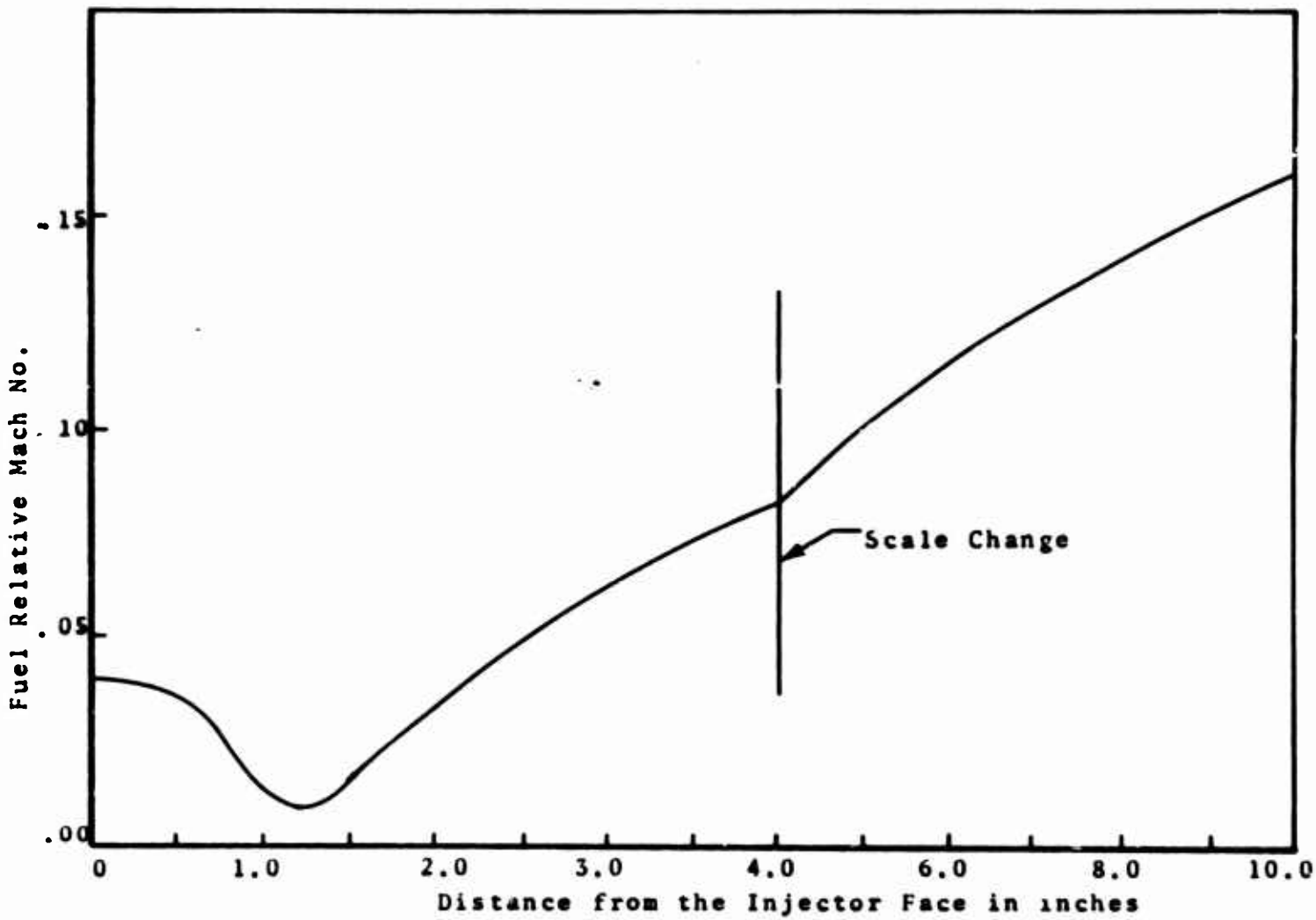

FIGURE 2. Profile of Steady-State Droplet Relative Mach Number

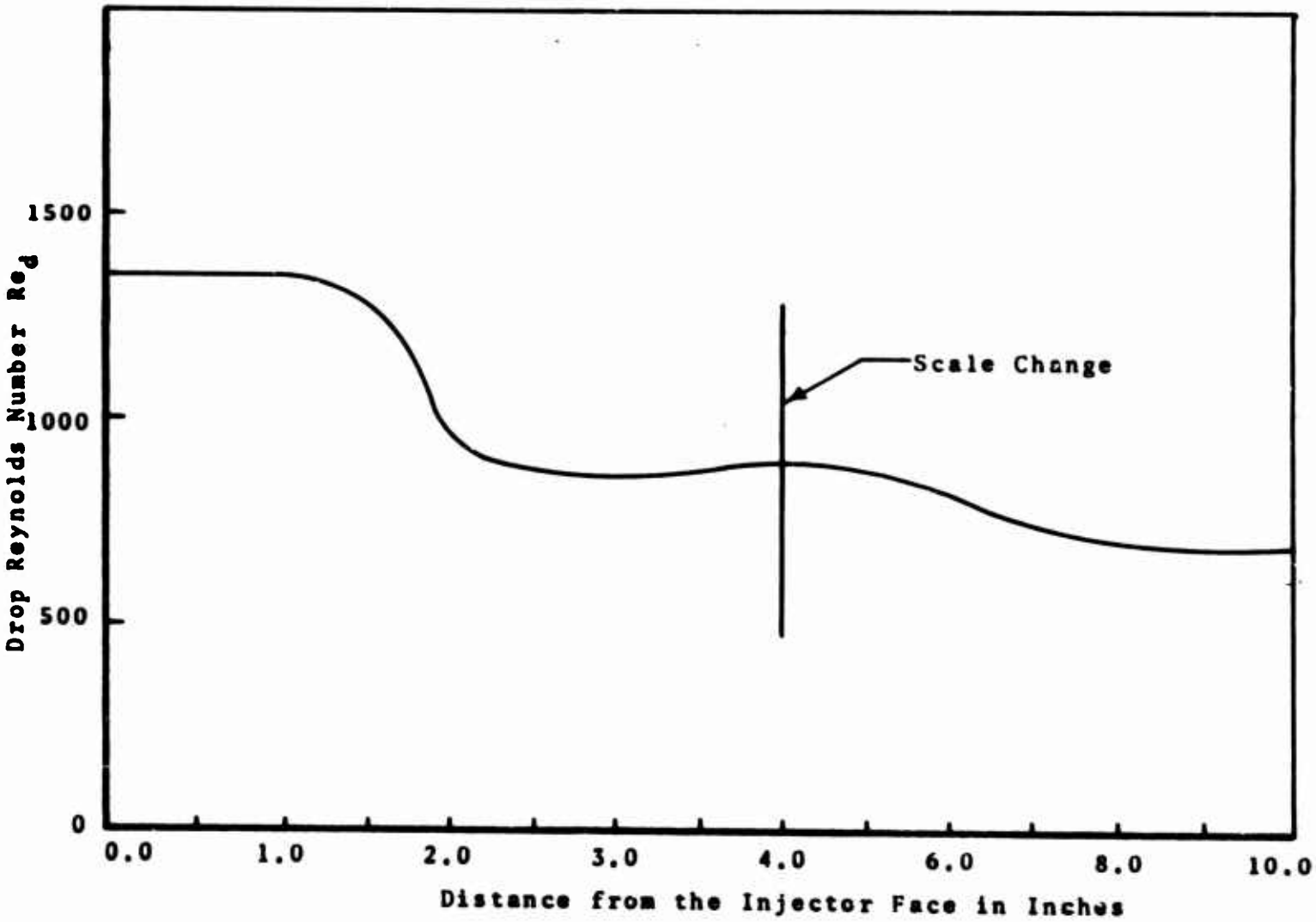

FIGURE 3. Profile of Drop Reynolds Number Re_d

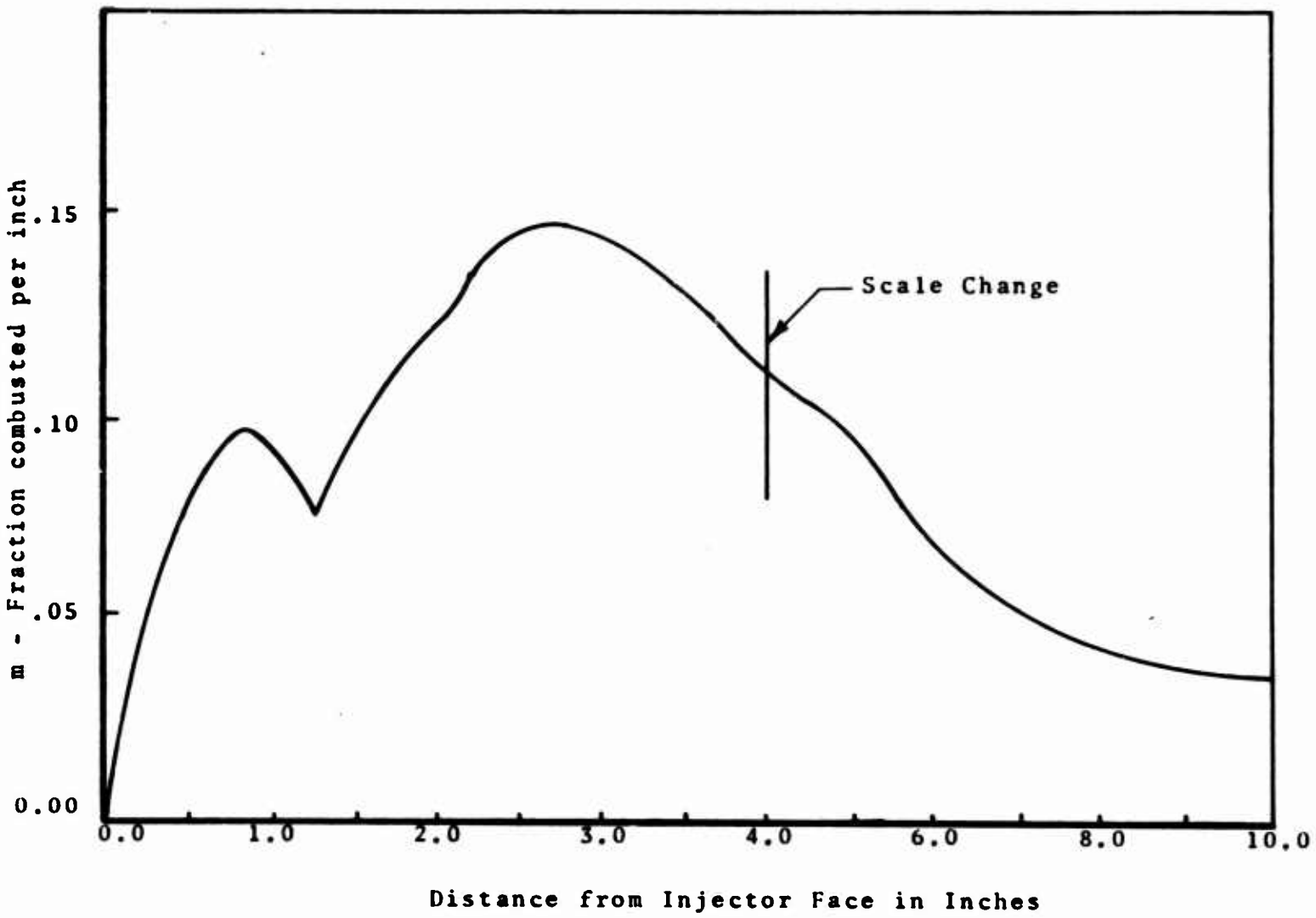

FIGURE 4. Profile of Steady-State Vaporization Rate

that it can be readily extended to treat distributed relative velocities.

In Figure 5, L is plotted versus r and z. Since L is directly proportional to r (equation II-2), it approaches zero at the centerline of the engine. Figure 6 is a plot of the pressure amplitude $\left(\frac{\Delta P}{P_c}\right)$ required to sustain a wave for various values of the parameter Δv. The upper boundary represents the equilibrium pressure amplitude that the wave will approach at steady-state and the lower boundary represents the minimum pressure amplitude necessary to initiate instability. These curves were plotted on the basis of Priem's stability limit curves. Figures 2-6 were cross-plotted to determine pulse pressure contour lines in the r-z plane in Figure 7. These isobaric lines describe the tangential threshold pulse required to initiate instability. It can be seen that the sensitive zone is from 0.2 to 3.0 inches from the injector face. For the case considered, this zone is largest at the outer radius. In general, the largest zone will occur where Re_d and Δv determine a point on the locus of minima of Figure 6. Thus, for a larger diameter engine the maximum sensitive zone may occur at some intermediate radius. A plot of ΔP required to induce instability versus z at the outer radius is shown in Figure 8. This plot shows that there is an extremely sensitive region occurring when the relative velocity between droplets and gas reverses direction, i.e., when Δv is minimum.

The method presented can be very useful in the design of stable rocket engines. In connection with engine design, it is useful to know the effect of various design parameters on the shape and extent of the sensitive zone. Although the analysis presented here can be extended to treat a variety of design conditions, certain qualitative observations are immediately evident. The most sensitive region can be moved closer to the injector face by (a) decreasing: 1) mass-median drop radius, 2) injection velocity, 3) chamber contraction ratio, or (b) increasing: 1) droplet geometric standard deviations, 2) propellant injection temperature, and 3) propellant volatility. The sensitive region can be moved away from the injector by opposite parameter changes. Since it is difficult to change one of the above parameters independently of the others, it is recommended that any proposed design change be analyzed in detail by the methods presented here before any conclusions are drawn.

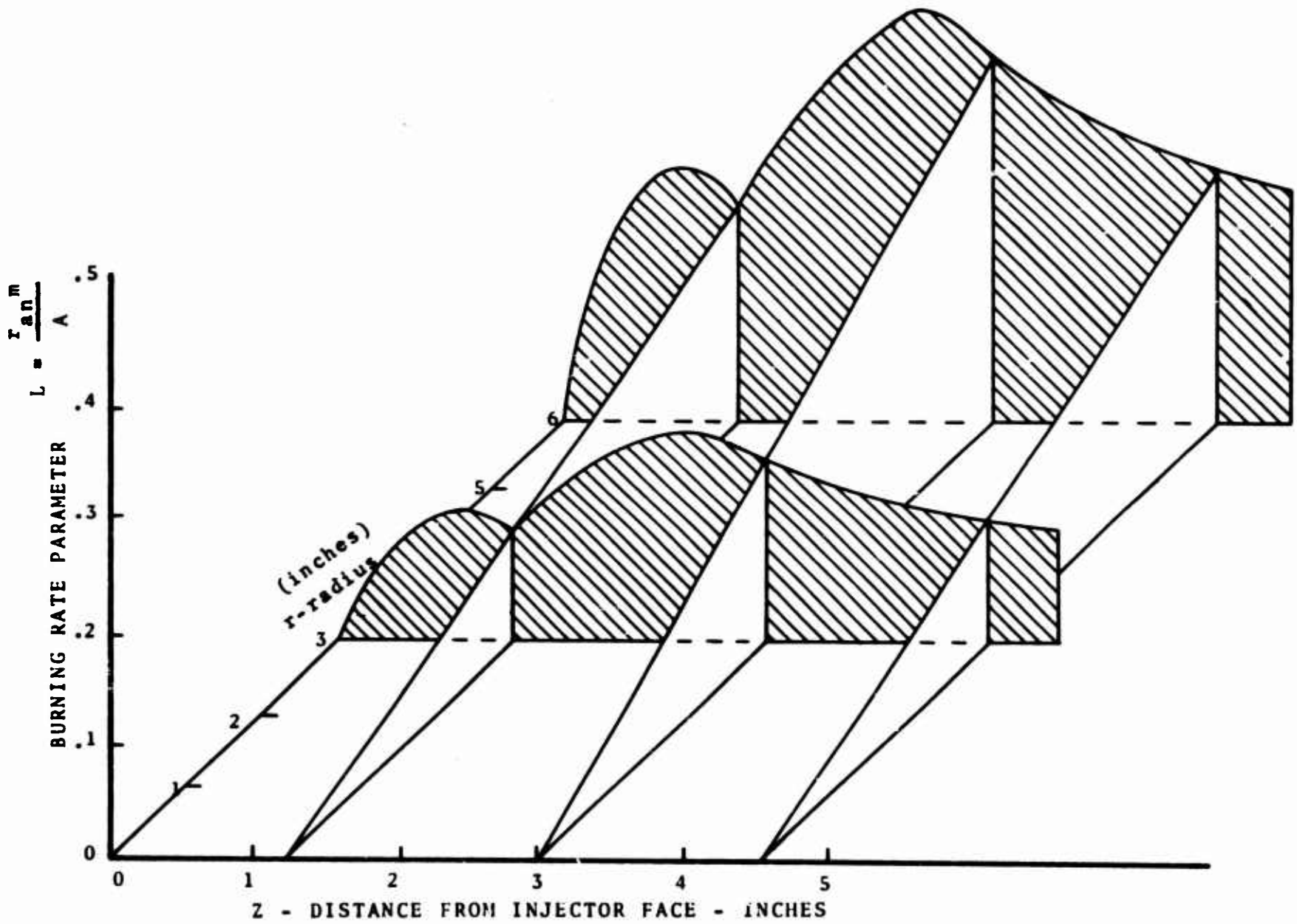

FIGURE 5. Burning Rate Parameter Distribution in Combustion Chamber

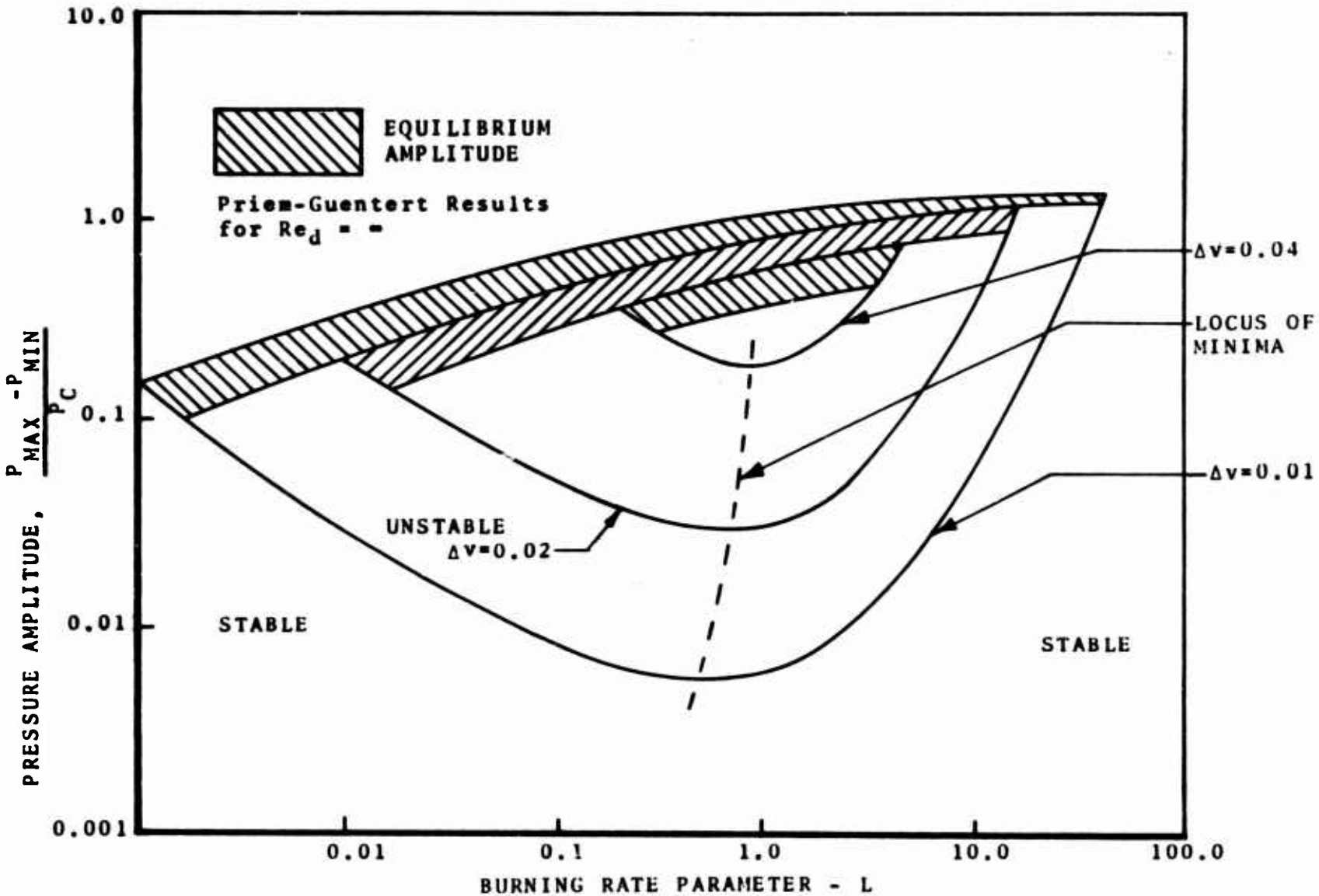

FIGURE 6. Stability Limit Curve (Reference 4)

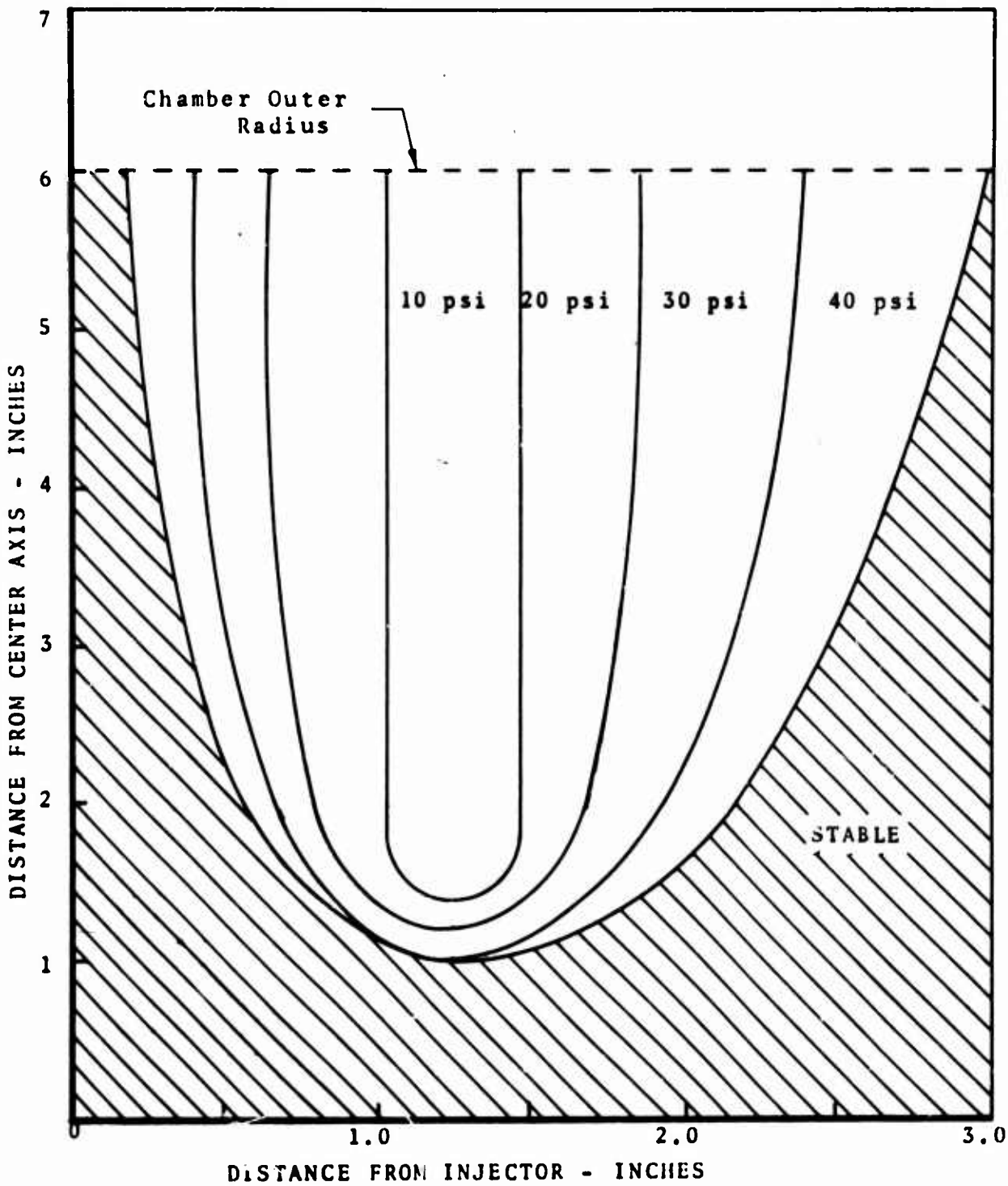

FIGURE 7. Pulse Pressure Contour Lines Defining Unstable Zones

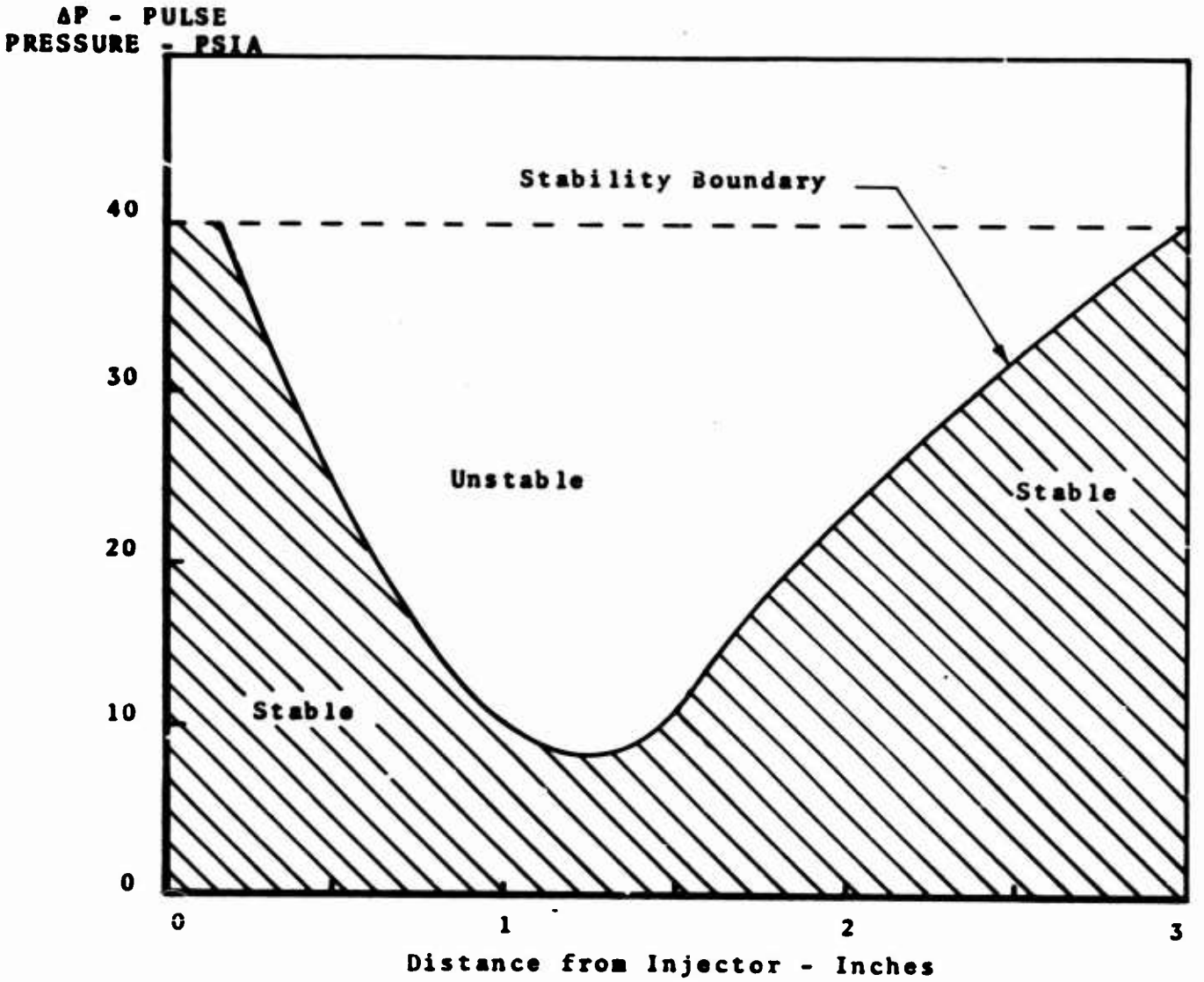
ΔP - PULSE
PRESSURE - PSIA
40
30
20
10
0
Stability Boundary
Unstable
Stable
Stable
0
1
2
3
Distance from Injector - Inches

FIGURE 8.

3. Conclusion.

Although the results presented here are reasonable in light of liquid rocket engine testing experience, it must be kept in mind that the basis of the model is a one-dimensional description of the transient processes. Two- and three-dimensional solutions would provide a description of the multidimensional nonlinear wave interactions and permit a more realistic consideration of the chamber boundary conditions which may significantly affect the results. However, it is felt that the agreement noted between the one-dimensional model and experimental findings (Ref. 8 and 9) indicate that the one-dimensional approximation leads to meaningful results. Thus, the model is valuable from an engineering standpoint since it relates design parameters directly to stability determination.

Results of this study show that: 1) the amplitude and position of a pressure disturbance required to initiate instability can be determined, thereby defining a sensitive zone; 2) this sensitive zone extends several inches from the injector face; 3) the most sensitive region in the zone occurs where the average droplets are moving the slowest relative to the gases; and 4) approximate baffle length can be determined, i.e., baffles must be extended past the instability zone. Dynamic Science Corporation has shown that as the droplet Reynolds number approaches zero, a rocket engine becomes more stable. A significant result of this work is that there are, for a vaporization controlled combustion process, three parameters affecting stability: 1) burning rate parameter; 2) absolute values of the relative velocity; and 3) Reynolds number of drop based on speed of sound-Re_d.

III. STEADY-STATE DROPLET COMBUSTION IN THE MONOMETHYLHYDRAZINE-NITROGEN TETROXIDE SYSTEM

1. Steady-State Vaporization with Vapor Phase Decomposition.

Analysis of high frequency instability in liquid rocket engines requires a spatial knowledge of such parameters as propellant burning rate, relative velocity between gases and propellant drops, and Reynolds number of propellant drops based on the local speed of sound. This section describes a steady-state combustion model which estimates these parameters in the combustion chamber.

A model for steady-state droplet combustion allowing for vapor phase decomposition of thermally unstable fuels has been developed and will be discussed. In this report the model was applied to the monomethylhydrazine/nitrogen tetroxide system. The model presented enables the computation of steady-state profiles within a rocket combustion chamber. From these profiles combustion instability parameters can be computed. Details of the computer program developed from the steady-state model are presented in Appendix I. With injection parameters specified, i.e., droplet size, injection velocity, chamber pressure, mixture, ratio, and droplet temperature, the computer program can compute droplet and gas histories along the chamber. This information is required for the design of combustion chambers and calculation of C* efficiency. From the results of the computer program the effects which any of the numerous design or physical parameters have upon chamber operation can be determined. Thus the influences of injector design parameters and physical properties on combustion instability can be evaluated.

This program assumes that droplet vaporization is the rate controlling step in liquid rocket chamber combustion. This approach has proven successful in previous studies, (Ref. 1, 10). The vaporization rate of a droplet is determined by transport phenomena across a boundary layer diffusion mantle. For such fuels as MMH and NTO, decomposition occurs within this diffusion mantle because of the extreme temperature gradient. Exothermic decomposition may change the mantle temperature gradient to such an extent that a decomposition flame appears within the boundary layer. This flame has the effect of maintaining high vaporization rates even under low convection (flow) conditions. Thus the physical two-flame model presented here determines higher combustion rates near the injector face than does the single-flame model of Reference 1 and 10.

2. The Model

Experiments and a literature search indicated that decomposition and oxidation flame fronts coexisted in the combustion of N_2H_4 type fuels. Thus a model which considers two different burning mechanisms, depending upon droplet Reynolds number, was developed. Such a model is compatible with the single-mechanism system of equations developed in Reference 1.

a. Oxidation Model (Single-Flame Regime).

This model incorporates features of two other models in the literature (Refs. 1, 10). The treatment of vaporization which allows for heating of the drops is essentially that of Priem and Heidmann (Ref. 1) while the treatments of drop ballistics and chamber gas dynamics are essentially those developed by Rocketdyne (Ref. 10). The combustion-flow process is considered to be one-dimensional. The model represents the continuous distribution of drop sizes by an arbitrary number of size groups as do both references. A logarithmiconormal distribution has been used to describe the spray pattern of the motor of interest; however, any type distribution may be substituted into the droplet size subroutine.

(1) System Equations. The equations describing combustion, assuming vaporization is rate controlling, are presented in this section. These equations are manipulated so that simultaneous computer solution is possible. The existence of a decomposition front, within the boundary layer mantle, is consistent with these equations except that a different mass vaporization rate must be defined as discussed in Section III-2.b.(2).

(a) Droplet Ballistics. A Force-momentum balance on the drop yields the equation

$$\frac{dv}{dx} = \frac{3C_d\rho_g|u-v|(u-v)}{8\rho_\ell \; r \; v} \qquad \text{(III-1)*}$$

---

* Equations following by an asterisk are applied individually to all drop sizes of both oxidizer and fuel.

where C_d is defined as in reference 10.

$$C_d = 27\ Re_g^{-0.84} \qquad 0<Re_g<80 \qquad \text{(III-2)*}$$

$$= 0.271\ Re_g^{0.217} \qquad 80<Re_g<10^4$$

$$= 2 \qquad 10^4<Re_g$$

$$Re_g = \frac{2r\Delta v\rho_g}{\mu_g} \qquad \text{(III-3)*}$$

(b) Droplet Mass. The rate of evaporation from a spherical drop of propellant is given by the equation (Ref. 1).

$$w = \frac{2\pi\ D_a r\ \ M_a\ \alpha Nu_m}{R\bar{T}}\ P_a \qquad \text{(III-4)*}$$

$$\text{where} \quad \alpha = \frac{P}{P_a}\ \ln\ [\frac{P}{P-P_a}], \text{ and} \qquad \text{(III-5)*}$$

the Nusselt number for mass transfer is determined from Ranz and Marshall's correlation (Ref. 11).

$$Nu_m = 2 + 0.6\ Re_m^{1/2}\ Sc^{1/3} \qquad \text{(III-6)*}$$

Thus the change in droplet mass with distance is given by

$$\frac{dm}{dx} = \frac{dm}{dt} \times \frac{dt}{dx} = -\frac{w}{v} \qquad \text{(III-7)*}$$

(c) Heat Transfer to Droplet. A heat balance on a single droplet yields the result that the rate of accumulation of energy must equal the net energy transferred to the drop at any time.

---

*Equations followed by an asterisk are applied individually to all drop sizes of both oxidizer and fuel.

Thus,

$$m\, C_{p_\ell} \frac{dT_\ell}{d\theta} = q_v - w\lambda - \frac{wv_f^2}{2} + Q_R \qquad \text{(III-8)}$$

The term Q_R represents the radiant heat transfer to the drop and has been omitted from this program; although, it could be included if values for emissivity justify it.

The third term on the right hand side of (III-8) represents the kinetic energy imparted to the vapor leaving the surface. This term is generally negligible but was included in the program since it can be important for small radii and/or for drops near their critical temperature (for which λ approaches zero).

The term q_v represents the heat transferred to the vaporizing drop by convection with mass transfer. This is defined in terms of a heat transfer coefficient as

$$q_v = 4\pi r^2 \dot{h}\, (T_g - T_\ell) \qquad \text{(III-9)}$$

Where the heat transfer coefficient with mass transfer, $\dot{h}$, is related to the coefficient without mass transfer by

$$\dot{h} = h \left[\frac{z}{e^z - 1}\right] \qquad \text{(III-10)}$$

and

$$z = \frac{wC_{pa,m}}{4\pi r^2 h} = \frac{wC_{pa,m}}{2\pi r\, Nu_h\, k_m} \qquad \text{(III-11)*}$$

Again the Nusselt number for heat transfer has been defined in the work of Ranz and Marshall (Ref. 11) to be

$$Nu_h = 2 + 0.6\, Re_m^{1/2}\, Pr^{1/3} \qquad \text{(III-12)*}$$

Substituting into (III-9)

$$q_v = \frac{w\, C_{pa,m}\, (T_g - T_\ell)}{(e^z - 1)} \qquad \text{(III-13)*}$$

Finally the heat balance (III-8) yields

$$\frac{dT_\ell}{dx} = \frac{q_v - w\lambda - \frac{wv_f^2}{2}}{m\, C_{p\ell} v} \qquad \text{(III-14)*}$$

(d) Chamber Pressure. A force balance on an incremental chamber length yields

$$\frac{d(PA_c)}{dx} = -\frac{dI}{dx} \qquad \text{(III-15)}$$

where

$$I = \frac{\rho_g u^2 A_c}{g} + \Sigma\, n\, m\, v \qquad \text{(III-16)}$$

The continuity equation is expressed as

$$\rho_g u A_c = \Sigma n (m_j - m) \qquad \text{(III-17)}$$

Use of equations (III-16) and(III-17) in equation (III-15) yields

$$\frac{dP}{dx} = -\frac{1}{A_c}\left\{\Sigma n(m_j - m)\frac{du}{dx} + \Sigma n\left[m\frac{dv}{dx} - (u-v)\frac{dm}{dx}\right] - P\frac{dA_c}{dx}\right\} \qquad \text{(III-18)}$$

Thus the pressure gradient has been expressed in terms of velocity gradient. However, another independent linear relationship between $\frac{du}{dx}$ and $\frac{dP}{dx}$ must be developed so that $\frac{dP}{dx}$ may be computed without iteration.

The following equations are necessary for this development.

$$\phi = \frac{[\Sigma n(m_{inj} - m]_o}{[\Sigma n(m_{inj} - m)]_f} \qquad \text{(III-19)}$$

$$T_g = T_{go}\left[1 - \frac{u^2(\gamma - 1)M_g}{2\gamma\, RT_o\, g}\right] \qquad \text{(III-20)}$$

$$\rho_g = \frac{P\, M_g}{R\, T_g} \qquad \text{(III-21)}$$

The analysis assumes the ability to evaluate properties of the combustion product gas (T_{go}, M_g, γ, k_g, and μ_g) as functions of chamber pressure and mixture ratio and propellant properties (P_a, k_a, ρ_ℓ, γ, $C_{p\ell}$, and C_{pa}) as functions of temperature. Furthermore, the diffusion coefficients, D, will have to be determined functions of mixture ratio, pressure, and temperature.

After considerable algebra involving equations (III-17, 19, 20, and 21) and their derivatives, an independent linear relationship between $\frac{du}{dx}$ and $\frac{dP}{dx}$ can be developed in the form

$$\frac{du}{dx} = F + G \frac{dP}{dx} \qquad \text{(III-22)}$$

where F and G are functions of quantities which are known at any step in the numerical integration, (e.g., m, v, $\frac{dm}{dx}$, $\frac{dv}{dx}$ P, u,---), of the combustion product gas properties and of the derivatives of those properties with respect to local mixture ratio, Φ.

If equation (III-18) is considered to have the form

$$\frac{dP}{dx} = H + J \frac{du}{dx} \qquad \text{(III-23)}$$

equations (III-22 and 23) result in

$$\frac{dP}{dx} = \frac{H + JF}{I - JG} \qquad \text{(III-24)}$$

Thus, equation (III-24) allows $\frac{dP}{dx}$ to be computed directly in this program.

(2) Physical Properties in the Vaporization Mantle.

(a) The NTO System. The nitrogen tetroxide system exhibits complex changes with very short equilibrium times (order of microseconds). The system exists in equilibrium in the following form

$$N_2O_4 \rightleftarrows 2NO_2 \rightleftarrows 2NO + O_2$$

The extent of either of the two decomposition reactions is a function of the system temperature and pressure. The actual function is not well defined by thermodynamic data because N_2O_4 and NO_2 exist in equilibrium at the mixture critical point. Thus it is impossible to separately determine either's critical properties.

For the temperature and pressure ranges to be considered in this work it was possible to postulate an approximate physical model. Utilizing such a model, liquid and vapor composition and thus such properties as thermal conductivity, heat capacity, and heat of vaporization could then be computed.

As shown in Figure 9, the entering liquid droplet is assumed to be N_2O_4. However, as the N_2O_4 evaporates it goes to

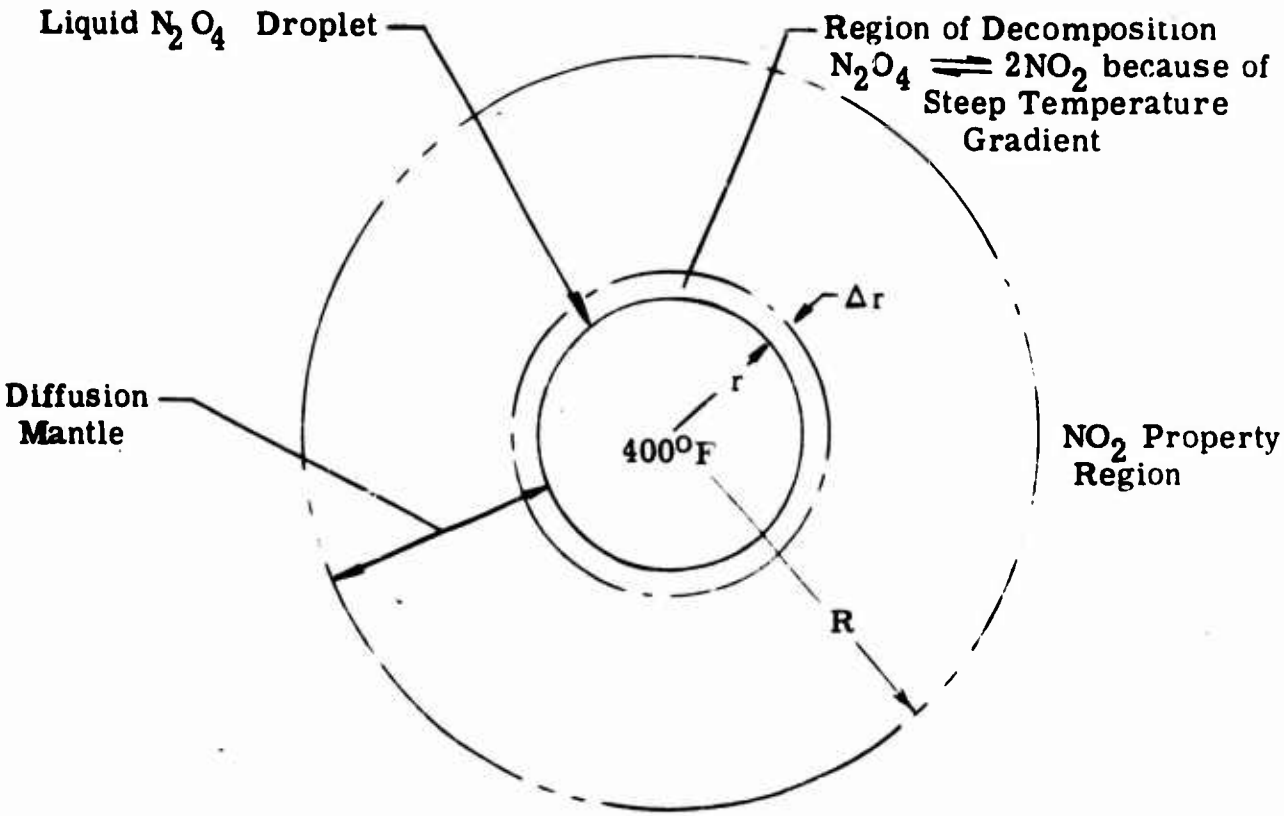

The assumption making possible the inclusion of heat of reaction with heat of vaporization is

$$\Delta r < 10\% \text{ of } (R - r).$$

FIGURE 9. Nitrogen-Tetroxide Droplet Vaporization Model.

approximately 50% NO_2. Then since the temperature gradient is very steep, (Figure 9) the vapor will be 100% NO_2 before it crosses even 10% of the diffusion mantle. The approximation that NO_2 is the vaporizing species was thus made. Using this approximation it was possible to account for chemical change by adding the heat of decomposition to the heat of vaporization for N_2O_4. The vapor was assumed to consist of NO_2 for the purpose of physical property calculation. The second decomposition $2NO_2 \rightleftharpoons 2NO + O_2$ was not considered in this approximate model.

(b) The MMH System. Monomethylhydrazine can support a decomposition front in the vapor mantle before undergoing oxidation. The occurrence of such phenomena not only changes such properties as thermal conductivity, heat capacity, density and diffusivity but also necessitates postulation of a decomposition model. A physically realistic model for vaporization with decomposition is discussed in the next section.

b. Decomposition Model (Two-flame Regime).

(1) Introduction. The equations presented in Section 2.a., describe a complex two-phase gasdynamics system. The vaporization description is one part of this coupled system. This part was modified, so that steady-state combustion with vapor phase decomposition of a thermally unstable fuel could be described. The modified combustion package was then incorporated into the system description.

Dynamic Science Corporation (Ref. 12) has completed experiments which indicate that a single diffusion flame front model is not realistic for such monopropellant systems as hydrazine and monomethylhydrazine. As shown in Figures 10 and 11, two flame fronts appear in the combustion of hydrazine and MMH in nitrogen tetroxide. The presence of these two flame fronts has been observed, but the exact nature of these fronts has not been fully determined.

This section reviews experimental and analytical studies of the MMH type system. A realistic two flame model is postulated along with its required assumptions. Equations are derived for this two flame decomposition-oxidation model and the method of solution is explained. The results of this work are:

i) Specification of a realistic steady-state vaporization model which includes vapor phase decomposition,

Note: The liquid drop is within the wire support.

Hydrazine burning in still nitrogen tetroxide, at one atmosphere

FIGURE 10. Photograph of Experimental Burning Drop Showing Two Flame Fronts (Reference 12)

Note: The liquid drop is within the wire support.

MMH Burning in still nitrogen tetroxide, at one atmosphere

FIGURE 11. Photograph of Experimental Burning Drop Showing Two Flame Fronts (Reference 12)

ii) Development of the technique used to solve these equations.

iii) Calculation of the spatial combustion properties with vapor phase decomposition.

The vaporization-diffusion model with a single stoichiometric diffusion flame front is shown in Figure 12b. For bipropellant combustion the outside boundary of the vapor mantle determines the position of the stoichiometric diffusion flame front. However, monopropellants may support a decomposition front within this diffusion mantle. The decomposition front is similar to a premixed gas flame front and cannot be analyzed as a diffusion flame. When a decomposition front occurs within the fuel diffusion mantle of an oxidizer-rich propellant combustor, two flame fronts will appear. The inside one is a decomposition front while the outer flame is an oxidizer diffusion flame front.

The postulated physical model involves two regions:

Region I, (Figure 12a) where the two-flame decomposition mechanism is rate controlling, and

Region II, (Figure 12b) where the single-flame, laminar boundary-layer oxidation mechanism is rate controlling.

The equations applicable to Regions I and II were used in specific calculations for the MMH-NTO system. The calculated burning rates for a distribution of MMH drops were determined and used to calculate the fraction combusted and the C* efficiency. The C* efficiencies for several engines were finally compared with experimental values determined by Priem (Ref. 1).

(2) Equations and Calculations. The existence of either region I or II depends upon the relative velocity between the liquid drop and the product gas. Region II corresponds to a large relative velocity (and small boundary layer), while region I corresponds to a small relative velocity (and relatively stagnate conditions). The applicability of the equations of either region are thus dependent upon the criterion that either the decomposition thickness is within the boundary layer, $r_t < B$ (region I), or the boundary layer is less than the decomposition thickness $r_t > B$ (region II). The equations, which allow calculation of r_t and B, were developed and used simultaneously to determine applicable regions.

Figure 12a. Decomposition Front Within Diffusion Mantle, Regime I

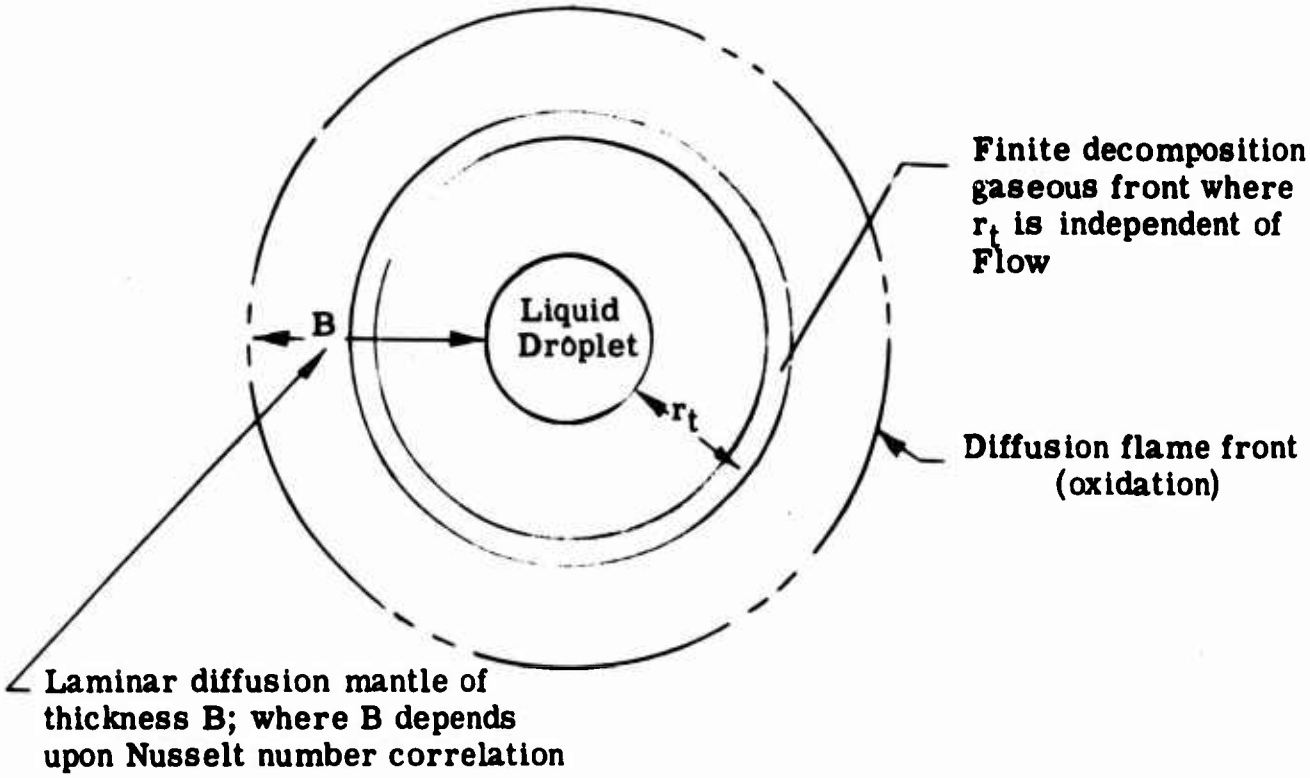

Figure 12b. Laminar Diffusion Model when $r_t \geqslant B$, Regime II

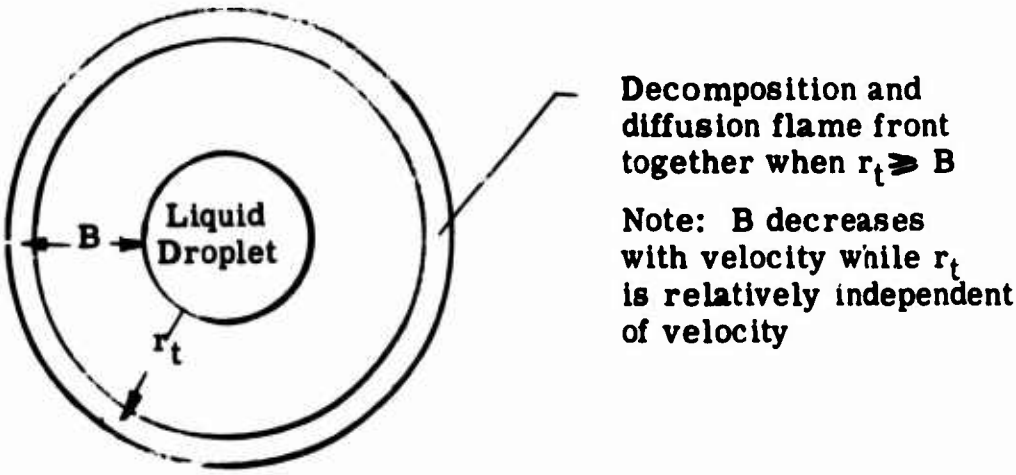

Figure 12. Two-Regime Model of Decomposition-Front Position, Adiabatic Oxidation Temperature the same in both cases.

Decomposition Equations (Region I)

The theoretical decomposition-flame model of Tarifa and Notario (Ref. 13) was extended to include the influence of adiabatic oxidation flame temperatures. The equations applicable for small drops in this region are not derived here; but are presented from the literature (Ref. 13) so that different liquid properties may be substituted in the program.

The decomposition film thickness is given in reference 13 as,

$$r_t = \frac{X_s}{X^*} r, \qquad \text{(III-25)}$$

And the decomposition evaporation rate constant (in^2/sec), [defined by $K = \frac{d(r^2)}{dt}$] is given in reference 13 by,

$$K = \frac{2k}{C_p \rho_l} X_s \qquad \text{(III-26)}$$

$$\text{where } X_s = \ln \left[\frac{\theta_m}{\theta_\ell} + \frac{X^*}{\theta_\infty}\right] \qquad \text{(III-27)}$$

$$X^* = \frac{3}{4\sqrt{6}} \left[\frac{\ln(\theta_\infty/\theta_l)}{(\theta_\infty - \theta_o)^{1/2}}\right] \exp \frac{-\theta_a}{2(\theta_\infty - \theta_o)} \sqrt{A_k}\, r \qquad \text{(III-28)}$$

$$\text{and } \theta = \frac{C_p}{q_r} \left(T - T_\ell + \frac{\lambda}{C_p}\right) \qquad \text{(III-29)}$$

$\theta = \theta_\infty$ for $T = T_\infty$ (adiabatic flame temperature)

$\theta = \theta_\ell$ for $T = T_\ell$ (liquid temperature)

$\theta = \theta_o$ for $T = 0$

$$\theta_a = \frac{C_p E}{R q_r} \qquad \text{(III-30)}$$

$$A_k = B \frac{C_p}{k} \left(\frac{\rho_\ell T_\ell C_p}{q_r}\right)^n \qquad \text{(III-31)}$$

where B and n are constants of the reaction velocity equation (Ref. 13).

Decomposition Parameters

In order to use the model proposed, the decomposition thickness and the evaporation rate constant must be calculated and used as input to the program. The decomposition-flame film thickness

and the evaporation rate constant were determined for several adiabatic oxidation temperatures and are shown in Figures 13 and 14 for the MMH-NTO system. An adiabatic decomposition flame temperature for a monopropellant corresponds to $\Theta_m = 1.0$; while $\Theta_m = 1.54$ corresponds to an adiabatic oxidation flame temperature for the MMH-NTO bipropellant system. The calculated curves of Figures 13 and 14 are thus extensions of the work of reference 13 to two flame front conditions.

(3) Calculation Procedure with Two-Flame Model. The decomposition thickness and evaporation rate curves of Figures 13 and 14 and burning rate curves similar to Figure 15 were used simultaneously to compute burning rates for the two regions. The values for the single flame model are shown in dashed lines (Fig. 15) for comparison.

Burning rate curves similar to Figure 15 are computed by the following steps for each group.

(a) Determine regions by the criteria.

$r_t < B$ region I

$r_t > B$ region II

Where B is the boundary layer thickness shown in Figure 15 and r_t is the decomposition film thickness shown in Figure 13 (B and r_t are input to the program).

(b) By this criteria the burning rate of Figure 15 was initially determined by the mechanism of region II.

(c) At $r_t = B$, the mechanism shifted to that of region I.

(d) The burning rate for region II was now determined by the K shown in Figure 14 and the rate equation:

$$\frac{3}{2} \frac{rK}{r_o^3 v} = -\frac{\text{fraction}}{\text{inch}} \qquad \text{(III-32)}$$

(e) At $r_t = B$ the mechanism shifted back to that of region II.

(f) If the drop had not yet reached its wet bulb temperature, while $B > r_t$, the distance to do so was calculated

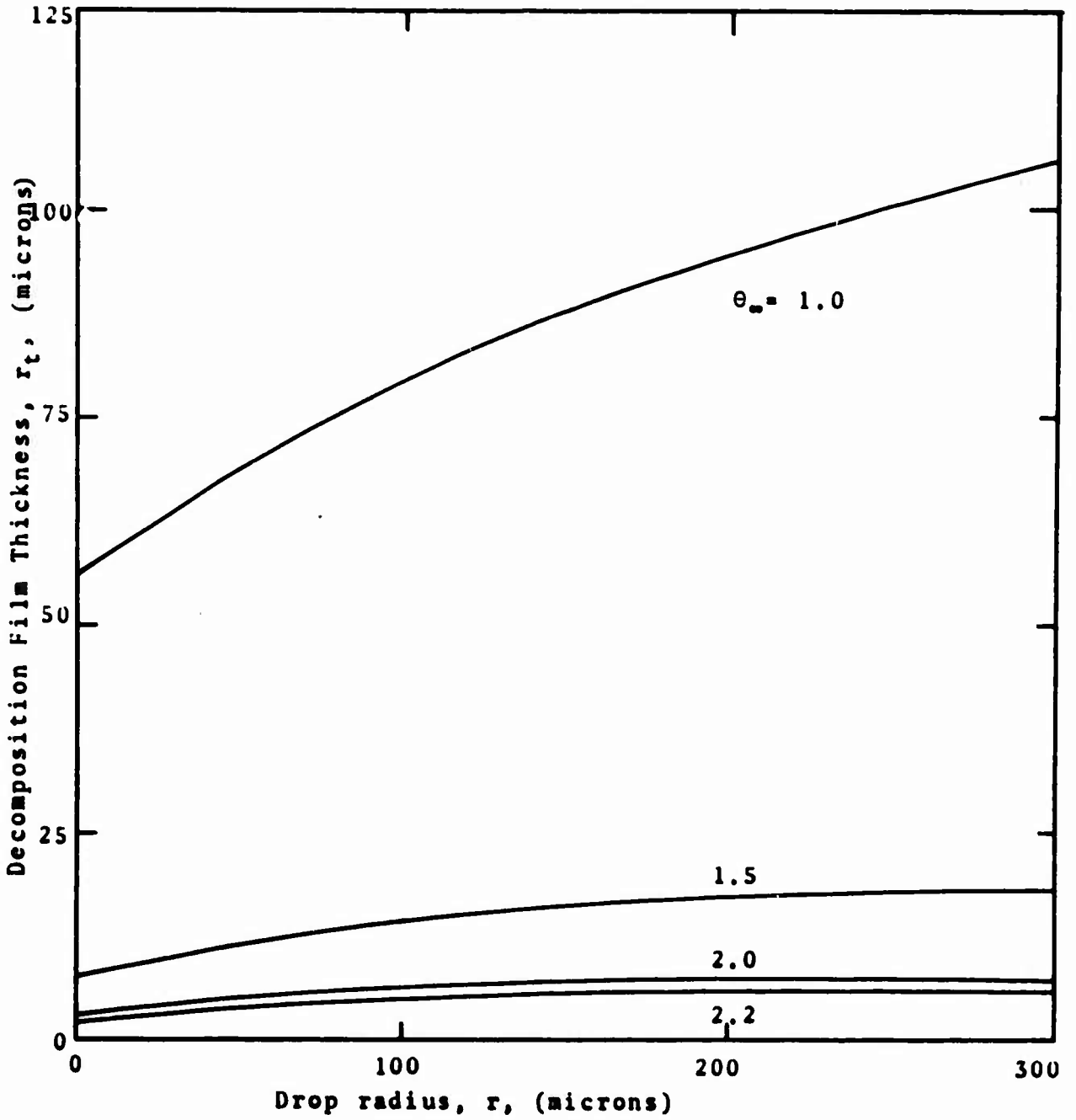

FIGURE 13. Film Thickness For Decomposition Flame

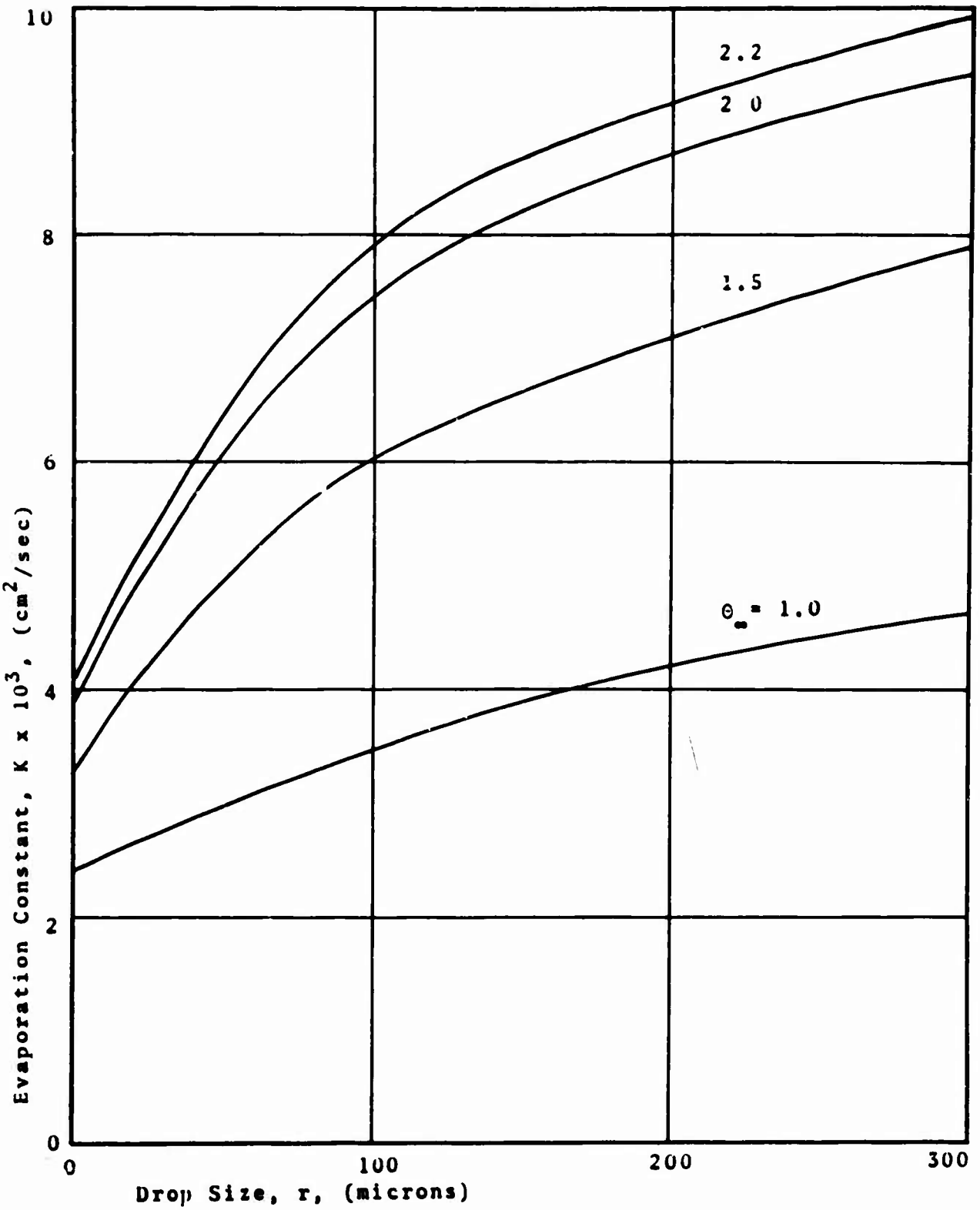

FIGURE 14. Evaporation Rate Constant for Decomposition

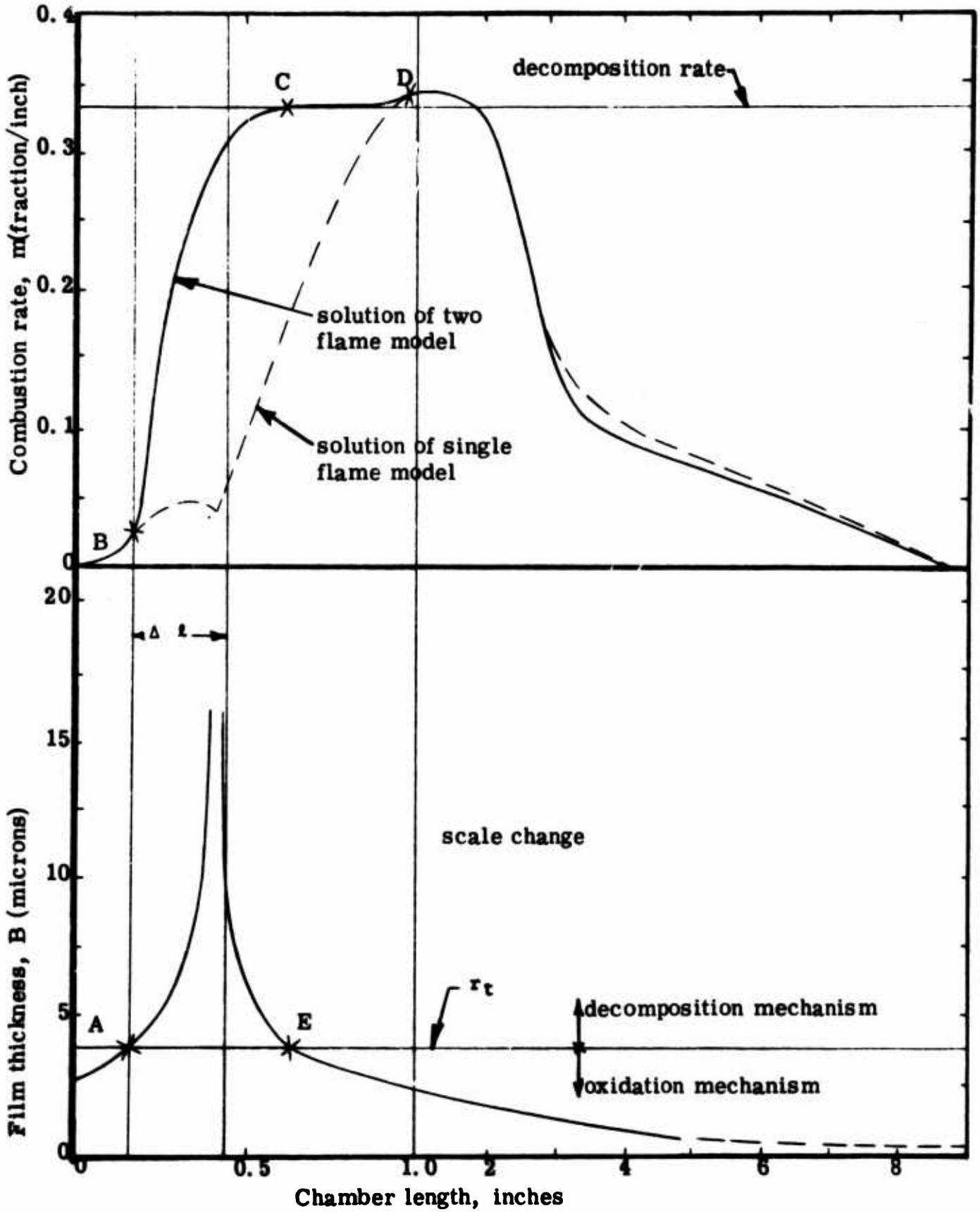

FIGURE 15. Combustion Rate, Initial Drop Size 49.4μ

by a heat balance which resulted in the equation

$$\Delta x = \frac{vmC_p(T_{w.b.} - T_\ell)}{2\pi \; q_r \; \rho_r \; k}$$

(g) The resulting burning rate curves, shown in Figure 15 are continually integrated by the program to determine the cumulative fraction of fuel vaporized. This curve is shown in Figure 16.

(4) Characteristic Results Using Two-Flame Model.

Burning Rates. The burning rates computed for the decomposition model are substantially higher than those computed using the single flame front model.

The maximum burning rates under either the single or double flame models are essentially the same (once wet bulb temperature is reached) because adiabatic conditions are assumed and the same amount of total enthalpy release is involved in both mechanisms.

The zero relative velocity point has a less pronounced effect upon the burning rate because the decomposition flame now determines the minimum rate at stagnation conditions.

Fraction Vaporized. The fraction vaporized under the two flame model is higher than under the single flame model as shown in Figure 16. At one inch chamber length the fraction is approximately 100% greater for the two-flame model than for the single-flame model.

C* Efficiency, η_{C^*}. The experimental data shown in Figure 17 were used by Priem and Heidmann (Ref. 1) to compare experimental and calculated hydrazine efficiencies. This comparison for a large number of propellant combinations is shown in Figure 18.

The hydrazine fraction vaporized, $\mathcal{F}$, (Figure 13) is vaporization rate controlling with the gaseous oxygen data of Fig. 17. Thus, the computed $\mathcal{F}$ was used with $\theta = 1.0$ for gaseous oxygen to compute the efficiency for hydrazine - GOX according to the formula

$$C^* = \frac{(C^*)_{O/\mathcal{F}}}{(C^*)_{O/F}} \; \frac{\frac{\dot{w}_o}{\dot{w}_F} + \mathcal{F}}{\frac{\dot{w}_o}{\dot{w}_F} + 1} \qquad \text{(III-33)}$$

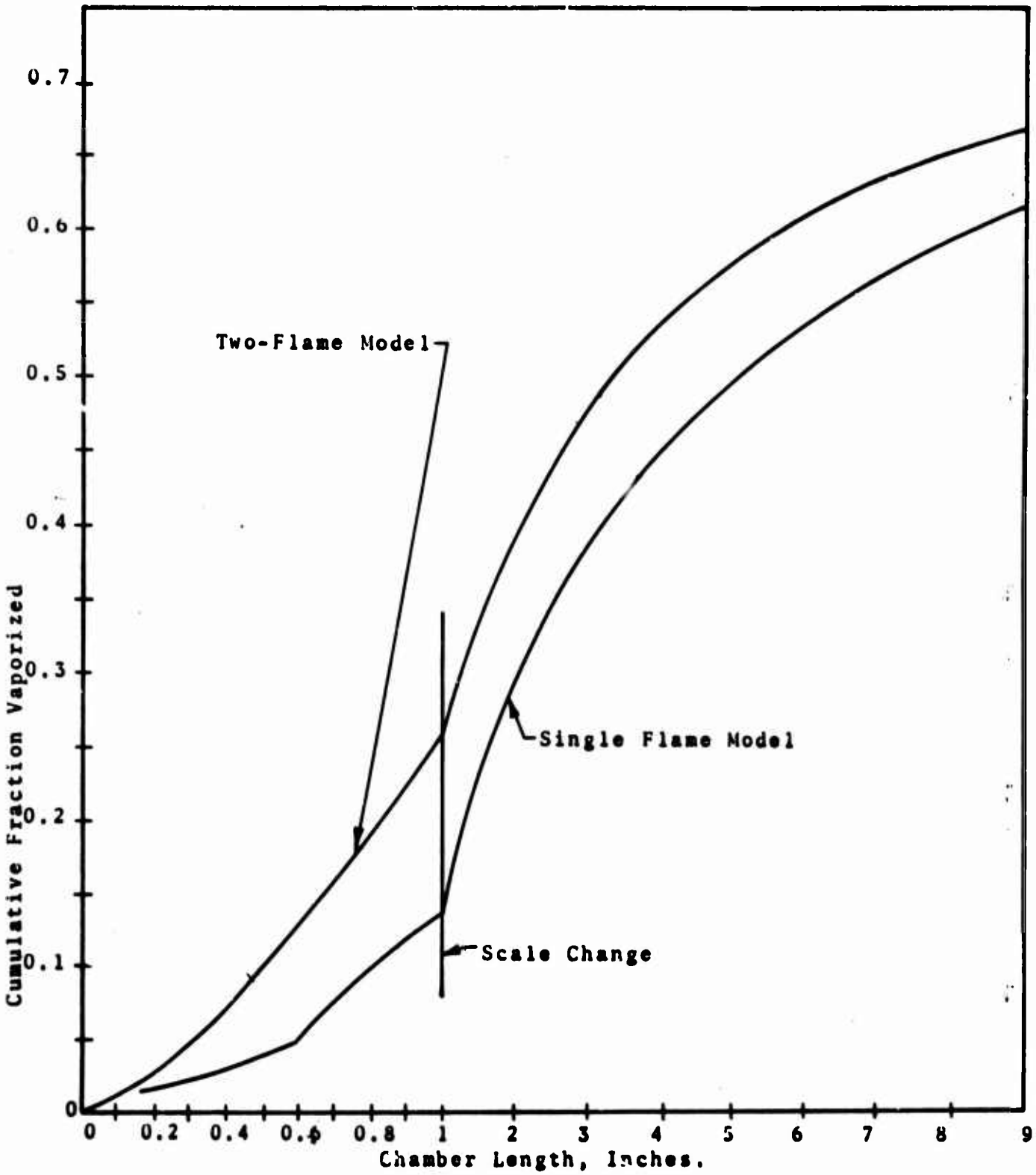

FIGURE 16. Fuel Fraction Vaporized, Mass Median Drop Size 75 μ

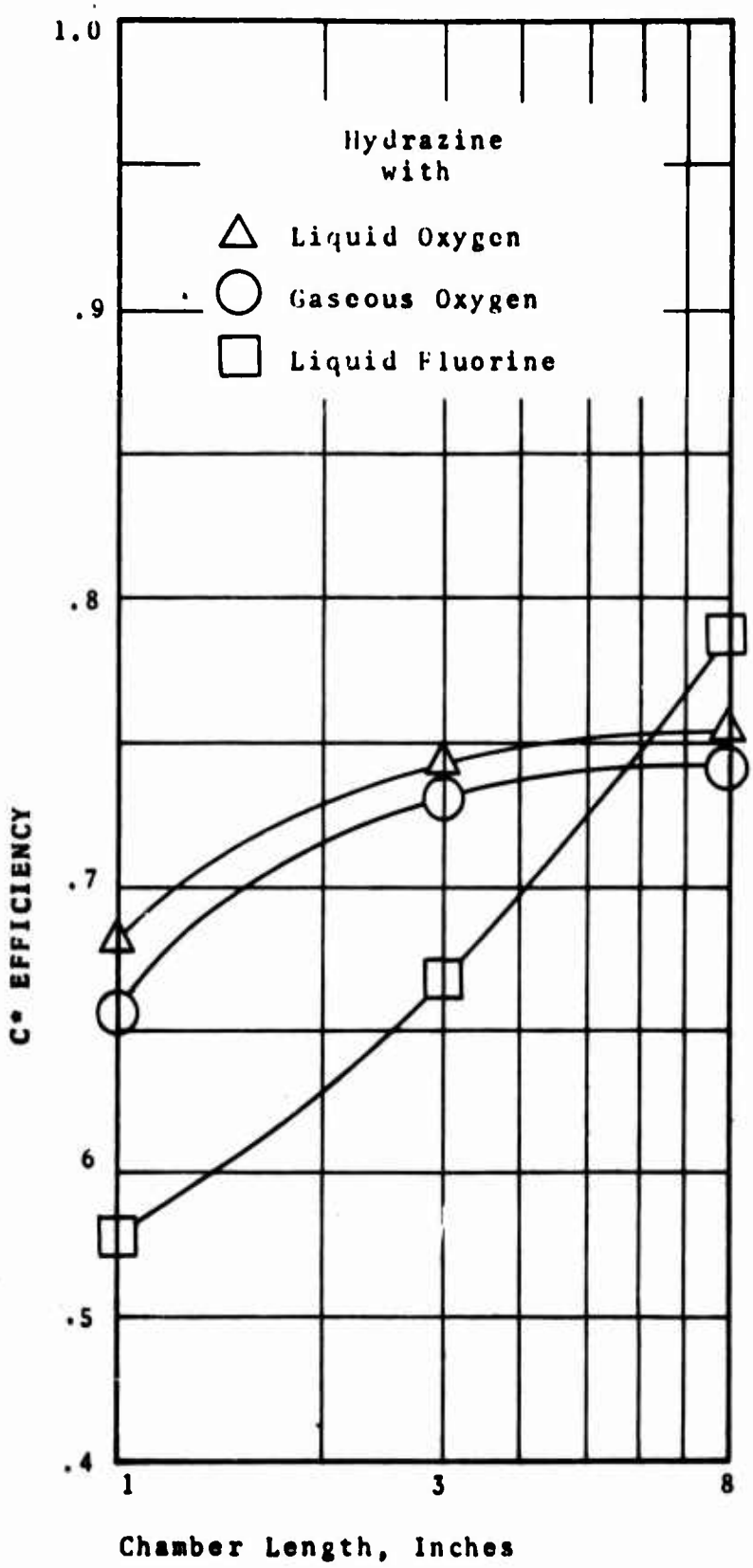

FIGURE 17. Experimental Performance of Hydrazine Propellant Combinations (Ref. 1).

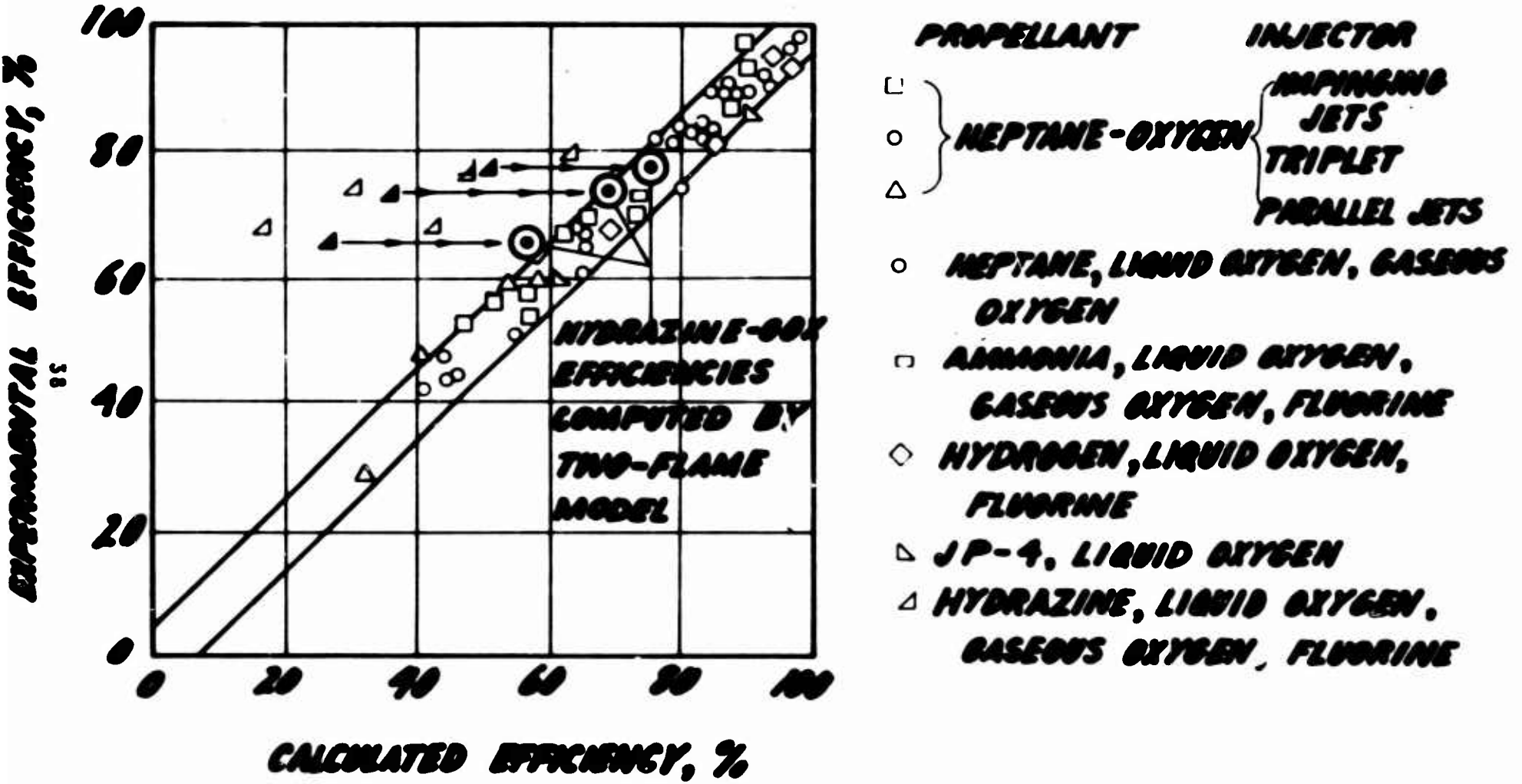

FIGURE 18. Comparison of Experimental and Calculated Efficiencies (Ref. 1) Showing Hydrazine Efficiencies computed by the two-flame model

The efficiencies computed, using the two-flame model, are in good agreement with the experimental efficiencies as shown in Figure 18.

The two-flame, vapor decomposition model of droplet combustion in hydrazine type fuel systems allows accurate prediction of the droplet history in a combustion chamber. This information is necessary for both efficiency and instability calculations. This model therefore, represents a significant advance in the state-of-the-art of analytical chamber design.

3. The Stability Drop Size

The model used for the analysis of stability treats droplets as if they were all of a single size. It is desirable to select a drop size which represents the vaporization properties of the spray distribution as accurately as possible.

The vaporization rate of a spray made up of a finite number of drop size groups (as used in the steady-state combustion model) is given by

$$\omega = \Sigma\, c_i \beta_i r_i \left(2 + k r_i^{1/2} \phi_i \delta_i\right) \qquad \text{(III-34)}$$

where

$$\beta_i = \frac{2\pi M_a D_i P}{R T_i} \ln \frac{P}{P - P_{a_i}} \qquad \text{(III-35)}$$

$$\phi_i = |u - v|^{1/2} \qquad \text{(III-36)}$$

$$\xi_i = (\rho_{mi}/\mu_{mi})^{1/2} \qquad \text{(III-37)}$$

$$K = .6\sqrt{2}\; S_c^{1/3} \qquad \text{(III-38)}$$

Combustion instability is related to changes in ω caused by disturbances in the state of the gas (p,T) and in the relative velocity term, ϕ. If we preserve $\omega, \frac{\partial\omega}{\partial\phi}, \frac{\partial\omega}{\partial p}$, and $\frac{\partial\omega}{\partial T}$ from a multigroup representation to a single-group model, the following equations are obtained:

Quantity Preserved	Equation	
ω	$c_s r_s \beta_s (2+kr_s^{1/2}\phi_s\xi_s) = \sum_i c_i r_i \beta_i (2+kr_i^{1/2}\phi_i\xi_i)$	(III-39)
$\frac{\partial\omega}{\partial\phi}$	$c_s r_s^{3/2}\beta_s\xi_s = \sum_i c_i r_i^{3/2}\beta_i\xi_i$	(III-40)
$\frac{\partial\omega}{\partial p}$	$c_s r_s [2\frac{\partial\beta}{\partial p} + k\, r_s^{1/2}\phi_s(\xi_s\frac{\partial\beta}{\partial p} + \beta_s\frac{\partial\xi}{\partial p})]$	
	$= \sum_i c_i r_i [2\frac{\partial\beta}{\partial p} + k\, r_i^{1/2}\phi_i(\xi_i\frac{\partial\beta}{\partial p} + \beta_i\frac{\partial\xi}{\partial p})]$	(III-41)
$\frac{\partial\omega}{\partial T}$	$c_s r_s [2\frac{\partial\beta}{\partial T} + k\, r_s^{1/2}\phi_s(\xi_s\frac{\partial\beta}{\partial T} + \beta_s\frac{\partial\xi}{\partial T})]$	
	$= \sum_i c_i r_i [2\frac{\partial\beta}{\partial T} + kr_i^{1/2}\phi_i(\xi_i\frac{\partial\beta}{\partial T} + \beta_i\frac{\partial\xi}{\partial T})]$	(III-42)

In equations (III-41 and 42) it has been assumed that the spray of only one propellant is controlling the stability and that β and ξ can be represented by functions which are linear in p and T so that the partial derivatives are constants determined from the propellant properties.

Partial solutions to equations (III-39 - 42) can be obtained under certain assumptions. If we assume that all ϕ are large, that $\frac{\partial\beta}{\partial p} = \frac{\partial\beta}{\partial T} = 0$ and, as a result, that all β_i are equal, we obtain

$$\phi_s = \frac{\sum c_i r_i^{3/2}\xi_i\phi_i}{\sum c_i r_i^{3/2}\xi_i} \qquad \text{(III-43)}$$

$$\xi_s = \frac{\sum c_i r_i^{3/2}\xi_i\phi_i}{\sum c_i r_i^{3/2}\phi_i} \qquad \text{(III-44)}$$

The assumptions made to arrive at equations (III-43 and 44) are equivalent to those made by Priem in his stability model (Ref. 4), namely that changes in vaporization rate are

attributed only to changes in the Nusselt number and that the Nusselt number is much larger than 2.

On the other hand, if interest is focused on regions of small velocity difference where stability criteria seem to be most critical, we seek a solution for small ϕ_i. The results are

$$\beta_s = \frac{\Sigma c_i r_i \beta_i}{\Sigma c_i r_i} \tag{III-45}$$

$$r_s^{1/2} \xi_s = \frac{\Sigma c_i r_i^{3/2} \beta_i \xi_i}{\Sigma c_i r_i \beta_i} \tag{III-46}$$

The quantity of ρ_m/ν_m is much less sensitive to drop temperature than β. If the ξ_i are considered to be nearly equal, equation (III-46) can reduce to

$$r_s^{1/2} = \frac{\Sigma c_i r_i^{3/2} \beta_i}{\Sigma c_i r_i \beta_i} \tag{III-47}$$

In the region between the injector and the point where drop velocity and gas velocity are equal, small drops are especially important for two reasons: 1) The absolute velocities of small drops are lower than those of larger drops, resulting in increased concentration, c, of small drops. 2) The small drops heat up faster and attain high vaporization rates due to high value of β which are quite sensitive to the large increases in vapor pressure which accompany the rise in drop temperature.

This analysis and results from the steady-state combustion program indicate that combustion instability may be governed by the properties of the smaller drops in a spray rather than by those of the drop of mass mean radius.

IV. COMBUSTION INSTABILITY MODEL

1. Introduction.

While there has been a great deal of research devoted to create linear models of the instability phenomena, little has been done on nonlinear models, in spite of the fact that combustion instability in liquid rocket engines is a nonlinear phenomena (Ref. 8 and 9). The fundamental conservation equations i.e., mass, momentum, energy, and state will result in a nonlinear model, by their very nature. Because of the complexity of the solution of these nonlinear partial differential equations, various authors, among them, Crocco (Ref. 14) and Priem (Ref. 1), have attempted to simplify them before solution with various assumptions. The conservation equations in their most general form consist of four independent variables (θ, r, z, t), making a closed-form solution impractical. With the advent of the high-speed digital computer and advanced numerical techniques, solving these equations becomes possible. However, solution with four independent variables is a paramount task and would exceed the practical cost of computer runs. Priem has solved these equations with two independent variables (θ,t) with simplifying assumptions. In this approach, functional dependencies are determined in every case from the basic equations for the phenomena, and simplifying assumptions are introduced that are considered reasonable in light of the combustion processes in a liquid rocket engine. The models advanced by Dynamic Science Corporation, Crocco and Priem utilize the same theory derived from the fundamental conservation equations, but with different assumptions.

Dynamic Science Corporation feels that combustion instability in liquid rocket engines is a nonlinear phenomena, in that: 1) stability depends on the disturbance; 2) there is a limiting amplitude of oscillations; and 3) the wave forms become steep fronted or nonsinuisoidal. In addition, the nonlinear model enables the combustion process to be described from the basic equations of the phenomena without the introduction of "empirical" or "intuitive" constants. Linear models cannot relate engine parameters to threshold disturbance. Either a linear system is stable or unstable regardless of the disturbance. Such linear models are derived from the nonlinear conservation equations by assuming that all variations are small. This assumption is necessary if a closed form solution is desired since mathematical techniques are not well developed for

solving simultaneous sets of nonlinear partial differential equations.

Dynamic Science Corporation model is based on the numerical solution of the conservation equations with mass-addition. The mass-addition or combustion rate is described by a quasi-steady-state expression for vaporization. This assumes that all the combustion processes, i.e., atomization, mixing, and kinetics are rapid compared to the vaporization process. The quasi-steady-state assumption implies that the droplet spray instantly responds to a change in the local environmental conditions.

2. Theory.

An annular section of a combustion chamber is chosen to predict the response of the spray to a disturbance. The use of an annular section is dictated by the limitations of present computers as to storage and speed in producing useful results. An annular section enables the variations of the dependent variables in the tangential direction. Such a model enables the description of a tangential disturbance propagated throughout the spray field. As shown in Figure 1 the annular section has a very small length Δz and thickness Δr. Physically this means that there are no gradients in the r and z direction in the annulus. It is assumed that the steady-state combustion is uniform around the annulus. However, the transient combustion rate is a function of the local environment and varies around the annulus. The assumption that steady-state properties are not a function of θ, implies that the propellants are injected uniformly, at the injector face, at that particular radius of injection. The annular model can be extended to injection profiles which are distributed across the injector face by use of the "nodal method" and a quasi two-dimensional steady-state model. While the annular model is one-dimensional, in order to describe the convective flow out of the annulus, the z derivatives are treated in a gross way by assuming that the dependent variables are constant through the annulus but the derivatives vary with time. The model does not treat the z direction in a purely two-dimensional manner since the z derivatives are lumped in the θ direction by an integration assuming mass, momentum, and energy is constant in the annulus as a function of time. The derivation of the transport or field equations is similar to the method of Priem-Guentert (Ref. 1) and will be repeated here for completeness of the nonlinear model.

The basic transport equations for two-phase flow have been developed by Bird, Stewart, and Lightfoot (Ref. 15):

Equation of Continuity

$$\frac{\partial \rho}{\partial t} = - \nabla \cdot \vec{\rho} v + \omega \qquad \text{(IV-1)}$$

Equation of Momentum

$$\frac{\partial}{\partial t} \rho \vec{v} = -\nabla \cdot \rho \vec{v}\vec{v} - \nabla \cdot \rho_l \vec{v}_l \vec{v}_l - g \nabla P - \nabla \cdot \tau \qquad \text{(IV-2)}$$

Equation of Energy

$$\frac{\partial}{\partial t} \left(\rho c_v T + \frac{1}{2gJ_H} \rho v^2\right) = - \nabla \cdot \rho \vec{v} \left(c_v T + \frac{1}{2gJ_H} v^2\right)$$

$$-\nabla \cdot \rho_l \vec{v}_l \left(U_l + \frac{1}{2gJ_H} v_l^2\right) - \nabla \cdot \vec{q}$$

$$- \frac{1}{J_H} \nabla \cdot P\vec{v} - \frac{1}{gJ_H} \nabla \cdot (\tau \cdot v) \qquad \text{(IV-3)}$$

After assuming the liquid velocity and temperature to be constant in the annulus and further manipulation of the equations IV-1, 2, 3, we obtain the transport equations for two phase flow with mass addition.

The conservation equations appear in the following form:

Continuity

$$\frac{\partial \rho}{\partial t} = - \nabla \cdot \rho \vec{v} + \omega \qquad \text{(IV-4)}$$

Momentum

$$\rho \frac{\partial \vec{v}}{\partial t} = - \rho (\vec{v} \cdot \nabla) \vec{v} - (\vec{v} - \vec{v}_l) \omega \quad g \nabla P - \nabla \cdot \tau \qquad \text{(IV-5)}$$

Energy

$$\rho c_v \frac{\partial T}{\partial t} = -\rho c_v (\vec{v} \cdot \nabla) T + \lambda \nabla^2 T - \frac{p}{J_H} \nabla \cdot \vec{v}$$

$$- \frac{1}{gJ_H} \tau : \nabla \vec{v} + \omega \left[U_l - c_v T + \frac{1}{2gJ_H} (\vec{v}_l - \vec{v}) \cdot (\vec{v}_l - \vec{v})\right]$$

(IV-6)

The above equations can be nondimensionalized by means of the following transforms:

$$t' = ta_o/r_{an} \tag{IV-7}$$

$$\nabla' = r_{an}\nabla \tag{IV-8}$$

$$\omega' = \omega/\omega_o \tag{IV-9}$$

$$\rho' = \rho/\rho_o \tag{IV-10}$$

$$P' = P/P_o \tag{IV-11}$$

$$\tau' = \tau r_{an}/\mu_o a_o \tag{IV-12}$$

$$T' = T/T_o \tag{IV-13}$$

$$v' = v/a_o \tag{IV-14}$$

Apply the transforms to the continuity equation

$$\frac{\partial(\rho'\rho_o)}{\partial\left(\frac{t' r_{an}}{a}\right)} = -\frac{\nabla'}{r_{an}} \cdot (\rho'\rho_o)(\vec{v}' \; a) + (\omega_o\omega') \tag{IV-15}$$

$$\left|\frac{\rho_o a}{r_{an}}\right| \frac{\partial\rho'}{\partial t'} = -\left|\frac{\rho_o a}{r_{an}}\right| \nabla' \cdot \rho' \vec{v}' + \omega_o \; (\omega') \tag{IV-16}$$

$$\frac{\partial\rho'}{\partial t'} = -\nabla' \cdot \rho'\vec{v}' + \left|\frac{r_{an}\omega_o}{\rho_o a}\right| \omega' \tag{IV-17}$$

After further manipulation the resulting equations are:

<u>Continuity</u>

$$\frac{\partial\rho'}{\partial t'} = -\nabla' \cdot \rho'\vec{v}' + \left|\frac{r_{an}\omega_o}{\rho_o a}\right|\omega' \tag{IV-18}$$

<u>Motion</u>

$$\rho' \frac{\partial\vec{v}'}{\partial t'} = -\rho'(\vec{v}' \cdot \nabla')\vec{v} - \left|\frac{g\bar{p}_c}{\rho_o a_o^2}\right|\nabla' p' - \left|\frac{\mu}{r_{an}\rho_o a_o}\right|\nabla' \cdot \tau'$$

$$- \left|\frac{r_{an}\omega_o}{\rho_o a_o}\right| (\vec{v}' - \vec{v}_i')\omega' \tag{IV-19}$$

Energy

$$\rho'\frac{\partial T'}{\partial t'} = -\rho'(v' \cdot \nabla')T' + \left|\frac{\lambda}{r_{an}\rho_o c_v a_o}\right| \nabla'^2 T' - \left|\frac{\bar{P}_c}{\rho_o c_v T_o J_H}\right|$$

$$P'\nabla' \cdot \vec{v}' - \left|\frac{a_o \mu}{r_{an}\rho_o c_v T_o g J}\right| \tau' : \nabla'\vec{v}' + \left|\frac{\omega_o r_{an}}{\rho_o a_o}\right| \omega' \left[\frac{U_i}{c_v T_o} - T' + \left(\frac{a_o^2}{2gJ_H c_v T_o}\right)(\vec{v}_i' - \vec{v}')^2\right] \qquad \text{(IV-20)}$$

By assuming that the gas is perfect and flow is one-dimensional and isentropic:

$$a_o^2 = g\frac{R}{M}\gamma T_o \qquad \text{(IV-21)}$$

$$\frac{c_v \mu}{\lambda} \cong 1 \qquad \text{(IV-22)}$$

$$\frac{c_p}{c_v} = \gamma \qquad \text{(IV-23)}$$

$$P = \rho\frac{R}{M}T \qquad \text{(IV-24)}$$

$$U_i \cong c_p T_o \qquad \text{(IV-25)}$$

$$c_v = \frac{R}{J_H M}\left(\frac{1}{\gamma - 1}\right) \qquad \text{(IV-26)}$$

$$\omega_o = m\frac{\dot{W}}{A_c} \qquad \text{(IV-27)}$$

$$A = \frac{A_c}{A_t} \qquad \text{(IV-28)}$$

$$C^* = \frac{\bar{P}_c A_t g}{\dot{W}} = \frac{1}{\gamma}\sqrt{\frac{g\,RT_o}{M\left(\frac{2}{\gamma+1}\right)^{\frac{\gamma+1}{\gamma-1}}}} \qquad \text{(IV-29)}$$

then equations IV-18, 19, and 20 can be reducted to

Continuity

$$\frac{\partial \rho'}{\partial t'} = - \Delta' \cdot \rho' \vec{v}' + \omega' \left| \frac{r_{an}\, o}{\rho_o\, a_o} \right| \qquad \text{(IV-30)}$$

Motion

$$\rho' \frac{\partial v'}{\partial t'} = \rho'(\vec{v}' \cdot \Delta')\vec{v}' - \frac{1}{\gamma}\Delta' P' - \left| \frac{\mu}{\rho_o r_{an} a_o} \right| \Delta' \cdot \tau'$$

$$-(\vec{v}' - \vec{v}'_1)\ \omega' \left| \frac{r_{an}\omega_o}{\rho_o\, a_o} \right| \qquad \text{(IV-31)}$$

Energy

$$\rho' \frac{\partial T'}{\partial t'} = - \rho'(v' \cdot \Delta')T + \Delta'^2 T \left| \frac{\mu}{\rho_o r_{an} a_o} \right| \ |\gamma - 1| P' \Delta' \cdot \vec{v}'$$

$$-|\gamma(\gamma-1)| \left| \frac{\mu}{\rho_o r_{an} a_o} \right| \tau' : (\Delta' \vec{v}') + \frac{r_{an}\omega_o}{\rho_o\, a_o}\ \omega$$

$$[\gamma - T' + \frac{(\gamma-1)\gamma}{2} (v'_1 - \vec{v}')^2] \qquad \text{(IV-32)}$$

Equations (IV-33) is similar to Damkohler's group based on the speed of sound. It can be thought of as the ratio of the wave time around the annulus at the speed of sound to the combustion time. L is defined by Priem as the burning rate parameter. Equation (IV-35) is similar to the reciprocal of a Reynolds number based on the speed of sound. J is defined as the viscous dissipation parameter and is a measure of the energy lost by viscous forces. By substitution of Equations (IV-33) and (IV-35) the following transport equations are obtained:

$$\frac{r_{an}\omega_o}{\rho_o a_o} = \frac{r_{an} m}{A} \sqrt{\frac{2}{\gamma+1}}^{\frac{\gamma+1}{\gamma-1}} = \frac{r_{an} m}{A}\ f(\gamma) \qquad \text{(IV-33)}$$

$$\frac{r_{an} m}{A} \equiv L \qquad \text{(IV-34)}$$

$$\frac{\mu}{\rho_o r_{an} a_o} = \frac{\mu C^*}{r_{an} P_c g} \sqrt{\frac{2}{\gamma+1}}^{\frac{\gamma+1}{\gamma-1}} = \frac{\mu C^*}{r_{an} P_c g} f(\gamma) \qquad \text{(IV-35)}$$

$$\frac{\mu C^*}{r_{an} P_c g} \equiv J \qquad \text{(IV-36)}$$

Continuity

$$\frac{\partial \rho'}{\partial t'} = -\nabla' \cdot \rho' \vec{v}' + \omega' L f(\gamma) \qquad \text{(IV-37)}$$

Motion

$$\rho' \frac{\partial \vec{v}'}{\partial t'} = -\rho'(\vec{v}' \cdot \nabla')\vec{v}' - \frac{1}{\gamma}\nabla' P' - J f(\gamma) \nabla' \cdot \tau'$$

$$- (\vec{v}' - \vec{v}'_{\iota})\omega' L f(\gamma) \qquad \text{(IV-38)}$$

Energy

$$\rho' \frac{\partial T'}{\partial t'} = -\rho'(\vec{v}' \cdot \nabla')T' + \nabla'^2 T J f(\gamma) - |\gamma - 1| P' \nabla' \cdot \vec{v}'$$

$$- |\gamma(\gamma-1)| J f(\gamma) \tau' : (\nabla' \vec{v}') + L f(\gamma) \omega' \left[\gamma - T' + \frac{(\gamma-1)\gamma}{2} (v'_{\iota} - \vec{v}')^2\right]$$

(IV-39)

Using the appropriate cylindrical coordinate transforms outlined in Bird, Stewart, and Lightfoot, (Ref. 15), equations (IV-37-39) can be simplified to describe an annular chamber section. If it is assumed that all dependent variables and derivatives of dependent variables in the radial direction are zero, that all axial dependent variables do not vary with angular position, and that all second derivatives in the axial direction are zero, the following transport equations result:

Continuity:

$$\frac{\partial \rho'}{\partial t'} = -\rho' \left(\frac{\partial v'_{\theta}}{\partial \theta'} + \frac{\partial v'_{z}}{\partial z'}\right) - v'_{\theta} \frac{\partial \rho'}{\partial \theta'} - v'_{z} \frac{\partial \rho'}{\partial z'} + \omega' L f(\gamma)$$

(IV-40)

Momentum (in the θ-direction):

$$\rho' \frac{\partial v'_{\theta}}{\partial t'} = -\rho v'_{\theta} \frac{\partial v'_{\theta}}{\partial \theta'} - \left|\frac{1}{\gamma}\right| \frac{\partial P'}{\partial \theta'} + J f(\gamma) \frac{4}{3} \frac{\partial^2 v'_{\theta}}{(\partial \theta')^2}$$

$$- v'_{\theta} \omega' L f(\gamma) \qquad \text{(IV-41)}$$

Momentum (in the axial or z-direction):

$$0 = -\rho' v'_z \frac{\partial v'_z}{\partial z'} - \left|\frac{1}{\gamma}\right| \frac{\partial P'}{\partial z'} - Lf(\gamma)\ (v'_z - v'_1)\omega' \qquad \text{(IV-42)}$$

Energy:

$$\rho' \frac{\partial T'}{\partial t'} = -\rho' \left(v'_\theta \frac{\partial T'}{\partial \theta'} + v'_z \frac{\partial T'}{\partial z'}\right) + Jf(\gamma) \frac{\partial^2 T'}{(\partial \theta')^2}$$

$$- |\gamma - 1|\ P' \left(\frac{\partial v'_\theta}{\partial \theta'} \quad \frac{\partial v'_z}{\partial z'}\right) \qquad \text{(IV-43)}$$

$$+ \frac{4}{3}|\gamma(\gamma-1)|\ J\left[\left(\frac{\partial v'_\theta}{\partial \theta'}\right)^2 \left(\frac{\partial v'_z}{\partial z'}\right)^2 - \frac{\partial v'_\theta}{\partial \theta'} \frac{\partial v'_z}{\partial z'}\right] f(\gamma)$$

$$+ Lf(\gamma)\ \omega' \left\{\gamma - T' + \frac{(\gamma-1)\gamma}{2} \left[(v'_1 - v'_z)^2 + v'^2_\theta\right]\right\}$$

To obtain the lumped derivatives of the axial dependent variable to account for convective flow through the annulus, it is assumed that conservation of mass, momentum, and energy must apply for the entire annular system as well as the incremental volumes described by equations (IV-41-43). Following the Priem-Guentert (Ref. 4) assumptions to determine the derivatives in the axial or z - direction the conservation equations are integrated through the entire volume of the annulus. Since it is assumed that none of the terms vary in the axial or radial direction, the equations only have to be integrated in the θ-direction. Further, if it is assumed that the total mass, momentum, and energy in the annulus does not vary with time. It is also assumed that all dependent variables are zero in the radial direction and constant across Δz. All axial derivatives do not vary with angular position and are thus lumped or averaged by the integration. Since the annulus is closed in the angular direction there can be no net loss or gain of mass, momentum, and energy in that direction. These assumptions result in the following integral equations for the axial derivatives:

Continuity:

$$0 = -\frac{\partial v'_z}{\partial z'}\int_0^{2\pi} \rho' \, d\theta' - 2\pi v'_z \frac{\partial \rho'}{\partial z'} + Lf(\gamma)\int_0^{2\pi} \omega' \, d\theta' \qquad \text{(IV-44)}$$

Momentum:

$$0 = -\frac{\partial v'_z}{\partial z'} v'_z \int_0^{2\pi} \rho' \, d\theta' - \frac{1}{\gamma}\left(\frac{\partial \rho'}{\partial z'}\int_0^{2\pi} T' \, d\theta' + \frac{\partial T'}{\partial z'}\int_0^{2\pi} \rho' \, d\theta'\right)$$

$$- Lf(\gamma)\,(v'_z - v'_1)\int_0^{2\pi} \omega' \, d\theta' \qquad \text{(IV-45)}$$

Energy:

$$0 = -\frac{\partial T'}{\partial z'} v'_z \int_0^{2\pi} \rho' \, d\theta' - (\gamma-1)\frac{\partial v'_z}{\partial z'}\int_0^{2\pi} P' \, d\theta' \qquad \text{(IV-46)}$$

$$+ \frac{8\pi}{3}|\gamma(\gamma-1)|\, Jf(\gamma)\left(\frac{\partial v'_z}{\partial z'}\right)^2$$

$$+ Lf(\gamma)\int_0^{2\pi} \omega'\left[\gamma - T' + (\gamma-1)\frac{\gamma}{2}(v_1 - v_z)^2\right] d\theta'$$

Ideal Gas:

$$2\pi \frac{\partial P'}{\partial z'} = \frac{\partial \rho'}{\partial z'}\int_0^{2\pi} T' \, d\theta' + \frac{\partial T'}{\partial z'}\int_0^{2\pi} \rho' \, d\theta' \qquad \text{(IV-47)}$$

To define the annular model an expression for the mass addition is required. In a liquid rocket engine four significant processes determine the mass addition or combustion rate: 1) atomization; 2) vaporization; 3) mixing; and 4) kinetics. It has been shown by many authors that for a well mixed chamber at typical pressures and temperatures encountered in a liquid rocket engine that atomization, mixing, and kinetics are much faster processes than vaporization. Thus it may be concluded that the combustion rate can be assumed to be controlled by vaporization. Further in a well mixed and atomized spray the combustion rate is controlled by droplet vaporization. Since high performance liquid rocket engine systems are

controlled by droplet vaporization, the instability model describes the response of a vaporizing droplet spray. With the above description of the droplet combustion model shown in Figure 19, a vaporization rate equation may be derived.

The vaporization rate equation may be derived analytically (Ref. 1) in terms

$$w = \frac{D\ M_\ell}{R\ \bar{T}}\ \bar{S}_d \left(\frac{1}{B} + \frac{1}{r}\right)\ \alpha\ P_a \qquad \text{(IV-48)}$$

However, the state-of-the-art does not allow for analytical calculation of the flow dependent film thickness, B. Thus, it is necessary to use the standard engineering driving force equation given by Sherwood and Pigford (Ref. 16):

$$w = (k4\pi r^2)\ (\alpha\ P_a) \qquad \text{(IV-49)}$$

Ranz and Marshall (Ref. 11) determined the mass transfer coefficient, k, for vaporizing drops, in terms of the Nusselt number for mass transfer, Nu_m:

$$k = \frac{Nu_m}{2r}\ \frac{D\ M_\ell}{R\ \bar{T}} \qquad \text{(IV-50)}$$

with the correlation

$$Nu_m = 2 + 0.6\ (Sc)^{1/3}(Re)^{1/2}. \qquad \text{(IV-51)}$$

Substituting equation (IV-50) into (IV-49) gives,

$$w = 2\pi r\ \frac{D\ M_\ell}{R\ \bar{T}}\ Nu_m\ \ \alpha P_a \qquad \text{(IV-52)}$$

The film thickness may be empirically determined from equations (IV-48 and 52) as

$$\frac{2r}{B} = Nu_m - 2 \qquad \text{(IV-53)}$$

Substitution of (IV-51) into (IV-52) for a concentration of drops, C_{dr} gives,

$$w = C_{dr} w = C_{dr} 2\ r\ \frac{D\ M_\ell}{R\ \bar{T}}\ \alpha P_a \left| 2 + 0.6 (Sc)^{1/3} (Re)^{1/2} \right| \qquad \text{(IV-54)}$$

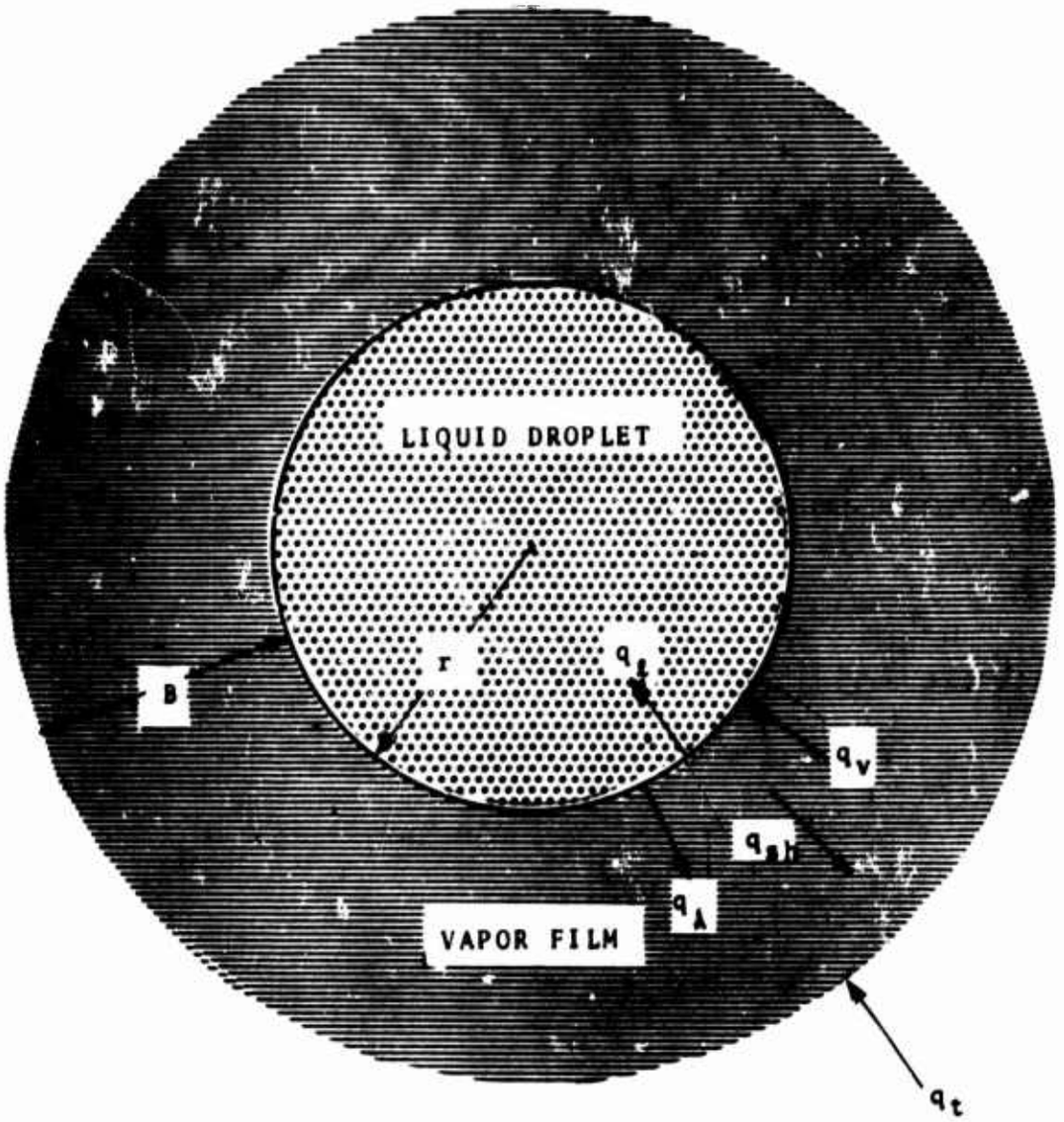

FIGURE 19. Schematic diagram of heat transfer to vapor film and liquid drop. (Reference 1)

This empirical expression shows the dependence of the vaporization rate upon physical properties and upon flow parameters.

Substituting for the Reynolds number, the vaporization rate equation takes the form:

$$\omega = \frac{C_{dr} D M_{\ell} \bar{S}_{d\alpha}}{R\bar{T} \quad 2r} \; P_a \left| 2 + 0.6 S_c^{1/2} \left(\frac{2r \, |\vec{v} - v_{\ell}| \rho}{\mu} \right)^{1/2} \right| \qquad \text{(IV-55)}$$

If the liquid temperature and vapor pressure do not vary with time, the following nondimensional vaporization rate is obtained:

$$\omega' = \frac{\omega}{\omega_o} = \frac{2 + 0.6 S_c^{1/3} (2r \, |\vec{v} - \vec{v}_{\ell}| \rho / \mu)^{1/2}}{2 + 0.6 S_c^{1/3} (2r \, |v_o - v_{\ell,o}| \rho_o / \mu_o)^{1/2}} \qquad \text{(IV-56)}$$

Equation (IV-56) may be written in terms of the Reynolds number of the drop based on the speed of sound (Re_d).

$$\omega' = \frac{2 + 0.6 S_c^{1/3} (\rho')^{1/2} \left| (v_{\theta}')^2 + (\Delta v')^2 \right|^{1/4} Re_d^{1/2}}{2 + 0.6 S_c^{1/3} (\Delta v')^{1/2} \; Re_d^{1/2}} \qquad \text{(IV-57)}$$

where

$$Re_d = \frac{2 r \rho_o a_o}{\mu_o} \qquad \text{(IV-58)}$$

Before the nonlinear partial differential equations can be numerically integrated, the boundary conditions must be defined. Since the response of the system is required, i.e., whether the system will amplify or attenuate, the conditions define an initial value problem. The boundary condition or initial value is analogous to the disturbance induced in a rocket engine. Presently, two types of disturbances are imposed. The first consists of an instaneous adiabatic pressure change at time $t' = 0$, given by

$$P' = 1 + A_p \, \mathrm{SIN}\theta' \qquad \text{(IV-59)}$$

$$T' = (1 + A_p \, \mathrm{SIN}\theta')^{(\gamma - 1)/\gamma} \qquad \text{(IV-60)}$$

$$\rho' = (1 + A_p \, \mathrm{SIN}\theta')^{(1/\gamma)} \qquad \text{(IV-61)}$$

$$v_{\theta}' = 0 \qquad \text{(IV-62)}$$

The second type of disturbance consists of an instantaneously imposed velocity component in the θ-direction.

$$v_\theta = A_v \text{ SIN}\theta \qquad \text{(IV-63)}$$

at constant pressure, temperature, and density.

The first type of disturbance is a pressure disturbance and corresponds to an ideal pulse gun disturbance. It should be noted that it is possible to introduce any wave shape desired. The second type of disturbance is a velocity change and corresponds to a standing or spinning transverse wave. Work done at Princeton (Ref. 17) shows that this type of field is produced by a real pulse gun disturbance as well as a pressure gradient. A third type disturbance which can be introduced in a vortex or a constant tangential velocity disturbance. This type of wave most closely represents a gas flow disturbance. This nonlinear model which relates instability to the disturbance character is very flexible and can be used to determine the effects of shape, amplitude and various combinations of pressure and velocity disturbances.

For times greater than t'=0, the pressure, the temperature, and the velocity at each position in the combustor or annulus are computed from Equations (IV-40) to (IV-47) and (IV-57). From these results, stability limits can be computed as shown in Figure 6.

The nonlinear differential equations are solved numerically using a marching technique. The computer program is outlined in Appendix II. This numerical technique involves solving for derivatives in the direction of march (time direction) in terms of the dependent variables (P', T', v', ρ') and their derivatives. Derivatives, with respect to other independent variables (θ), are obtained from values of the dependent variables by a finite-difference scheme. Using the computed derivatives in the t direction, values of the dependent variables may be computed for the incremented time. The process is repeated, and dependent variables are computed for successive values of time. Initial conditions are introduced in the form of a disturbance at time = 0. By analyzing the magnitude and rate of growth or decay, stability can be determined.

Stability limit curves can be computed as a function of the significant instability parameters Δv, L, and Re_d. Results of the calculation of the disturbance amplitude required to trigger instability show that the annulus is most stable

when Δv approaches infinity, Re_d approaches zero and L is less than 0.1 and greater than 5.0. Second order effects have been shown for the viscous-dissipation parameter, specific heat ratio and axial gas Mach number.

Work is presently in progress at Dynamic Science Corporation to include the effects of droplet damping and drift terms. Since the simplified model presented here requires the use of an instability drop average, development of a model based on polydispersed sprays and bipropellant droplet sprays is under development. As the models become more complicated simplified nondimensional groups become harder to use, since the number of family curves required become prohibitive. Work is in progress to integrate the steady-state model and the instability model directly so that stability zones for a given engine may be generated by computer.

APPENDIX I

Dynamic Science Corporation Steady-State Spray Combustion Model with Two Flame Fuel Burning for MMH-NTO System Program.

APPENDIX I

STEADY-STATE PROGRAM

1. Introduction.

A FORTRAN IV computer program has been written which integrates the solution of the simultaneous first order differential equations describing steady-state droplet vaporization with vapor phase decomposition. The equations involve simultaneous heat, mass, and momentum transfer coupled with varying gas dynamics. The equations are solved simultaneously at distance (x) increments along the axis of the chamber for each of a finite number of drop groups describing the spray distribution of the propellants. Paragraph 2 describes the required input data. Paragraph 3, describes the program logic, important variables, and numerical integration technique. A program listing is given in Paragraph 4 and the solution of a sample problem is shown in Paragraph 5.

2. Input Data.

The computer program as formulated is general in that any propellant combination whose burning can be described by the model can be analyzed providing that the thermodynamic properties are available. The input data to the program includes:

(a) Propellant thermodynamic and physical properties.

(b) Chamber geometry.

(c) Injection parameters.

Each of the above areas will be discussed separately. The propellant thermodynamic and physical propellants required are tabulated in Table I. These properties are input as function subprograms and are curve-fit to yield continuous values. Table I also shows the subprogram of the respective properties. The program listing shows the property subprograms as used in the analysis of the MMH-NTO propellant system.

Chamber geometry is input in two function subprograms A(x) and AP(x). Function A(x) describes the variation of chamber area with distance (x) while AP(x) specifies the derivative of the chamber area with respect to distance (x). These functions as shown in the listing are for a conical chamber configuration.

The injection parameters are input in card form. The

TABLE I. PROPELLANT PROPERTIES

NAME	SYMBOL	UNITS	SUBROUTINE
Liquid Density	ρ_ℓ	#/in^3	RHO
Liquid Specific Heat	C_{p_ℓ}	BTU/#-°F	CPL
Vapor Pressure	P_A	#/in^2	PVAP
Vapor Viscosity	μ_a	#/in-sec	VISCV
Vapor Specific Heat	C_{p_a}	BTU/#-°F	CVAP
Vapor Thermal Conductivity	k_a	BTU/sec-°F-In	FKA
Heat of Vaporization	λ	BTU/#	
PRODUCT PROPERTIES			
Adiabatic Flame Temperature	T_g	°R	TGINT
Viscosity, Thermal Cond. & Specific Heat	μ_g, k_g, C_{p_g}		VKSGAS
Diffusivity	D	In^2/sec	DIFFU

input variables and format with their respective units are represented in Figures 20 and 21. Specifying these parameters as card input easily permits parametric studies to be made for a particular propellant system and chamber configuration. Thus the effects of changing such conditions as initial drop temperature, injection velocity, O/F ratio, and droplet distribution may conveniently be determined.

3. Program Nomenclature.

The logical flow diagram of the steady-state program is shown in Figure 22. The FORTRAN variable names describing the important parameters of the model are shown in (Program Nomenclature). The equations solved at each calculation box of the flow diagram are described in Section III of the text.

The program uses a second order Runge-Kutta integration technique which is described below.

say, $\frac{dy}{dx} = f(x, y)$

and, $\frac{\Delta y}{2} = \frac{dy}{dx} \quad \frac{\Delta x}{2} - f\ (x_n, y_n).$

Then the slope of y(x) midway across the Δx increment (a) is approximated by

$$\left[\frac{dy}{dx}\right]_a = f(x + \frac{\Delta x}{2},\ y + \frac{\Delta y}{2})$$

this gives

$$(\Delta y)_a = \left[\frac{dy}{dx}\right]_a \quad \Delta x$$

and calculating y (x)

$$y_{n+1} = y_n + (\Delta y)_a$$

IBM

Form X28-7327-4
Printed in U.S.A.

FORTRAN CODING FORM

Program MMH		Punching Instructions	Page 1 of 2
Programmer	Date	Graphic / Punch	Card Form # *	Identification 73 80

C FOR COMMENT

STATEMENT NUMBER 1 5 | Cont. 6 | FORTRAN STATEMENT 7 10 15 20 25 30 35 40 45 50 55 60 65 70 72

CARD NUMBER ONE

---------- Title (Header) ----------

CARD NUMBER TWO

---------- Title (Header) ----------

CARD NUMBER THREE

Pressure(P) PSIA	$\dot{w}_o/\dot{w}_f$(RAT)	Specific Heat Ratio(GAM)
300.	1.50	1.20

CARD NUMBER FOUR

Initial Liquid Temp. (TL) IN °R	Injection Velocity (V) in In/Sec	Injection Flow Rate (EMDOT) in lb/sec	Mass Mean Drop Radius (RM) in In.	Standard Deviation (σ)	Molecular Weight (WTMOL)	No. of Drops Groups (NSET)	← Oxidizer
530.	1000.	18.	.003	2.3	82.	5	

CARD NUMBER FIVE

Initial Liquid Temp. (TL) IN °R	Injection Velocity (V) in In/Sec	Injection Flow Rate (EMDOT) lb/sec	Mass Mean Drop Radius (RM) in In.	Standard Deviation (σ)	Molecular Weight (WTMOL)	No. of Drops Groups (NSET)	← Fuel
530.	1000.	9.	.003	2.3	47.	5	

FIGURE 20

* A standard card form, IBM electro 888157, is available for punching source statements from this form.

IBM

FORTRAN CODING FORM

Program MMH

Programmer

Date

Punching Instructions

Graphic

Punch

Card Form #

C FOR COMMENT

STATEMENT NUMBER | Cont. | FORTRAN STATEMENT

CARD NUMBER SIX

O/F Min. Allowable (RATMN)	O/F Max. Allowable (RATMX)	Min.Chamber Area (AXMIN)	Max.Chamber Area (AXMAX)	Stoichiometric O/F
0.7	2.5	44.	123.	1.65

CARD NUMBER SEVEN*

Step Size (DX) in In.	Distance for Which (DX) will be used as step size (XT) in In.	Program Will Print Every (IP) Cycle	Program Will Plot Every (IPOT) Cycle
.015	1.00	2	2

*Note: Subsequent cards of this type will change step size and continue running of program to distance of X=XT. To terminate, follow last step size card with a blank.

FIGURE 21

* A standard card form, IBM electro 888157, is available for punching source statements from this fo

FLOW CHART FOR DYNAMIC SCIENCE CORPORATION
STEADY-STATE PROGRAM

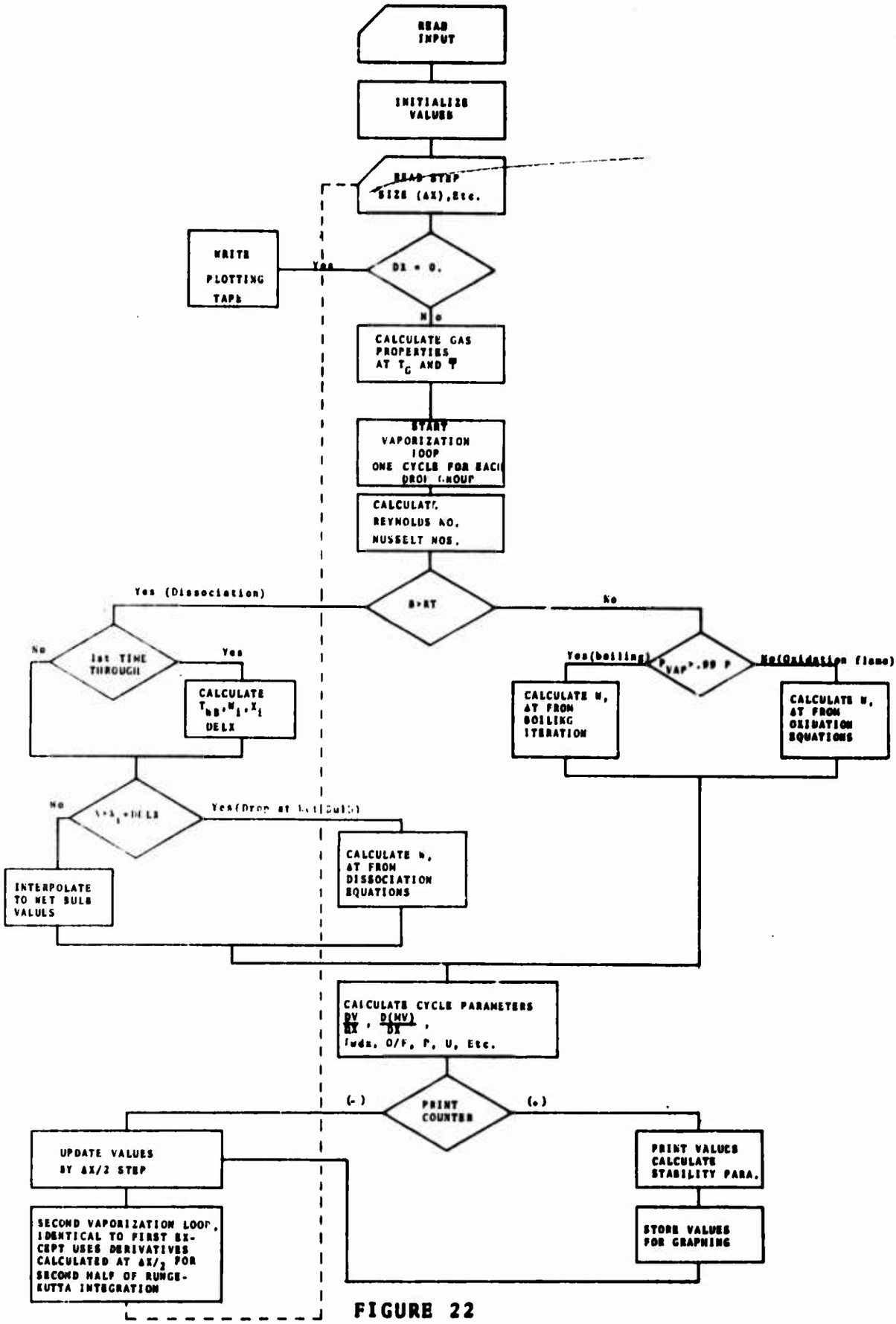

FIGURE 22

Program Nomenclature*

FORTRAN	SYMBOL	DESCRIPTION
ETA	A	nozzle contraction ratio
AX from Fcn A (X)	A_c	chamber cross-sectional area, function of x
AXMIN	A_t	area of throat
B	B	boundary layer film thickness
	C^*	characteristic exhaust velocity
CD(RE) from Fcn CD(RE)	C_d	drag coefficient
	C_p	heat capacity
Fcn CPL		-- of liquid
Fcn CVAP		-- of vapor
CPA from Fcn CVAP		-- of vapor at average mantle temperature
CPB from Fcn VKSGAS		-- of bulk products at average mantle temperature
CPG from Fcn VKSGAS		-- of bulk products at static temperature
CPAV		-- of mantle mixture
DFU from Sub DIFFU	D	molecular diffusion coefficient
	D_o	injector orifice diameter
	E	activation energy
	F	injected fuel fraction
FVAP2		local fuel fraction vaporized
G	g	acceleration of gravity
	I	momentum flux
XL from Fcn XK	K	evaporation rate constant
	k	thermal conductivity

*Fcn means function subprogram
Sub means subroutine

FORTRAN	SYMBOL	DESCRIPTION
FCN FKA		-- of vapor
		-- of vapor at average mantle temperature
FKB from Sub VKSGAS		-- of bulk products at average mantle temperature
FKG from Sub VKSGAS		-- of bulk products at static temp.
FKAV		-- of mantle mixture at av.temp.
	l	length
EM	m	mass of drop
RVAP	m	vaporization rate of spray (fraction/in.)
WTML from Sub WTMINT	M	molecular weight of vapor
WTMAV		-- of mantle mixture
WTMOL (input)		-- of propellant
DN	n	number of drops/sec. in each drop size group or reduc-duction velocity constant
FNUH	Nu_h	Nusselt number, heat transfer
FNUM	Nu_m	Nusselt number, mass transfer
	O	injected oxidizer fraction
FVAP1	θ	local oxidizer fraction vaporized
P	P	static bulk gas pressure
PA from Fcn PVAP	P_a	vapor pressure
PR	Pr	Prandtl number
SDSPD	a	speed of sound
	q_r	heat of reaction
	q_v	heat arriving at drop surface
RS	r	drop radius
	r_{mo}	$[\Sigma n\, r^m/\Sigma n]^{1/m}$ summation over all size groups when m = 2; area mean m = 3; volume mean

FORTRAN	SYMBOL	DESCRIPTION
RM	r_m	radius of mass median droplet
	r_{max}	maximum droplet diameter
RL from Fcn RT	r_t	distance from drop surface to decomposition flame
R	R	universal gas constant
	Re	drop Reynolds number
RE		-- bulk gas properties
REP		-- mantle properties
REN		-- based on speed of sound
SC	Sc	Schmidt number
	T	temperature
TG		--static gas
TL		--liquid
TBR		--mean mantle temperature
TSTG		--stagnation
TB from Fcn TBL	T_b	boiling point temperature
TWB	T_{wb}	wet bulb temperature
U	u	gas velocity
VD	V	u - v
ABSF of VD	ΔV	$\lvert u - v \rvert$
V	v	drop velocity
V(input)	v_j	liquid injection velocity
W	w	vaporization rate of single drop (lbm/sec)
EMDOT (input)	$\dot{W}$	flow rate (lbm/sec)
	X	defined by equations 27 & 28
X	x	axial position (x-0 at injector)
	z	defined by equation (correction factor for mass transfer)

FORTRAN	SYMBOL	DESCRIPTION
	α	defined by equation (6)
	β	reaction velocity constant
	ρ	density
RH from Fcn RHO		-- of liquid
RHOG		-- of bulk gas at static temp.
RHOAV		-- of mixture in mantle at average temperature
GAM	γ	ratio of specific heats of product gas
	η_{C^*}	efficiency based on characteristic velocity
Fcn ALM	λ	heat of vaporization
	μ	viscosity
VIS from Sub VKSGAS		-- of bulk products at static temperature
VISB		-- of bulk products at average mantle temperature
VISAV		-- of mantle mix.at aver.temp.
	ν	kinematic viscosity
	σ	surface tension
RAT	ϕ	mixture ratio, O/F

SUBSCRIPTS

a	vapor
c	combusted
d	droplet
f	fuel
g	product gas
j	at injector
ℓ	liquid
o	oxidizer or stagnation
p	particle
v	vaporized

4. Program Listing

```
      PROGRAM MMH
C     STEADY STATE SPRAY COMBUSTION MODEL -- TWO FLAME FULL BURNING
C     DYNAMIC SCIENCE CORPORATION
C    1900 WALKER AVENUE
C     MONROVIA,  CALIFORNIA
C     359 - 3251  (A.C. 213)
C     BREEN          KOSVIC
      COMMON OR
       DIMENSION AB(150), OR(150,90) , BCDX(7), BCDY(3)
       DIMENSION LOB(9)
C
C
      TYPE INTEGER BCDX,BCDY,BD1,BD2,BD3
      DIMENSION TITLE(39),TL(40),  V(40),  EMDOT(2),RM(2),SIG(2),Y(5),
     1          WTMOL(2),PR(2),SC(2),NSET(2),FA(2),DNT(2),FKM(2),FKH(3
     2          WCON(2)          ,RSS(20),EMS(20),EM(40), PE(2),
     3          RS(40),  DN(40),  DNS(20),ENMP(2),VD(40),EMINT(40),
     4          VDOUT(40),DV(40),DM(40),DT(40),BETA(40),SR(2),SR3(2),
     5          SVR(2),SVR32(2),SBVR(2),SBVR32(2),BRN(3),
     6          R10(2),R30(2),RV321(2),RBV321(2),RMEAN(6),RLN(12)
      EQUIVALENCE(RMEAN,R10),(RMEAN(3),R30),(RMEAN(5),RV321),
     1           (RMEAN(7),RBV321)
      DIMENSION KK(20),XENTR(20),WENTR(20),TWBINT(20),DELX(20),
     1  DUMITL(20),DUMTL(20)
      DIMENSION VD10(2),VD30(2),VD321(2),VDB321(2)
      DIMENSION WW(20)
      DIMENSION KDISC(40)
C
C
      DATA(R=18540.),(TWOPI=6.2831853),(G=386.4),(FTPI=4.1887902)
C           IN LBF/MOLE R                IN/SEC/SEC
    5 READ(5,10)(TITLE(I),I=1,39)
   10 FORMAT(13A6)
      IF(EOF,5)15,16
   15 STOP
   16 WRITE(6,20)(TITLE(I),I=1,39)
   20 FORMAT(45H1SN7002 STEADY-STATE SPRAY COMBUSTION MODEL  /(1H 13A6
      READ(5,30)P,RAT,GAM,       (TL(I),  V(I)  ,EMDOT(I),RM(I),SIG(I),
     1          WTMOL(I),              NSET(I),I=1,2)
   30 FORMAT(3F9.0/(6F9.0,I4))
      WRITE(6,40)(EMDOT(I),RM(I),SIG(I),WTMOL(I),              I=1,2)
   40 FORMAT(1H0
     1 8X     50H MASS FLOW    RM          SIG   MOLE WT                /
     12H O          F15.2,    E12.3,    2F7.2          /
     22H F          F15.2,    E12.3,    2F7.2          )
         READ (5,41)  RATMN,RATMX,AXMIN,AXMAX,OFSTOC
   41     FORMAT(5F10.5)
C
C
C     ----------------
      U=0.
      IBZ=0
      JZ = 1
      X=0.
      FA(1)=0.
      FA(2)=0.
      PHI=0.
      GAM1=GAM-1.
      GAM2=GAM1/2.
      GAM3=GAM2/GAM
      GAM4=GAM1/GAM
```

```
      GAM5 = GAM/GAM1
      EMD=EMDOT(1)+EMDOT(2)
      THRD=1./3.
      NP = 1
      KSW=1
C
C
      DO 100 I=1,2
      DNT(I)=0.
      WCON(I)=TWOPI*WTMOL(I)/R
      N=NSET(I)
      CALL LOGNRM(RM(I),SIG(I),N,RSS)
      CALL MASSET(EMS,RHO(TL( I ),I),RSS,EMDOT(I),N,DNS)
      NSET(I) = N+4
      N = NSET(I)
      DO 100 J=1,N
      K=J+J-2+I
      TL( K )=TL(I)
      V( K )=V(I)
      EM( K )=EMS(J)
      EMINT(K)  =  EM(K)
      RS( K )=RSS(J)
      DN( K )=DNS(J)
      DNT(I)=DNT(I)+DNS(J)
      KK(K)=1
      WW(K) = 0.
  100 CONTINUE
C
      DNTT=DNT(1)+DNT(2)
      XT=5.
      DX=6.
      RVAP = 0.20
      GO TO 106
C
C     ***** END INITIALIZATION - START CALCULATION
C
C     ******************************************************************
C     ******************************************************************
C
  104 IF(X+DX-XT)105,105,999
  105 IF(X-0.25)110,110,107
  106 READ(5,50)DX,XT,IP,IPLOT
   50 FORMAT(2F9.0 ,2I9)
      GO TO 108
  107 DX = XDEL(RVAP)
  108 DX2 = DX/2.
      IF (DX)999,999,110
  110 P2=P*2.
      P2R=P2/R
C
C     ***** OBTAIN STAGNATION TEMP,TSTG, AND THE DERIVATIVE OF TEMP
C     WITH RESPECT TO O/F, TGOD
         CALL TGINT (RAT,P,TSTG,TGOD)
C
C     ***** OBTAIN MOLECULAR WEIGHT OF PRODUCTS AS FUNCTION  O/F
         CALL WTMINT (RAT,P,WTML,WTMLDT)
C
      RG=R/WTML
      U2=U*U
C
C     ***** CALCULATE STATIC TEMP. FROM TOTAL TEMP. AND GAMMA
```

```
      TG=TSTG*(1.-GAM3*U2/RG/TSTG/G)
C
C
C     ***** CALCULATE GAS DENSITY
      RHOG=P/RG/TG
C
C
C     ***** CALCULATE VISCOSITY, THERMAL CONDUCTIVITY, AND SPECIFIC HE
C     OF GAS AS FUNCTION OF P, TG, O/F
         CALL VKSGAS (RAT,P,TG,VIS,FKG,CPG)
C
      RHOVS=RHOG/VIS*2.
      RHOTE=.375*RHOG
C
C
C     ***********************************************************************
C
C     ***** START DROP VAPORIZATION LOOP
C
  120 DO 200 I=1,2
      N=NSET(I)
      ENMP(I)=0.
C
      DO 200 J=1,N
      K=J+J-2+I
      KDISC(K) = 0
C
C     ***** TEST FOR ZERO MASS OF DROP - SKIP IF ZERO
      IF(EM(K))   200,200,130
  130 TBR=(TG+TL(K))/2.
         CALL VKSGAS (RAT,P,TBR,VISB,FKB,CPB)
C
C     ***** OBTIAN VAPORIZATION PRESSURE ,PA, AT LIQUID TEMP.,TL,
      PA=PVAP(TL(K),I)
      PA2P=PA/P2
      DPA2P=1.-PA2P
      CPA=CVAP(TBR,I)
      RH=RHO(TL(K),I)
         RV=WTMOL(I)*P/R/TL(K)
      VD(K)=U-V(K)
      RS(K)=(EM(K)/FTPI/RH)**THRD
C
C     ***** RE = REYNOLDS NUMBER OF DROP AT GAS PROPERTIES
      RE=    RS(K)*RHOVS*ABSF(VD(K))
C
         WTMAV = PA2P*WTMOL(I) + DPA2P*WTML
         VISAV = VISCV(TBR,I)*PA2P + DPA2P*VISB
         FKAV = PA2P*FKA(TBR,I) + DPA2P*FKB
         RHOAV = P*WTMAV/R/TBR
         CPAV = (PA2P*WTMOL(I)*CPA + DPA2P*WTML*CPB)/WTMAV
         REP= 2.*RS(K)*RHOAV*ABSF(VD(K))/VISAV
            PAIP = PA / 2.
         CALL DIFFU (RAT,P,TBR,PAIP,I,DFU)
         DPOT = DFU*P/TBR
         PR(I) = CPAV*VISAV/FKAV
         SC(I) = VISAV/RHOAV/DFU
         RTRE = SQRTF(REP)
         FNUM = 2. + 0.6 * SC(I)**THRD * RTRE
         FNUH = 2. + 0.6 * PR(I)**THRD * RTRE
C
C
```

```
C
C
C       -----------------
C       CHECK FOR ENTRANCE TO DISSOCIATION LOOP
        GO TO (149,160)I
  160 B= 2. *RS(K)/(FNUH-2.)
        IF DIVIDE CHECK 161,162
  161 B = 1.E30
  162 RL = RT(RS(K))
        IF (B-RL) 149,163,163
C       ENTER DISSOCIATION FLAME LOOP
  163 II =KK(K)
        KDISC(K) = 1
        GO TO (164,165),II
  164 KK(K)=2
C       CALCULATE AND STORE INITIAL QUANTITIES ON 1ST CYCLE
        IF(X) 601,601,600
  600 XENTR(K) = X
        WENTR(K) = WW(K)
        XL = XK(RS(K))
             W = XL * TWOPI * RS(K) * RHO(TL(K),I)
        ZZ =          W * CPA * RL / FKAV / 2. / TWOPI / RS(K) / RS(K)
        GO TO 602
  601 XENTR(K) = -.001
        XL = XK(RS(K))
         WENTR(K)=XL* TWOPI * RS(K) * RHO(TL(K),I)
        ZZ = WENTR(K) * CPA * RL / FKAV / 2. / TWOPI / RS(K) / RS(K)
  602 TWBINT(K) =  817.0
        DELX(K) = V(K)*EM(K)*CPL(TL(K),I)*(TWBINT(K)-TL(K))/
       1  TWOPI /RS(K) /RHO(TL(K),I) / 562. /XL
        DUMITL(K) =TL(K)
        DUMTL(K)= TL(K)
C       MAIN DISSOCIATION FLAME CALCULATION LOOP
  165 XL = XK(RS(K))
        W  = XL * TWOPI * RS(K) * RHO(TL(K),I)
        ZZ =          W * CPA * RL / FKAV / 2. / TWOPI / RS(K) / RS(K)
        TWB = 817.0
C       TEST FOR X GREATER THAN XENTR + LENGTH TO REACH WET BULB
        XTRA = XENTR(K) + DELX(K)
        IF ( X-XTRA)166,167,167
  166 CONTINUE
C       INTERPOLATE TO FIND WO AND TWB WHEN X L.TH. XENTR + DELX
        W  = WENTR(K) +(W -WENTR(K))/ DELX(K) *(X-XENTR(K))
        TWB = DUMITL(K)+(TWB-DUMITL(K))/DELX(K)*(X-XENTR(K))
        DT(K) =(TWB-DUMTL(K))/DX2
        DUMTL(K) = TWB
        DM(K) = -W /V(K)
C       BACK TO MAIN
        BETA(K) = W / RS(K) / FNUM
        GO TO 156
C       CALCULATIONS WHEN X GR.TH. XENTR + DELX
  167 DM(K) = -W /V(K)
        DT(K) = (TWB-DUMTL(K))/DX2
        DUMTL(K) = TWB
        BETA(K) = W / RS(K) / FNUM
        GO TO 156
C       -----------------
C
C
C
  149 PMDP=0.99*P
```

```
          IF(PA.GE.PMOP)  150,  155
  150   TB=TBL(P,I)
      WRITE(6,2000)
 2000 FORMAT(21HOSTATEMENT NUMBER 150)
      K1 = 0
        W1=-DM(K)*V(K)
       W1 = ABSF(W1)
         RRS=RV*RS(K)*RS(K)
C
         COE=FNUH*FKAV*RS(K)*TWOPI/CPA
      COE = ABSF(COE)
C
  152  W=COE*LOGF(1.+CPA*(TG-TB)/(ALM(TB,I)+8.78E-10*(W1/RRS)**2))
C
         WR=ABSF((W-W1)/W)
      K1 = K1 + 1
      IF(K1.GT.15)154,153
  153 W1 = (W + W1)/2.0
      IF(WR.LE.0.02)154,152
  154    DM(K)=-W/V(K)
         DT(K)=0.0
            TL(K)=TB
      BETA(K) = W / RS(K) / FNUM
         GO TO  156
  155    CONTINUE
C
C
         CALL COMP (RAT,P,Y)
      PE(1) = 0.0
      GO TO(3400,3410)KSW
 3400                 PE(1) = 0.0
 3410                 PE(2) = 0.0
         BETA(K) = WCON(I)*DPOT*LOGF((P-PE(I))/(P-PA))
C
      W=BETA(K)*RS(K)*FNUM
C
         IF(W)  190,  192,  192
  190      W = 0.
      WRITE(6,2050)
 2050 FORMAT(19HOW NEG. SET TO ZERO)
C
C
         DM(K)=0.
         DT(K)=TWOPI*FNUH*FKAV*(TG-TL(K))/EM(K)/CPL(TL(K),I)/V(K)*RS(K)
          GO TO 156
C
C      ----------------
C
  192 DM(K)=-W/V(K)
      Z=W*CPA/TWOPI/RS(K)/FNUH/FKAV
      EZ=EXPF(Z)-1.
      DIF=ALM(TL(K),I)-CPA*(TG-TL(K))/EZ+8.78E-10*(W/RV/RS(K)/RS(K))**2
      DT(K)=-DIF      /CPL(TL(K),I)/EM(K)*W/V(K)
C
      IF(DT(K)+100.)7711,156,156
 7711 DT(K) = -100.
C
C
C
  156    CONTINUE
      DV(K)=RHOTE*VD(K)*ABSF(VD(K))*CD(RE)/RH/V(K)/RS(K)
```

```
      ENMP(I)=ENMP(I)+DN(K)*DM(K)
      WW(K) = W
  200 CONTINUE
C     ***********************************************************
C
C
      RR = RG * TG
      SDSPD = SQRTF (RR * GAM * G)
      IF(U.GT.SDSPD)205,210
  205 XT=0.
      NP=0
  210 AX=A(X)
      PHIP = -(ENMP(1)+ENMP(2))
      PHI=FA(1)+FA(2)
      U = PHI/RHOG/AX
      EMACH=U/SDSPD
      EMACH2 = EMACH**2
      GO TO (230,220)KSW
  220   RATP = (FA(1)/FA(2)*ENMP(2)-ENMP(1))/FA(2)
        IF(RAT.GT.RATMN.AND.RAT.LT.RATMX)  224,  222
  222         RATP=0.
  224         CONTINUE
      GO TO 240
  230 KSW=2
      NP = IP
C
C
C     ***********************************************************
C
  240 IF(NP - IP)250,300,300
C
C     ***********************************************************
C
  250 CONTINUE
      NP=NP+1
      X=X+DX2
C
      DO 260 I=1,2
      FA(I)=EMDOT(I)
      N=NSET(I)
C
      DO 260 J=1,N
      K=J+J-2+I
      IF(EM(K)) 260,260,255
C
C     ----------------
  255 EM(K)=EM(K)+DX2*DM(K)
      FA(I)=FA(I)-DN(K)*EM(K)
      TL(K)=TL(K)+DX2*DT(K)
      V(K)=V(K)+DX2*DV(K)
C     ----------------
C
      IF(EM(K))180,180,260
  180 EM(K)=0.
      TL(K)=0.
      V(K)=0.
      RS(K)=0.
      VD(K)=0.
      DNT(I)=DNT(I)-DN(K)
      DN(K)=0.
  260 CONTINUE
```

```
C
      RAT=FA(I)/FA(2)
         IF(RAT.LT.RATMN)  261,  262
  261    RAT = RATMN
         GO TO   264
  262    CONTINUE
         IF(RAT.GT.RATMX)  263,  264
  263    RAT = RATMX
  264      CONTINUE
C
      P2=P*2.
      P2R=P2/R
         CALL TGINT (RAT,P,TSTG,IGOD)
         CALL WTMINT (RAT,P,WTML,WTMLDT)
C
      RG=R/WTML
      U2=U*U
      TG=TSTG*(1.-GAM3*U2/RG/TSTG/G)
      RHOG=P/RG/TG
C
         CALL VKSGAS (RAT,P,TG,VIS,FKG,CPG)
      RHOVS=RHOG/VIS*2.
      RHOTE=.375*RHOG
C
      SUMP=0
      SUMPA = 0.0
      SUMPB = 0.0
      WDSUM = 0.0
C
C     ***********************************************************************
 1120 DO1200 I=1,2
      N=NSET(I)
      ENMP(I)=0.
C
C     ----------------
      DO1200 J=1,N
      K=J+J-2+I
      KDISC(K) = 0
      IF(EM(K))1200,1200,1130
 1130 TBR=(TG+TL(K))/2.
         CALL VKSGAS (RAT,P,TBR,VISB,FKB,CPB)
      PA=PVAP(TL(K),I)
      PA2P=PA/P2
      DPA2P=1.-PA2P
      CPA=CVAP(TBR,I)
      RH=RHO(TL(K),I)
         RV=WTMOL(I)*P/R/TL(K)
      VD(K)=U-V(K)
      RS(K)=(EM(K)/FTPI/RH)**THRD
      RE=    RS(K)*RHOVS*ABSF(VD(K))
         WTMAV = PA2P*WTMOL(I) + DPA2P*WTML
         VISAV = VISCV(TBR,I)*PA2P + DPA2P*VISB
         FKAV = PA2P*FKA(TBR,I) + DPA2P*FKB
         RHOAV = P*WTMAV/R/TBR
         CPAV = (PA2P*WTMOL(I)*CPA + DPA2P*WTML*CPB)/WTMAV
         REP= 2.*RS(K)*RHOAV*ABSF(VD(K))/VISAV
            PAIP = PA / 2.
         CALL DIFFU (RAT,P,TBR,PAIP,I,DFU)
         DPOT = DFU*P/TBR
         PR(I) = CPAV*VISAV/FKAV
         SC(I) = VISAV/RHOAV/DFU
```

```
      RTRE = SQRTF(REP)
      FNUM = 2. + 0.6 * SC(I)**THRD * RTRE
      FNUH = 2. + 0.6 * PR(I)**THRD * RTRE
C
C
C     -----------------
C     CHECK FOR ENTRANCE TO DISSOCIATION LOOP
      GO TO (1149,1160)I
 1160 B= 2. *RS(K)/(FNUH-2.)
      IF DIVIDE CHECK 1161,1162
 1161 B = 1.E30
 1162 RL = RT(RS(K))
      IF (B-RL) 1149,1163,1163
C     ENTER DISSOCIATION FLAME LOOP
 1163 II =KK(K)
      KDISC(K) = 1
      GO TO (1164,1165)II
 1164 KK(K)=2
C     CALCULATE AND STORE INITIAL QUANTITIES ON 1ST CYCLE
      IF(X) 611,611,610
  610 XENTR(K) = X
      WENTR(K) = WW(K)
      XL = XK(RS(K))
            W = XL * TWOPI * RS(K) * RHO(TL(K),I)
      ZZ = WENTR(K) * CPA * RL / FKAV / 2. / TWOPI / RS(K) / RS(K)
      GO TO 612
  611 XENTR(K) = -.001
      XL = XK(RS(K))
       WENTR(K)=XL* TWOPI * RS(K) * RHO(TL(K),I)
      ZZ = WENTR(K) * CPA * RL / FKAV / 2. / TWOPI / RS(K) / RS(K)
  612 TWBINT(K) = 817.0
      DELX(K) = V(K)*EM(K)*CPL(TL(K),I)*(TWBINT(K)-TL(K))/
     1  TWOPI /RS(K) /RHO(TL(K),I) / 562. /XL
      DUMITL(K) =TL(K)
      DUMTL(K)= TL(K)
C     MAIN DISSOCIATION FLAME CALCULATION LOOP
 1165 XL = XK(RS(K))
      W  = XL * TWOPI * RS(K) * RHO(TL(K),I)
      ZZ =          W * CPA * RL / FKAV / 2. / TWOPI / RS(K) / RS(K)
      TWB = 817.0
C     TEST FOR X GREATER THAN XENTR + LENGTH TO REACH WET BULB
      XTRA = XENTR(K) + DELX(K)
      IF ( X-XTRA)1166,1167,1167
 1166 CONTINUE
C     INTERPOLATE TO FIND WB AND TWB WHEN X L.TH. XENTR + DELX
      W  = WENTR(K) +(W -WENTR(K))/ DELX(K) *(X-XENTR(K))
      TWB = DUMITL(K)+(TWB-DUMITL(K))/DELX(K)*(X-XENTR(K))
      DT(K) =(TWB-DUMTL(K))/DX2  -DT(K)/2.
      DUMTL(K) = TWB
      DM(K) = -W /V(K) - DM(K)/2.
      DMC = -W / V(K)
C     BACK TO MAIN
      BETA(K) = W / RS(K) / FNUM
      GO TO 1156
C     CALCULATIONS WHEN X GR.TH. XENTR + DELX
 1167 DM(K) = -W /V(K) -DM(K)/2.
      DMC = -W / V(K)
      DT(K) = (TWB-DUMTL(K))/DX2 -DT(K)/2.
      DUMTL(K) = TWB
      BETA(K) = W / RS(K) / FNUM
      GO TO 1156
```

```
C       ----------------
C
C
C
 1149 PMDP=0.99*P
          IF(PA.GE.PMDP) 1150, 1155
 1150   TB=TBL(P,I)
      KI = 0
        W1=-DM(K)*V(K)
       W1 = ABSF(W1)
        RRS=RV*RS(K)*RS(K)
        COE=FNUH*FKAV*RS(K)*TWOPI/CPA
      COE = ABSF(COE)
 1152  W=COE*LOGF(1.+CPA*(TG-TB)/(ALM(TB,I)+8.78E-10*(W1/RRS)**2))
        WR=ABSF((W-W1)/W)
      KI = KI + 1
      IF(KI.GT.15)1154,1153
 1153 W1 = (W + W1)/2.0
      IF(WR.LE.0.02)1154,1152
 1154 DMC = -W1 / V(K)
      DM(K)  = DMC  - DM(K)/2.
        DT(K)=0.0
           TL(K)=TB
      BETA(K) = W / RS(K) / FNUM
        GO TO 1156
C
 1155   CONTINUE
        CALL COMP (RAT,P,Y)
        PE(1) = Y(5) * P
        PE(2) = 0.
        BETA(K) = WCON(I)*DPOT*LOGF((P-PE(I))/(P-PA))
      W=BETA(K)*RS(K)*FNUM
        IF(W) 1190, 1192, 1192
 1190     W = 0.
        DM(K)=0.
      DMC = 0.0
        DT(K)=TWOPI*FNUH*FKAV*(TG-TL(K))/EM(K)/CPL(TL(K),I)/V(K)*RS(K)
        GO TO  1156
C
 1192 DMC  =-W/V(K)
      DM(K)=DMC-DM(K)/2.
      Z=W*CPA/TWOPI/RS(K)/FNUH/FKAV
      EZ=EXPF(Z)-1.
      DIF=ALM(TL(K),I)-CPA*(TG-TL(K))/EZ+8.78E-10*(W/RV/RS(K)/RS(K))**2
      DT(K)=-DIF      /CPL(TL(K),I)/EM(K)*W/V(K) -DT(K)/2.
C
      IF(DT(K)+100.)7712,1156,1156
 7712 DT(K) = - 100.
C
C     ***************************************************************
 1156   CONTINUE
      DVC  =RHOTE*VD(K)*ABSF(VD(K))*CD(RE)/RH/V(K)/RS(K)
      DV(K)=DVC-DV(K)/2.
C
      ENMP(I)=ENMP(I)+DN(K)*DMC
      SUMP = SUMP + DN(K) * DMC    * (V(K)-U) * DX
      SUMPA = SUMPA + DVC  *EM(K)*DN(K)*DX
      WW(K) = W
C
 1200 CONTINUE
C     ***************************************************************
```

```
C
      RR=RG*TG
      SDSPD=SQRTF(RR*GAM*G)
      IF(U.GT.SDSPD)1205,1210
 1205 XT=0.
      NP=0
 1210 AX=A(X)
      PHIP=-(ENMP(1)+ENMP(2))
      PHI=FA(1)+FA(2)
      U = PHI/RHOG/AX
      EMACH=U/SDSPD
      EMACH2 = EMACH**2
        RATP = (FA(1)/FA(2)*ENMP(2)-ENMP(1))/FA(2)
          IF(RAT.GT.RATMN.AND.RAT.LT.RATMX) 1224, 1222
 1222          RATP=0.
 1224          CONTINUE
C
      A1 = AX -AP(X) * DX
      A2 = AX
      A1DA2 = A1/A2
      P1 = U * ENMP * DX / (G*A2)
      P2 = -SUMP / (G*A2)
      P3 = -SUMPA / (G*A2)
      P4 =-RHOG * U**2 * (A1/A2 - 1.0) / G
C
      P = P + P1 + P2 + P3 + P4
C     -----------------
      IF(KKKKK-10)9891,9892,9892
 9891 KKKKK=KKKKK+1
      GO TO 9893
 9892 WRITE(6,8009)SUMP,SUMPA,P,P1,P2,P3,P4, RHOG,U,A1,A2,A1DA2
 8009 FORMAT(1H-,6F15.8/6F15.8)
      KKKKK = 0
 9893 CONTINUE
C
      X=X+DX2
C
      DO1260 I=1,2
      FA(I)=EMDOT(I)
      N=NSET(I)
      DO1260 J=1,N
      K=J+J-2+I
      IF(EM(K)) 1260,1260,1255
C
 1255 EM(K)=EM(K)+DX*DM(K)
      FA(I)=FA(I)-DN(K)*EM(K)
      TL(K)=TL(K)+DX*DT(K)
      V(K)=V(K)+DX*DV(K)
C
      IF(EM(K))1180,1180,1260
 1180 EM(K)=0.
      TL(K)=0.
      V(K)=0.
      RS(K)=0.
      VD(K)=0.
      DNT(I)=DNT(I)-DN(K)
      DN(K)=0.
 1260 CONTINUE
C
      RAT=FA(1)/FA(2)
         IF(RAT.LT.RATMN) 1261, 1262
```

```
1261    RAT = RATMN
        GO TO  1264
1262    CONTINUE
        IF(RAT.GT.RATMX) 1263, 1264
1263    RAT = RATMX
1264       CONTINUE
      GO TO 104
  300 NP = 0
C
C     ***********************************************************************
C     ***********************************************************************
C
      RAN = SQRTF(AX/3.14159)
      ETA = AX / AXMIN
      IF(RAT -OFSTOC)  31,31,32
   31 RCOMB = -ENMP(1) * (1./OFSTOC + 1.) / EMD
      FCOMB = FA(1) * (1. + 1./OFSTOC) / EMD
      GO TO 33
   32 RCOMB = -ENMP(2) * (OFSTOC + 1.) / EMD
      FCOMB = FA(2) * (1.+OFSTOC) / EMD
   33 RLCOMB = RCOMB * RAN / ETA
C     CALCULATE TOTAL PRESSURE
      PO = P*(TSTG/TG)**GAM5
      REC=RHOVS*SDSPD
      FVAP1=FA(1)/EMDOT(1)
      FVAP2=FA(2)/EMDOT(2)
      FVAP= PHI/EMD
      RVAP1=-ENMP(1)/EMDOT(1)
      RVAP2=-ENMP(2)/EMDOT(2)
      RVAP= PHIP/EMD
      DO 320 I=1,2
      SBVR(I)=0.
      SBVR32(I)=0.
      SVR(I)=0.
      SVR32(I)=0.
      SR(I)=0.
      SR3(I)=0.
      N=NSET(I)
      DO 320 J=1,N
      K=J+J-2+I
      IF(EM(K))320,320,310
  310 ENR=DN(K)*RS(K)
      SR(I)=SR(I)+ENR
      SR3(I)=SR3(I)+ENR*RS(K)*RS(K)
      ENVR=ENR/V(K)
      SVR(I)=SVR(I)+ENVR
      ENBVR=BETA(K)*ENVR
      SBVR(I)=SBVR(I)+ENBVR
      R12=SQRTF(RS(K))
      SVR32(I)=SVR32(I)+ENVR*R12
      SBVR32(I)=SBVR32(I)+ENBVR*R12
      VDOUT(K)=VD(K)/SDSPD
  320 CONTINUE
      IF(IBZ/IPLOT*IPLOT-IBZ)328,324,328
  324 AB(JZ) = X
      OR(JZ,1) = RAT
      OR(JZ,2) = FVAP2
      OR(JZ,3) = FVAP1
      OR(JZ,4) = FVAP
      OR(JZ,5) = RVAP2
      OR(JZ,6) = RVAP1
```

```
      OR(JZ,7) = RVAP
      OR(JZ,8) = EMACH
      OR(JZ,49) = U
       OR(JZ,80) = FCOMB
       OR(JZ,81) = RCOMB
      OR(JZ,18) = P
      OR(JZ,28) = PO
      OR(JZ,38) = TG
      OR(JZ,48) = TSTG
      JZ = JZ + 1
  328 IBZ = IBZ + 1
      WRITE(6,330)(TITLE(I),I=1,39)
  330 FORMAT(1H1/(1H 13A6))
      WRITE(6,340)X,U,TG,TSTG,P,PO,RAT,EMACH
  340 FORMAT(3H0X=F6.3,4H  U=F7.1,4H  T=F4.0,4H TO=F4.0,4H  P=F7.2,
     1        4H PO=F7.2,6H  O/F=F7.3,7H  MACH=F5.3)
      WRITE(6,350)FVAP1,FVAP2,FVAP
  350 FORMAT(26H VAPORIZED FRACTION       OF9.6,4H   FF9.6,7H   BOTHF9.6)
      WRITE(6,360)RVAP1,RVAP2,RVAP
  360 FORMAT(26H VAPORIZATION RATE/IN     OF9.6,4H   FF9.6,7H   BOTHF9.6)
      N=NSET(1)
      WRITE(6,370)
  370 FORMAT(70H0OXIDIZER DROPS   R(MIL)  MASS(LB)  V(IN/SEC) U-V/A  TEM
     1P     NUMBER          )
      DO 380 J=1,N
      K=J+J-1
      IF(EM(K))371,371,375
  371 RPD = 0.0
      VDOUT(K) = 0.0
      GO TO 377
  375 RPD = DM(K)/EMINT(K)
  377 FRACT = (EMINT(K) -EM(K)) /EMINT(K)
       MNM = J + 8
       OR(JZ-1,MNM) = RS(K)  * 1.E+3
      MZM = J + 28
      OR(JZ-1,MZM) = ABSF(VDOUT(K))
      MZN = J + 49
      OR(JZ-1,MZN) = V(K)
  380 WRITE(6,390)J,RS(K),EM(K),V(K),VDOUT(K),TL(K),DN(K) ,FRACT,RPD
  390 FORMAT(13X,I2,3PF9.4,0PE13.5 ,       F5.0,F9.4,F8.2,E11.3,4X,
     1  E11.3,4X,E11.3)
      WRITE(6,400)
  400 FORMAT(12H0FUEL DROPS    )
      N=NSET(2)
      DO 410 J=1,N
      K=J+J
      IF(EM(K))401,401,405
  401 RPD = 0.0
      VDOUT(K) = 0.0
      GO TO 407
  405 RPD = DM(K)/EMINT(K)
  407 FRACT = (EMINT(K) -EM(K)) /EMINT(K)
      MNM = J+18
      OR(JZ-1,MNM) = RS(K) * 1.E+3
      MZM = J + 38
      OR(JZ-1,MZM) = ABSF(VDOUT(K))
      MZN = J +  59
      OR(JZ-1,MZN) = V(K)
  410 WRITE(6,391)J,RS(K),EM(K),V(K),VDOUT(K),TL(K),DN(K) ,FRACT,RPD,
     1KDISC(K)
  391 FORMAT(13X,I2,3PF9.4,0PE13.5 ,       F5.0,F9.4,F8.2,E11.3,4X,
```

```
     1  E11.3,4X,E11.3,I15)
        DO 430 I=1,2
        R10(I)=SR(I)/DNT(I)
        R30(I)=(SR3(I)/DNT(I))**THRD
        RV321(I)=(SVR32(I)/SVR(I))**2
        RBV321(I)=(SBVR32(I)/SBVR(I))**2
  430   CONTINUE
        CALL TERP (R10,RS,VDOUT,NSET,VD10)
        CALL TERP (R30,RS,VDOUT,NSET,VD30)
        CALL TERP (RV321,RS,VDOUT,NSET,VD321)
        CALL TERP (RBV321,RS,VDOUT,NSET,VDB321)
        RT10 = (SR(1) + SR(2)) / (DNT(1) + DNT(2))
        RT30 = ((SR3(1) + SR3(2)) / (DNT(1) + DNT(2)))**THRD
        RTV321 = (RV321(1) + RV321(2)) / 2.
        RTBV321 = (RBV321(1) + RBV321(2)) / 2.
        VDT30 = (VD30(1)*R30(1)  +  VD30(2)*R30(2)) / (R30(1) + R30(2))
        VDT10 = (VD10(1)*R10(1)  +  VD10(2)*R10(2)) / (R10(1) + R10(2))
        VDT321 = (VD321(1)*RV321(1)  +  VD321(2)*RV321(2)) / (RV321(1) +
     1  RV321(2))
        VDTB321 = (VDB321(1)*RBV321(1) + VDB321(2)*RBV321(2)) /
     1 (RBV321(1) + RBV321(2))
        DO403I=1,2
        REN(I) = R10(I) * REC
        REN(I+2) = R30(I) * REC
        REN(I+4) = RV321(I) * REC
        REN(I+6) = RBV321(I) * REC
  403   CONTINUE
        REN(9) = RT10 * REC
        REN(10) = RT30 * REC
        REN(11) = RTV321 * REC
        REN(12) = RTBV321 * REC
        BD3 =  8HTOTAL
        BD2 = 8HFUEL
        BD1 = 8HOXIDIZER
        BRN(1) = RVAP1 * RAN / ETA
        BRN(2) = RVAP2 * RAN / ETA
        BRN(3) = RVAP * RAN / ETA
        OR(JZ-1,82) = REN(7)
        OR(JZ-1,83) = REN(8)
        OR(JZ-1,84) = REN(12)
        OR(JZ-1,85) = RLCOMB
        OR(JZ-1,86) = BRN(3)
        OR(JZ-1,87) = ABSF(VDB321(2))
        OR(JZ-1,88) = ABSF(VDB321(1))
        OR(JZ-1,89) = ABSF(VDTB321)
        IF(JZ-150)7375,7375,999
 7375   WRITE(6,420)
        WRITE (6,430)BD1,R10(1),VD10(1),REN(1),R30(1),VD30(1),REN(3),
     1 RV321(1),VD321(1),REN(5),RBV321(1),VDB321(1),REN(7)
        WRITE(6,430)BD2,R10(2),VD10(2),REN(2),R30(2),VD30(2),REN(4),
     1 RV321(2),VD321(2),REN(6),RBV321(2),VDB321(2),REN(8)
        WRITE(6,430) BD3,RT10,VDT10,REN(9),RT30,VDT30,REN(10),RTV321,
     1 VDT321,REN(11),RTBV321,VDTB321,REN(12)
  420   FORMAT(1H0,15X,6HR(MIL) ,7X,4HDELV ,8X,3HRED  )
  430   FORMAT(1H0,A8/(14X,3PF8.4,0PF12.4,0PF12.4/))
        WRITE(6,440)(BRN(I),I=1,3)
  440   FORMAT(1H0,13X,23HBURNING RATE PARAMETERS  /14X-8HOXIDIZER  ,
     1 F11.2,4HFUEL  , F11.2,5HTOTAL ,F11.2)
        WRITE (6,441) RCOMB,RLCOMB,FCOMB
  441   FORMAT(1H0,16HCOMBUSTION RATE ,F9.6,5X,16HCOMB. PARAMETER ,F5.2,
     1 5X,14HFRACTION COMB. ,F9.6)
```

```
      WRITE(6,55)DX,GAM
   55 FORMAT(18HOINTEGRATION STEP=F7.4,5H INCH5X6HGAMMA=F5.3)
      GO TO 250
  999 BCDY(1) = 8HO/F RATI
       JZ = JZ-1
       KZ = AB(JZ) + 2.0
       UPA = KZ
      XUU = UPA
       UPAM = UPA - 1.0
       DO 990 I = 1,JZ
       K = I
       IF(AB(K) - 1.0) 990, 990, 991
  990   CONTINUE
       K = K + 1
  991  M = K - 1
       DO 993 I = 1,M
  993   AB(I) = AB(I)*3.5 + 1.0
       IF(JZ - K) 996, 996, 994
  994    DO 995 I = K , JZ
  995  AB(I) = (AB(I)-1.0)/UPAM*3.5 + 4.5
  996   BCDY(2) = 8HO OF COM
      BCDY(3) = 8HB. GASES
       BCDX(1) = 8HDISTANCE
       BCDX(2) = 8H IN INCH
       BCDX(3) = 8HES
      ID = RATMX
      UO = ID + 1
       CALL GRAPH(AB,OR(1,1),XUU,UO ,BCDX,BCDY,JZ,1)
      BCDY(1) = 8HFRACTION
      BCDY(2) = 8H VAPORIZ
      BCDY(3) = 8HED
       BCDX(4) = 8H FUEL
       BCDX(5) = 8HOXIDIZER
       BCDX(6) = 8H TOTAL
      BCDX(7) = 8HCOMBUST
       CALL GRAPH(AB, OR(1,2),-XUU,-1.0, BCDX, BCDY, JZ, 1)
       CALL GRAPH(AB, OR(1,3),-XUU,-1.0, BCDX, BCDY, JZ,-2)
      CALL GRAPH(AB,OR(1, 4),-XUU,-1.0,BCDX,BCDY, JZ, -3)
      CALL GRAPH(AB,OR(1,80),+XUU,-1.0,BCDX,BCDY, JZ, -4)
       BCDY(1) = 8HVAPORIZA
       BCDY(2) = 8HTION RAT
       BCDY(3) = 8HE
       UO = 0.0
       DO 831 I = 1, JZ
  831   UO = MAX1(UO, OR(I,5), OR(I,6), OR(I,7))
       UO = UO + 1.0
       CALL GRAPH(AB, OR(1,5),-XUU,-UO , BCDX, BCDY, JZ,+1)
       CALL GRAPH(AB, OR(1,6),-XUU,-UO , BCDX, BCDY, JZ,-2)
      CALL GRAPH(AB,OR(1, 7),-XUU,-UO ,BCDX,BCDY, JZ, -3)
      CALL GRAPH(AB,OR(1,81),+XUU,-UO ,BCDX,BCDY, JZ, -4)
       BCDY(1) = 8HGAS MACH
       BCDY(2) = 8H NUMBER
       BCDY(3) = 8H
       CALL GRAPH(AB, OR(1,8), XUU, 1.0, BCDX, BCDY, JZ, 1)
       BCDY(1) = 8HOXIDIZER
       BCDY(2) = 8H DROP RA
       BCDY(3) = 8HD (MILS)
       UO = 0.0
        KZ = NSET(1) + 8
       DO 1000 I = 1,JZ
 1000  UO = MAX1F(UO,OR(I,KZ))
```

```
      DO 1015 I = 1,JZ
 1015 OR(I,90) = OR(I,49)
      MZN=UO
      UO = MZN+1
        NMN = NSET(1) - 2
      CALL GRAPH(AB,OR(1, 91),-XUU,UO   ,BCDX,BCDY,JZ,+1)
         DO 1020 I = 1, NMN
       NZ = I + 9
 1020 CALL GRAPH(AB,OR(1,NZ),-XUU,UO   ,BCDX,BCDY,JZ,-2)
      CALL GRAPH(AB,OR(1,KZ),+XUU,UO   ,BCDX,BCDY,JZ,-3)
      BCDY(1) = 8H FUEL DR
      BCDY(2) = 8HOP RAD (
      BCDY(3) = 8HMILS)
       UO = 0.0
       KZ = NSET(2) + 18
       DO 1050 I = 1,JZ
 1050  UO = MAX1F(UO,OR(I,KZ))
      MZN=UO
      UO = MZN+1
       NMN = NSET(2) - 2
      CALL GRAPH(AB,OR(1,19),-XUU,UO   ,BCDX,BCDY,JZ,+1)
       DO 1070  I = 1, NMN
       NZ = I + 19
 1070 CALL GRAPH(AB,OR(I,NZ),-XUU,UO   ,BCDX,BCDY,JZ,-2)
      CALL GRAPH(AB,OR(1,KZ),+XUU,UO   ,BCDX,BCDY,JZ,-3)
       NMN = NSET(1)
      BCDY(1) = 8HOXIDIZER
      BCDY(2) = 8H REL. MA
      BCDY(3) = 8HCH NO.
       NM1 = NSET(1) - 2
       KZ = NSET(1) + 28
        UO = 0.0
      DO 1075 I = 1, JZ
 1075   UO = MAX1 (UO, 100.*OR(I,KZ))
       UO = (UO + 2.0)/100.
      CALL GRAPH(AB,OR(1,29),-XUU,UO,BCDX,BCDY,JZ, 1)
       DO 1080  I = 1, NM1
       NZ = I + 29
 1080  CALL GRAPH(AB, OR(1,NZ),-XUU,UO,BCDX,BCDY,JZ, -2)
      CALL GRAPH(AB, OR(1,KZ), XUU,UO,BCDX,BCDY,JZ, -3)
       BCDY(1) = 8H  FUEL
       NM2 = NSET(2) -2
       KZ2 = NSET(2) + 38
       UO = 0.0
       DO 1085 I = 1, JZ
 1085   UO =  MAX1(UO, 100.*OR(I,KZ2))
       UO = (UO + 2.0)/100.
       CALL GRAPH(AB, OR(1,39),-XUU,UO, BCDX,BCDY,JZ, 1)
       DO 1086 I = 1,NM2
       NZ = I + 39
 1086  CALL GRAPH(AB,OR(1,NZ),-XUU,UO,BCDX,BCDY,JZ,-2)
       CALL GRAPH(AB,OR(1,KZ2),XUU,UO,BCDX,BCDY,JZ,-3)
        KZ = NSET(1) + 49
      BCDY(1) = 8HOXIDIZER
      BCDY(2) = 8H DROP VE
      BCDY(3) = 8HL IN/SEC
      BCDX(4) = 8H GAS VEL
       DO 677 I = 1, 9
       KK = I + 49
            DO 676 J = 1,JZ
       K = J
```

```
          IF(OR(J,KK)) 676, 677, 676
  676  CONTINUE
       K = K + 1
  677   LOB(I) = K - I
       UO = 0.0
       DO 1088 I = 1,JZ
 1088  UO = MAX1F(UO,OR(I,49))
       NZZ = UO/1000. + 1.0
       UO = NZZ * 1000
        MNM = NSET(I) - I
       CALL GRAPH(AB,OR(1,49),-XUU,-UO,BCDX,BCDY,JZ, 1)
       DO 1089  I = 1,MNM
       NZ = I + 49
          KK = LOB(I)
 1089  CALL GRAPH(AB,OR(1,NZ),-XUU,UO,BCDX,BCDY,KK, -2)
       KK = LOB(9)
       CALL GRAPH(AB,OR(1,KZ),XUU,UO,BCDX,BCDY,KK, -3)
       BCDY(1) = 8H  FUEL
       DO 687 I = 1, 9
       KK = I + 59
          DO 686 J = 1,JZ
       K = J
          IF(OR(J,KK)) 686, 687, 686
  686  CONTINUE
       K = K + 1
  687   LOB(I) = K - I
       NMN = NSET(2) -1
       KZ = NSET(2) +  59
       CALL GRAPH(AB,OR(1,90),-XUU,-UO,BCDX, BCDY,JZ, 1)
       DO 1091 I = 1,NMN
       NZ = I +  59
          KK = LOB(I)
 1091  CALL GRAPH(AB,OR(1,NZ),-XUU, UO,BCDX,BCDY,KK,-2)
       KK = LOB(9)
       CALL GRAPH(AB,OR(1,KZ),XUU,UO, BCDX,BCDY,KK, -3)
       BCDY(1) = 8H DROP RE
       BCDY(2) = 8HYNOLDS N
       BCDY(3) = 8HUMBER
          BCDX(4)  = 8HOXIDIZER
          BCDX(5)  = 8H  FUEL
       UO = 0.0
       DO 1110 I = 1,JZ
 1110  UO = MAX1(UO,OR(I,82),OR(I,83),OR(I,84))
       IF(UO - 1000.) 656, 656, 657
  656    UO = 1000.
       GO TO 658
  657  NZZ = UO/1000.
       UO = (NZZ + 1)*1000
  658  CALL GRAPH (AB,OR(1,82),-XUU,-UO,BCDX,BCDY,JZ, 1)
       CALL GRAPH (AB,OR(1,83),-XUU,-UO,BCDX,BCDY,JZ,-2)
       CALL GRAPH (AB,OR(1,84),+XUU,-UO,BCDX,BCDY,JZ,-3)
       BCDY(1) = 8HBURNING
       BCDY(2) = 8HRATE PAR
       BCDY(3) = 8HAMETER
        BCDX(4) = 8HCOMBUST
        BCDX(5) = 8HTOTAL
       UO = 0.0
       DO 1121 I = 1,JZ
 1121    UO = MAX1 (UO,10.*OR(I,85), 10.*OR(I,86))
       IF(UO - 10.) 821, 822, 822
  821  UO = (UO + 1.0)/10.
```

```
      GO TO 824
822   UO = (UO + 10.)/10.
824  CALL GRAPH(AB, OR(1,85), -XUU, -UO, BCDX, BCDY, JZ, 1)
     CALL GRAPH (AB,OR(1,86),+XUU,-UO,BCDX,BCDY,JZ,-2)
     BCDY(1) = 8HSTABILIT
     BCDY(2) = 8HY DROP D
     BCDY(3) = 8HELTA V
     BCDX(4) = 8H FUEL
     BCDX(5) = 8HOXIDIZER
      UO = 0.0
     DO 1131 I = 1,JZ
1131   UO = MAX1 (UO,100.*OR(I,87),100.*OR(I,88),100.*OR(I,89))
      UO = (UO + 2.0)/100.
     CALL GRAPH (AB,OR(1,87),-XUU,-UO,BCDX,BCDY,JZ, 1)
     CALL GRAPH (AB,OR(1,88),-XUU,-UO,BCDX,BCDY,JZ,-2)
     CALL GRAPH (AB,OR(1,89),+XUU,-UO,BCDX,BCDY,JZ,-3)
     BCDY(1) = 8HCHAMBER
     BCDY(2) = 8HPRESSURE
     BCDY(3) = 8H
     BCDX(4) = 8HSTAT PR.
     BCDX(5) = 8HTOT. PR.
     UO = 0.0
     DO 801 I = 1,JZ
801  UO = MAX1(UO,OR(I,18),OR(I,28))
     NZZ = UO/100. + 1.0
     UO = NZZ*100
      CALL GRAPH(AB, OR(1,18), -XUU, -UO, BCDX, BCDY, JZ, 1)
     CALL GRAPH(AB,OR(1,28),XUU,-UO,BCDX,BCDY,JZ,-2)
     BCDY(2) = 8HTEMPERAT
     BCDY(3) = 8HURE
     BCDX(4) = 8HSTAT T.
     BCDX(5) = 8HTOT. T.
     UO = 0.0
     DO 802 I = 1,JZ
802  UO = MAX1(UO,OR(I,38),OR(I,48))
     NZZ = UO/1000. + 1.0
     UO = NZZ*1000
     CALL GRAPH (AB,OR(1,38),-XUU,-UO,BCDX,BCDY,JZ,1 )
     CALL GRAPH (AB,OR(1,48), XUU,-UO,BCDX,BCDY,JZ,-2)
      END FILE 17
      GO TO 5
     END
```

```
      SUBROUTINE GRAPH(ABS,ORD,UPA,UPO,BCDX,BCDY,NP, NC)
      DIMENSION ABS(600), ORD(150), BCDX(7), BCDY(3), G(400)
      DATA (JZ=0)
C     UNIT 17 USED FOR PLOTTED OUTPUT  (INCLUDE CONTROL CARD EQUIP,17=PL
      IF(JZ) 9,8,9
    8 CALL PLOTS(G,225,17)
      JZ = 1
C     SCALE  INCOMING  DATA
    9   NPT = NP
      NCT = XABSF(NC)
      APA  = ABSF(UPA)
      APO  = ABSF(UPO)
   13 DO 14  I = 1,NPT
   14  ORD(I) = ABSF(ORD(I)/UPO*9.0) + 0.5
      IF(NC) 71, 3, 3
C     COMPUTE SUBDIVISIONS FOR ORDINATE LABEL  LAYOUT ORD LABELS
    3 IF(APO - 10.) 124, 124, 22
  124 MZ = 1
      DO 125 I = 1,3
      N = I - 1
      IF(APO - 1.0/10.0**N) 125, 125,9126
  125  CONTINUE
 9126  YB = 1.0/10.0**N
      MZ = MZ - N
        IF(APO - 3.0/10.**N) 134, 134, 135
  134  YB = YB/2.0
  135    YZ = 9.0/APO*YB
      YZ = 9.0/APO*YB
         GO TO 25
   22 MZ = 2
      IF(APO - 20.) 24, 24, 23
   23 IF(APO - 1000.) 126, 26, 27
  126  YB = 100.
      IF(APO - 300.) 142, 142, 143
  142 YB = YB/2.0
  143 YZ = 9.0/APO*YB
      GO TO 25
   26 YB = 200.
      YZ = 1.8
      GO TO 25
   27  IF(APO - 2000.) 28, 28, 29
   28  YB = 500.
       YZ = 2.25
       GO TO 25
   29     YB = 1000.
      YZ = 9.0/APO*1000.
         GO TO 25
   24 YZ = 9.0/APO
      YB = 1.0
   25 XLA = 0.0
      XAB = 1.0
      X = XAB - .07
   41 CALL NUMBER(X,0.4,.07,XLA,0.0,2)
      CALL PLOT(XAB, 0.5,3)
      CALL PLOT(XAB, 9.5,2)
       XAB = XAB + .875
      CALL PLOT(XAB, 9.5,3)
      CALL PLOT(XAB, 0.5,2)
      XLA = XLA + .25
      X = XAB - .07
      CALL NUMBER(X,0.4,.07,XLA,0.0,2)
```

```
      XLA = XLA + .25
       XAB = XAB + .875
      X = XAB - .07
      IF(XLA - 1.0) 41, 42, 42
42    CALL SYMBOL(3.0,0.2,0.14,BCDX, 0.0, 24)
      CALL NUMBER(X,0.4,.07,XLA,0.0,2)
      CALL PLOT(XAB, 0.5,3)
      CALL PLOT(XAB, 9.5,2)
       IF(APA - 1.0) 41, 41, 45
45     Z = 3.5/(APA-1.0)
      XAB = 4.5
      IF(Z - .875) 46, 47, 47
46    Z = 2.0*Z
      XLA = 3.0
      XB = 2.0
      GO TO 48
47    XLA = 2.0
      XB = 1.0
48    XAB = Z + XAB
      IF(XAB - 8.00001) 49, 49, 54
49     X = XAB - .07
50    CALL PLOT(XAB, 9.5,3)
      CALL PLOT(XAB, 0.5,2)
      CALL NUMBER(X,0.4,.07,XLA,0.0,2)
      XAB = XAB + Z
      IF(XAB - 8.00001) 51, 51, 55
51     X = XAB - .07
       XLA = XLA + XB
52    CALL NUMBER(X, 0.4,.07, XLA, 0.0,2)
       CALL PLOT( XAB,0.5, 3)
       CALL PLOT( XAB,9.5, 2)
       XLA = XLA + XB
      GO TO 48
54    XAB = XAB - Z/2.0
       X = XAB - .07
      XLA = XLA - XB/2.0
      IF( XAB - 8.0) 50, 50, 58
55    XAB = XAB - Z/2.0
       X = XAB - .07
      XLA = XLA - XB/2.0
      IF(XAB - 8.0) 52, 52, 59
58     YZ = -YZ
       YLA = APO
      YB = -YB + .000015
       YAB = 9.5
         AZ = 0.0
         A = -1.0
      GO TO 60
59     YLA = 0.0
       YAB = 0.5
       AZ = 9.5
       A = 1.0
60      CALL PLOT ( 8.0,YAB, 3)
        CALL PLOT ( 1.0,YAB, 2)
      Y = YAB - .035
      IF(MZ) 103, 104, 105
103    CALL NUMBER(0.7,Y, .07, YLA, 0.0, 3)
      GO TO 106
104   CALL NUMBER(0.7,Y, .07, YLA, 0.0, 2)
      GO TO 106
105   IF(MZ - 1) 108, 108, 109
```

```
108   CALL NUMBER(0.7,Y, .07, YLA, 0.0, 1)
      GO TO 106
109   CALL NUMBER(0.7,Y, .07, YLA, 0.0, 0)
106   YAB = YAB + YZ
         IF((AZ - YAB)/A) 70, 62, 62
 62    YLA = YLA + YB
      Y = YAB - .035
      IF(MZ) 113, 114, 115
113    CALL NUMBER(0.7,Y, .07, YLA, 0.0, 3)
      GO TO 116
114   CALL NUMBER(0.7,Y, .07, YLA, 0.0, 2)
      GO TO 116
115   IF(MZ - 1) 118, 118, 119
118   CALL NUMBER(0.7,Y, .07, YLA, 0.0, 1)
      GO TO 116
119   CALL NUMBER(0.7,Y, .07, YLA, 0.0, 0)
116   CALL PLOT(1.0, YAB, 3)
         CALL PLOT( 8.0, YAB, 2)
         YAB = YAB + YZ
         YLA = YLA + YB
            IF((AZ - YAB) / A) 70, 60, 60
 70    CALL SYMBOLT 0.6, 3.0, 0.14, BCDY, 90.0,24)
C     DRAW CURVES ON GRAPH  WHERE  NC REPRESENTS NUMBER OF CURVES ON
C     THIS PLOT
 71   CALL PLOT(ABS(1), ORD(1),3)
      IF(NCT-1) 72,63,72
 63   DO 65 J = 1,NPT
 65   CALL SYMBOL(ABS(J), ORD(J),.04,1,0.0,-2)
      GO TO 91
 72   IF(NCT - 2) 75 , 73, 75
 73   DO 74 J = 1,NPT
 74   CALL SYMBOL(ABS(J), ORD(J),.04,2,0.0,-2)
      GO TO 91
 75   IF(NCT - 3) 79, 76, 79
 76   DO 77 J = 1,NPT
 77   CALL SYMBOL(ABS(J), ORD(J),.04,3,0.0,-2)
      GO TO 91
 79   IF(NCT - 4) 82, 80, 82
 80   DO 81 J = 1,NPT
 81   CALL SYMBOL(ABS(J), ORD(J),.04,4,0.0,-2)
      GO TO 91
 82   IF(NCT - 5) 86, 83, 86
 83   DO 84 J = 1,NPT
 84   CALL SYMBOL(ABS(J), ORD(J),.04,5,0.0,-2)
      GO TO 91
 86   DO 87 J = 1,NPT
 87   CALL SYMBOL(ABS(J), ORD(J),.04,6,0.0,-2)
 91   IF(UPO) 911,90, 90
911   IF(NCT- 2) 912, 913, 914
912   CALL SYMBOL(6.0, 1.50,.04, 1, 0.0, -1)
      CALL SYMBOL(6.3, 1.50, .07, BCDX(4), 0.0, 8)
      GO TO 90
913   CALL SYMBOL(6.0, 1.25,.04, 2, 0.0, -1)
      CALL SYMBOL(6.3, 1.25, .07, BCDX(5), 0.0, 8)
      GO TO 90
914 IF(NCT - 3) 915, 915, 916
915 CALL SYMBOL(6.0, 1.00,.04, 3, 0.0, -1)
      CALL SYMBOL(6.3,1.0,.07,BCDX(6),0.0,8)
      GO TO 90
916 CALL SYMBOL(6.0,.75, .04, 4, 0.0, -1)
      CALL SYMBOL( 6.3, 0.75, .07, BCDX(7), 0.0, 8)
```

```
      SUBROUTINE  COMP (OFR,P,Y)
C     COMPOSITION OF COMBUSTION GASES AT ADIABATIC FLAME TEMPERATURE
C     AS A FUNCTION OF      O/F RATIO, PRESSURE
      DIMENSION R(6),YCOT1(6),YCO2T1(6),YH2T1(6),YH2OT1(6),YO2T1(6),
     1YN2T1(6), Y(7),YNOT1(6),YCO2T2(6),YCOT2(6),YH2T2(6),YH2OT2(6),
     2YO2T2(6),YN2T2(6),YNOT2(6),YCOB(6),YCO2B(6),YH2B(6),YH2OB(6),
     3YO2B(6),YN2B(6),YNOB(6)
      DATA (R= 0.687,0.923,1.083,1.326,1.778,10.),
     1( YCOT1= 0.052,0.045, .043, .041, .039,.039),
     2(YCO2T1=  .052, .051, .049, .047, .045,.045),
     3(YH2T1=  .331, .213, .147, .073, .019,.019),
     4(YH2OT1=  .287, .378, .423, .466, .450,.450),
     5( YO2T1=  .000, .001, .020, .049, .056,.056),
     6( YN2T1=  .380, .397, .402, .403, .397,.397),
     7( YNOT1=  .001, .006, .021, .077, .080,.080),
      DATA
     1( YCOT2=  .056, .045, .042, .040, .035,.035),
     2(YCO2T2=  .059, .053, .049, .047, .042,.042),
     3( YH2T2=  .330, .211, .149, .080, .026,.026),
     4(YH2OT2=  .286, .375, .415, .449, .447,.477),
     5( YO2T2=  .000, .004, .019, .030, .050,.050),
     6( YN2T2=  .382, .399, .405, .403, .398,.398),
     7( YNOT2=  .001, .009, .027, .083, .019,.019),
      A = (P - 300.)/ 700.
      DO 10 I=1,6
      YCOB(I) = YCOT1(I) + A * (YCOT2(I)- YCOT1(I))
      YCO2B(I) = YCO2T1(I) + A * (YCO2T2(I)- YCO2T1(I))
      YH2B(I) =  YH2T1(I) + A * (YH2T2(I) - YH2T1(I))
      YH2OB(I)=  YH2OT1(I) + A * (YH2OT2(I) - YH2OT1(I))
      YO2B(I) =  YO2T1(I) + A * (YO2T2(I) - YO2T1(I))
      YN2B(I)  = YN2T1(I) + A*(YN2T2(I)-YN2T1(I))
      YNOB(I)  = YNOT1(I) + A*(YNOT2(I)-YNOT1(I))
   10 CONTINUE
      CALL LNGRIN  (OFR,YCO, R , YCOB,DYDX,6)
      CALL LNGRIN  (OFR,YCO2,R ,YCO2B,DYDX,6)
      CALL LNGRIN  (OFR,YH2 ,R ,YH2B ,DYDX,6)
      CALL LNGRIN  (OFR,YH2O, R,YH2OB,DYDX,6)
      CALL LNGRIN  (OFR,YO2, R ,YO2B, DYDX,6)
      CALL LNGRIN (OFR,YN2,R,YN2B,DYDX,6)
      CALL LNGRIN (OFR ,YNO,R,YNOB,DYDX,6)
      Y(1)= YCO
      Y(2)= YCO2
      Y(3)= YH2
      Y(4)= YH2O
      Y(5)= YO2
      Y(6) = YN2
      Y(7) = YNO
      SUM = 0.
      DO 20 I=1,7
      IF (Y(I).LT.0.) 19,20
   19 Y(I)= 0.
   20 SUM = SUM + Y(I)
      DO 30   I = 1, 7
   30 Y(I) = Y(I) / SUM
      RETURN
      END
```

```
      SUBROUTINE TERP(X,RS,VD,NSET,RR)
      DIMENSION X(2),RS(40),VD(40),NSET(2),RR(2)
      LBB = NSET(2)
      LBJ = NSET(1)
      J = 1
   10 K = J-2
      DO 20 I=1,LBJ
      N = 2*I+K
      IF(RS(N)-X(J))20,30,40
   20 CONTINUE
      WRITE (6,25)X(J)
   25 FORMAT(1H0,E18.8,22H ABOVE RANGE OF TABLE      )
   30 RR(J) = VD(N)
      LBJ = LBB
      J = J + 1
      IF (J-3)10,50,50
   40 RR(J) = (X(J)-RS(N-2))/(RS(N)-RS(N-2)) *(VD(N)-VD(N-2)) + VD(N-2)
      LBJ = LBB
      J = J + 1
      IF(J-3)10,50,50
   50 RETURN
      END
```

```
      FUNCTION XDEL(RVAP)
      IF(RVAP-.5)10,5,5
    5 XDEL = 0.005
      GO TO 1000
   10 IF(RVAP-.3)20,15,15
   15 XDEL = 0.01
      GO TO 1000
   20 IF(RVAP-0.2)30,25,25
   25 XDEL = 0.02
      GO TO 1000
   30 IF(RVAP-0.1)40,35,35
   35 XDEL = 0.05
      GO TO 1000
   40 IF(RVAP-0.05)50,45,45
   45 XDEL = 0.100
      GO TO 1000
   50 IF(RVAP-0.02)60,55,55
   55 XDEL = 0.200
      GO TO 1000
   60 XDEL = 0.500
 1000 RETURN
      END
```

```
      FUNCTION PVAP (T,I)
C     VAPOR PRESSURE OF N2O4(I=1), MMH(I=2)
      DIMENSION A(2),B(2),C(2)
      DATA (A=20.47,14.3287), (B=12630.,7363.22), (C=181.,-63.1213)
      PVAP =EXPF(A(I)-B(I)/(T+C(I)))
      RETURN
      END


   90 IF(UPA) 95, 92, 92
C     TERMINATION POINT AND EOF WRITE FOR PLOT TAPE
   92          CALL PLOT (8.5, 0, -3)
   95     RETURN
          END


      FUNCTION TBL(P,I)
C     BOILING TEMP OF N2O4(I=1), MMH(I=2)
      DIMENSION A(2),B(2),C(2)
      DATA (A=20.47,14.33),(B=12630.,7363.2),(C=181.,-63.121)
      TBL = B(I)/(A(I)-LOGF(P))-C(I)
      RETURN
      END


      FUNCTION RHO (T,I)
C     LIQUID DENSITY OF N2O4(I=1), MMH(I=2)
      DIMENSION A(2),B(2),C(2)
      DATA (A=0.0616,0.030623), (B =0.1082,0.40289),
     1     (C=-0.54321,0.0)
      RHO = A(I)+B(I)*T/1.E4 +C(I)*T/1.E8*T
      RETURN
      END


      FUNCTION VISCV(T,I)
C     VAPOR VISCOSITY FOR N2O4(I=1), MMH(I=2)
      DIMENSION A(2),B(2)
      DATA (A=0.41998,0.41998),(B=0.009581,0.009581)
      VISCV = (A(I)+B(I)*T)/1.E7
      RETURN
      END
```

```
      FUNCTION CVAP (T,I)
C     VAPOR SPECIFIC OF N2O4(I=1),  MMH(I=2)
      DIMENSION A(2),B(2),C(2)
      GO TO (10,20),I
   10 TR=T-1800.
      CVAP=.274+TR*(2.305E-5-(TR*5.33E-9))
      RETURN
   20 CVAP=.336+1.804E-4*T
      RETURN
      END
```

```
      FUNCTION FKA (T,I)
C     VAPOR THERMAL CONDUCTIVITY OF N2O4(I=1), MMH(I=2)
      DIMENSION A(2),B(2)
      DATA (A=-1.67,0.1237), (B=0.00652,0.002236)
      FKA = (A(I)+B(I)*T)/1.E7
      RETURN
      END
```

```
      FUNCTION CPL (T,I)
C     LIQUID SPECIFIC HEAT OF N2O4(I=1),  MMH(I=2)
      GO TO (10,20),I
   10 CPL =0.354 +5.3E-6 *(T-450.)**2
      RETURN
   20 CPL =0.589125 + 2.80708E-4 *T
      RETURN
      END
```

```
      FUNCTION CD(RE)
C     DRAG COEF OF DROP
      IF (RE-80.)10,10,20
   10 CD =27. *RE **(-.84)
      RETURN
   20 IF(RE-1.E4)30,30,40
   30 CD =0.271*RE**.217
      RETURN
   40 CD=2.
      RETURN
      END
```

```
      FUNCTION ALM (T,I)
C     HEAT OF VAPORIZATION OF N2O4(I=1), MMH(I=2)
      GO TO (10,20),I
   10 TR =780. -T
      ALM = 272.
      IF(TR)16,16,15
   15 ALM = ALM + 174.*SQRTF(TR/230.)
   16 RETURN
   20 ALM = 150.747 -T*(.3591305-1.214E-4*T)
      RETURN
      END
```

```
      SUBROUTINE WTMINT (OFR,P,WM,DWMDOFR)
C     MOLECULAR WT OF COMBUSTION GASES AS A FUNCTION OF O/F RATIO
      DIMENSION OFTAB (7),WMTAB(7)
      DATA (OFTAB =   0.0,  1.0,  1.5,  2.0,  2.5, 3.0 ,  5.0),
     1      (WMTAB = 14.00,14.67,19.75,22.93,23.81,23.00,23.00)
      CALL LNGRIN (OFR,WM,OFTAB,WMTAB,DWMDOFR,7)
      RETURN
      END
```

```
      FUNCTION A(X)
C     CROSS SECTIONAL AREA OF CHAMBER VS X
      A = 107. -3.55*X
      RETURN
      END
```

```
      SUBROUTINE MASSET(EMO,RHO,RS,EMDOT,N,DROPN)
      DIMENSION EMO(20),RS(20),DROPN(20)
      CRHO=4.188790204*RHO
      FRAC=EMDOT/FLOATF(N)
C
      FRAC1 = FRAC/5.0
      NP4 = N+4
      DO 2 I =1,5
      EMO(I) = CRHO*RS(I)**3
    2 DROPN(I) = FRAC1/EMO(I)
      DO 5 I=6,NP4
      EMO(I)=CRHO*RS(I)**3
    5 DROPN(I)=FRAC/EMO(I)
      RETURN
        END
```

```
      SUBROUTINE  VKSGAS (OFR,P,T,VISG,TKG,CPG)
C     VISCOSITY,  THERMAL CONDUCTIVITY,  AND  SPECIFIC HEAT OF
C     COMBUSTION  GASES AS A FUNCTION OF O/F RATIO, PRESSURE, AND
C     TEMPERATURE
      DIMENSION TTAB(7),VCO(7),VCO2(7),VH2(7),VH2O(7),VO2(7),VN2(7),
     1          VNO(7),SUM(7),WM(7),V(7),Y(7),VR(7),WMR(7),PHI(7),
     2          YPHI(7),CP(7)
      DATA (TTAB = 500.0,1000.0,2000.0,3000.0,4000.0,5000.0,7000.0),
     1     (VCO  = 0.971, 1.635,  2.51,  3.34,  3.90,  4.51,  5.50),
     2     (VCO2 = 0.791, 1.425,  2.32,  3.21,  3.75,  4.19,  4.70),
     3     (VH2  = 0.484, 0.750,  1.18,  1.64,  1.95,  2.22,  2.65),
     4     (VH2O = 0.512, 1.100,  2.22,  3.34,  4.36,  5.23,  6.80),
     5     (VO2  = 1.100, 1.787,  2.85,  3.75,  4.43,  5.13,  6.30),
     6     (VN2  = 0.980, 1.323,  2.32,  3.47,  4.21,  4.98,  5.62),
     7     (VNO  = 0.850, 1.112,  2.15,  3.02,  4.10,  4.50,  5.30),
     8     (WM   =   28.,   44., 2.016,   18.,   32.,   28.,   30.)
      CALL LNGRIN  (T,V(1),TTAB,VCO,DYDX,7)
      CALL LNGRIN  (T,V(2),TTAB,VCO2,DYDX,7)
      CALL LNGRIN  (T,V(3),TTAB,VH2,DYDX,7)
      CALL LNGRIN  (T,V(4),TTAB,VH2O,DYDX,7)
      CALL LNGRIN  (T,V(5),TTAB,VO2,DYDX,7)
      CALL LNGRIN  (T,V(6),TTAB,VN2,DYDX,7)
      CALL LNGRIN  (T,V(7),TTAB,VNO,DYDX,7)
      CALL COMP (OFR,P,Y)
      SUMVIS = 0.
      DO 20 I=1,7
      IF(Y(I).LT.0.001) 20, 9
    9 SUM(I) = 0.
      DO 10 J=1,7
      VR (J) =  V(I)/ V(J)
      WMR (J) =  WM(J) / WM(I)
      PHI(J) = (1. + SQRTF(VR(J)* SQRTF(WMR(J))))**2/(2.828 * SQRTF (
     1          1. + 1. / WMR(J)))
      YPHI(J) =  Y(J) * PHI(J)/Y(I)
   10 SUM(I) = SUM (I) + YPHI(J)
      SUMVIS =  SUMVIS  + V(I) / SUM(I)
   20 CONTINUE
      VISG = SUMVIS /1.E6
      CP(1)= 9.46 -  3290./T  + 1.07E6/T/T
      CP(2)= 16.2  - 6530. /T  + 1.41E6/T/T
      CP(3)= 5.76  + 5.78E-4*T + 20./SQRTF(T)
      CP(4)= 19.86 - 597./SQRTF(T) + 7500./ T
      CP(5)= 11.515 -        173./ SQRTF(T)  + 1530./T
      CP(6) = 6.9562 + 3.573E-4 * T
      CP(7) = 7.7205 + 2.463E-4 * T
      SIGA = 0.
      SIGB=  0.
      DO 30 I=1,7
      SIGA = SIGA  +  Y(I) * CP(I)
   30 SIGB = SIGB  +  Y(I) * WM(I)
      CPG  = SIGA / SIGB
      TKG  = VISG * ( CPG +  2.484/ SIGB)
      RETURN
      END
```

```
      SUBROUTINE  LNGRIN (XARG,YARG,XTAB,YTAB,DYDX,N)
C     QUADRATIC LANGRANGIAN INTERPOLATION OR EXTRAPOLATION FOR F(X)
C    AND DF(X)DX
      DIMENSION  XTAB(50),YTAB(50)
      IF(XARG.LT.XTAB(1)) 10, 20
   10 WRITE (6,100) XARG
  100 FORMAT (10H0  XARG = F12.6,  41H  15 OUTSIDE THE RAN OF TABULATE
     1D VALUES.78X,71H VALUES OF F(X) AND F (X) RETURNED TO CALLING PROG
     2RAM ARE EXTRAPOLATED.)
   11 K=1
      GO TO 50
   20 IF (XARG.GT.XTAB(N)) 30,40
   30 WRITE (6,100) XARG
   31 K = N - 2
      GO TO 50
   40 IF (XARG.GT.XTAB(1).AND.XARG.LT.XTAB(2)) 11,41
   41 IF (XARG.LT.XTAB(N).AND.XARG.GT.XTAB(N-1)) 31,42
   42  M = N - I
      DO  43  I = 3, M
      IF (XTAB(I).GT.XARG) 44, 43
   43 CONTINUE
   44 DIF1 = ABSF (XARG - XTAB(I-2))
      DIF2 = ABSF (XARG - XTAB(I+1))
      IF (DIF1.LE.DIF2) 45, 46
   45 K = I - 2
      GO TO 50
   46 K = I -1
   50 A = XARG - XTAB(K)
      B = XARG - XTAB(K+1)
      C = XARG - XTAB(K+2)
      R = XTAB(K) - XTAB(K+1)
      S = XTAB(K) - XTAB(K+2)
      T = XTAB(K+1) - XTAB(K+2)
C    INTERPOLATION FOR F(X)
      YARG = YTAB(K) * B * C /R/S - YTAB(K+1) * A * C /R/T + YTAB(K+2)
     1 * A * B /S/T
C     DIFFERENTIATION FOR F (X)
      DYDX = YTAB(K) * (B+C)/R/S - YTAB(K+1) * (A+C)/R/T + YTAB(K+2)
     1* (A+B)/S/T
      IF (XARG.LT.XTAB(1).OR.XARG.GT.XTAB(N)) 60, 61
   60 WRITE (6,200)  YARG, DYDX
  200 FORMAT (20X,7HYARG = F12.6,10X,7HDYDX = F20.10)
   61 CONTINUE
      RETURN
      END
```

```
      SUBROUTINE TGINT (OFR,PC,T,DTDOFR)
C     ADIABATIC FLAME TEMPERATURE AS A FUNCTION OF O/F RATIO , PRESS.
C     PRESSURE EFFECTS ASSUMED NEG. FOR FIRST APPROX. (INCLUDED LATER)
      DIMENSION TC1(9) , OFTAB(9)
      DATA(OFTAB=  0.0, 0.94,  1.0,  1.2,  1.4,  1.5, 1.75,  2.0,  3.0),
     1     (TC1  =4780.,4780.,5082.,5516.,5650.,5650.,5393.,5287.,3820.)
      CALL LNGRIN (OFR,T,OFTAB,TC1,DTDOFR,9)
      RETURN
      END


      FUNCTION RT(RS)
C     CALCULATES DISTANCE OF DISSOCIATION FLAME AS FUNCTION OF RADIUS
      DIMENSION RRS(5),RRT(5)
      DATA (RRS =  0.0,100.,200.,300.,500.),
     1      (RRT =  8.0, 13., 17., 18., 18.)
C     CONVERT RS(K) TO MICRONS
      RST = RS
      RST =RST * 2.54E+4
      CALL LNGRIN  (RST,RT,RRS,RRT,DRTDRS,5)
      RT = RT / 2.54E+4
      RETURN
      END


      FUNCTION XK(RS)
C     CALCULATES DISSOCIATION BURNING RATE CONSTANT AS FUNCTION OF
C     RADIUS
      DIMENSION XXK(5),RRS(5)
      DATA (XXK =  3.2, 6.3, 7.3, 8.2, 11.),
     1      (RRS =  0.0,100.,200.,300.,500.)
C     CONVERT RS(K) TO MICRONS
      RST = RS
      RST = RST * 2.54E+4
      CALL LNGRIN  (RST,XK,RRS,XXK,DXKDRS,5)
      XK = XK *1.E-3/2.54/2.54
      RETURN
      END


      FUNCTION AP(X)
      AP = -3.55
      RETURN
      END
```

```
      SUBROUTINE LOGNRM(RM,SIG,N,RS)
C     COMPUTES RADII OF N DROPS ABOUT WHICH I/N TH OF THE MASS IS
C     CENTERED IN THE LOGARITHMICO-NORMAL DISTRIBUTION WITH MASS-MEAN
C     RADIUS RM AND STANDARD DEVIATION LN SIG.  XP, THE INVERSE
C     PROBABILITY FUNCTION IS APPROXIMATED BY A RATIONAL FRACTION.
      DIMENSION RS(20)
      DEL=1.00/FLOATF(N)
      SIGLN=LOGF(SIG)
      P=-DEL/2.
      NP4 = N+4
      MED = (N+1)/2 + 4
      J = NP4
      DO 4 I = 1,NP4
      IF(I-2)10,15,11
   10 P=P+ 0.6*DEL
      GO TO 2
   11 IF(I-5) 15,15,20
   15 P=P+0.2*DEL
      GO TO 2
   20 P=P+DEL
   30 IF(I.GT.MED)5.2
    2 T=SQRTF(-LOGF(P*P))
      XP=T-(2.30753+.27061*T)/(1.+T*(.99229+.04481*T))
      ESIGX=EXPF(SIGLN*XP)
      IF(I-3)4,3,40
   40 IF(I-5)4,49,50
   49 P = DEL/2.0
      GO TO 4
   50 J=N - I + 9
    3 RS(J)=RM*ESIGX
    4 RS(I)=RM/ESIGX
    5 RETURN
        END
```

```
      SUBROUTINE DIFFU (DFR,P,T,VPO2,I,DFU)
C     DIFFUSIVITY OF N2O4(I=1) , MMH(I=2) IN VAPOR FILM
      DIMENSION  FACA(7),FACB(7),Y(7),EPSA(7),EPSB(7),ETAB(14),
     1  OMEGT(14), PD(7)
      DATA (FACA =  4.86, 3.67, 17.5, 7.41, 5.85, 4.77, 4.93),
     1     (EPSA =  344., 453., 203., 638., 349., 314., 356.),
     2     (FACB =  4.77, 3.80, 17.2, 7.27, 5.74, 4.67, 4.84),
     3     (EPSB = 423., 557., 284., 785., 428., 386., 438.),
     4     (ETAB =   0.3,  1.0,  2.0,  3.0,  4.0,  6.0,  8.0,
     5              10.0, 20.0, 30.0, 40.0, 60.0, 80.0,100.0),
     6     (OMEGT= 2.622,1.439,1.075,0.949,0.884,0.812,0.771,
     7             0.742,0.644,0.623,0.596,0.559,0.535,0.517)
      CALL COMP (DFR,P,Y)
      DO 10 J=1,7
   10 Y(J) = Y(J) * (P-VPO2)/P
      SUMD = 0.
      IF (I.EQ.1) 20,40
   20 XNUM = 1. - VPO2/P
      DO 30 J=1,7
      E = T / EPSA(J)
      CALL LNGRIN (E,OMEGA,ETAB,OMEGT,DYDX,14)
      PD(J) = FACA(J)*T **1.5 /OMEGA
   30 SUMD  = SUMD +Y(J) /PD(J)
      GO TO 60
   40 XNUM =1. - VPO2/P
      DO 50 J=1,5
      E = T /EPSB(J)
      CALL LNGRIN (E,OMEGA,ETAB,OMEGT,DYDX,14)
      PD(J) = FACB(J)*T**1.5 /OMEGA
   50 SUMD = SUMD + Y(J)/PD(J)
   60 DFU = XNUM / SUMD /P /1.E6 * 14.7
      RETURN
      END
```

5. Sample Problem with Output

A sample problem was solved and typical program output is presented here. The input parameters are shown in Figures 20 and 21. The following pages show the printout of droplet histories at arbitrary x increments along the chamber length. Printed output in this solution involve:

(a) State of x position (inches).

(b) Calculated gas velocity u,

(c) Chamber temperature, T, and pressure P.

(d) Calculated local bulk gas O/F ratio.

(e) Local Mach number of gas.

(f) Cumulated fraction of O, F and both vaporized.

(g) Local vaporization rate.

(h) Drop size and mass for each group.

(i) Drop absolute and relative velocity.

(j) Droplet liquid temperature.

(k) Reynolds number of each drop based on the speed of sound.

Figures 23, 24 and 25 are samples of the printed output at various chamber stations.

In addition to the printed output the parameters of most interest are machine plotted. These plots display trends in these parameters in a more meaningful format than the printing. The results for the sample case follow the sample printouts.

STEADY STATE COMBUSTION MODEL
MMH AND NTO PROPERTIES

[illegible] 0.000 U= 0.0 T=5082 TO=5082 P= 100.00 PO= 100.00 O/F= 1.000 MACH=0.000
VAPORIZED FRACTION O 0.000000 F 0.000000 BOTH 0.000000
VAPORIZATION RATE/IN O 0.097539 F 0.369856 BOTH 0.188311

OXIDIZER DROPS	R(MIL)	MASS(LB)	V(IN/SEC)	U-V/A	TEMP	NUMBER			
1	0.5420	4.38802-011	1000	-0.0183	530.00	1.641+010	0.000+000	-7.698-001	
2	0.8221	1.53178-010	1000	-0.0183	530.00	4.700+009	0.000+000	-3.623-001	
3	1.0329	3.03783-010	1000	-0.0183	530.00	2.370+009	0.000+000	-2.432-001	
4	1.2220	5.02981-010	1000	-0.0183	530.00	1.431+009	0.000+000	-1.818-001	
5	1.4024	7.60311-010	1000	-0.0183	530.00	9.470+008	0.000+000	-1.434-001	
6	1.9428	2.02148-009	1000	-0.0183	530.00	1.781+009	0.000+000	-8.213-002	
7	3.0000	7.44273-009	1000	-0.0183	530.00	4.837+008	0.000+000	-3.947-002	
8	4.6324	2.74032-008	1000	-0.0183	530.00	1.314+008	0.000+000	-1.917-002	
9	8.7132	1.82351-007	1000	-0.0183	530.00	1.974+007	0.000+000	-6.826-003	
FUEL DROPS									
1	0.5420	3.46569-011	1000	-0.0183	530.00	1.039+010	0.000+000	-2.970+000	1
2	0.8221	1.20981-010	1000	-0.0183	530.00	2.976+009	0.000+000	-1.383+000	1
3	1.0329	2.39930-010	1000	-0.0183	530.00	1.500+009	0.000+000	-9.189-001	1
4	1.2220	3.97258-010	1000	-0.0183	530.00	9.062+008	0.000+000	-6.831-001	1
5	1.4024	6.00499-010	1000	-0.0183	530.00	5.995+008	0.000+000	-5.373-001	1
6	1.9428	1.59658-009	1000	-0.0183	530.00	1.127+009	0.000+000	-3.075-001	1
7	3.0000	5.87832-009	1000	-0.0183	530.00	3.062+008	0.000+000	-1.486-001	1
8	4.6324	2.16433-008	1000	-0.0183	530.00	8.317+007	0.000+000	-7.182-002	1
9	8.7132	1.44022-007	1000	-0.0183	530.00	1.250+007	0.000+000	-2.297-002	1

	R(MIL)	DELV	RED
OXIDIZER			
	0.8479	-0.0183	289.0257
	1.3218	-0.0183	450.5520
	1.1048	-0.0183	376.5608
	1.1048	-0.0183	376.5608
FUEL			
	0.8479	-0.0183	289.0257
	1.3218	-0.0183	450.5520
	1.1048	-0.0183	376.5608
	1.1002	-0.0183	375.0236
TOTAL			
	0.8479	-0.0183	289.0257
	1.3218	-0.0183	450.5520
	1.1048	-0.0183	376.5608
	1.1025	-0.0183	375.7922

FIGURE 23

[illegible]

[illegible] Po [illegible] PO= [illegible] 1.024 MACH=0.024

[illegible] F [illegible] DOTH [illegible]

[illegible] F [illegible] DOTH [illegible]

OXIDIZER DROPS	R(MIL)	MASS(LB)	V(IN/SEC)	U-V/A	TEMP	NUMBER			
1	[illegible]	[illegible]	[illegible]	[illegible]	[illegible]	[illegible]	[illegible]	[illegible]	
2	[illegible]	[illegible]	930	[illegible]	[illegible]	[illegible]	[illegible]	[illegible]	
3	[illegible]	[illegible]	932	[illegible]	[illegible]	[illegible]	[illegible]	[illegible]	
4	[illegible]	[illegible]	964	[illegible]	[illegible]	[illegible]	[illegible]	[illegible]	
5	[illegible]	[illegible]	972	0.0053	572.40	9.470+000	8.621-002	-3.301-001	
6	[illegible]	[illegible]	984	0.0051	570.80	1.701+009	4.112-002	-1.761-001	
7	[illegible]	[illegible]	[illegible]	[illegible]	[illegible]	[illegible]	[illegible]	[illegible]	
8	[illegible]	[illegible]	997	[illegible]	[illegible]	[illegible]	[illegible]	[illegible]	
9	[illegible]	[illegible]	999	[illegible]	[illegible]	[illegible]	[illegible]	[illegible]	
FUEL DROPS									
1	[illegible]	3.23770-012	919	0.0063	820.00	1.039+010	9.066-001	-1.544+000	1
2	[illegible]	[illegible]	918	[illegible]	[illegible]	[illegible]	[illegible]	[illegible]	1
3	[illegible]	[illegible]	940	[illegible]	[illegible]	[illegible]	[illegible]	[illegible]	1
4	[illegible]	[illegible]	[illegible]	[illegible]	[illegible]	[illegible]	[illegible]	[illegible]	1
5	[illegible]	[illegible]	964	0.0054	[illegible]	[illegible]	[illegible]	[illegible]	1
6	1.8424	1.43999-009	980	0.0051	603.77	1.127+009	9.035-002	-3.127-001	1
7	[illegible]	[illegible]	991	0.0049	[illegible]	[illegible]	4.714-002	-1.499-001	1
8	[illegible]	[illegible]	[illegible]	[illegible]	[illegible]	[illegible]	[illegible]	[illegible]	1
9	[illegible]	[illegible]	999	[illegible]	[illegible]	[illegible]	[illegible]	[illegible]	1

	R(MIL)	DELV	REQ
OXIDIZER			
	[illegible]	[illegible]	[illegible]
	1.2909	0.0050	439.0824
	1.0443	0.0056	351.0711
	[illegible]	[illegible]	322.1791
FUEL			
	0.6010	0.0063	202.0612
	[illegible]	[illegible]	420.7711
	1.0970	0.0056	355.3730
	1.0352	0.0056	348.0366
TOTAL			
	0.6899	0.0062	231.9482
	1.2778	0.0054	429.5972
	1.0506	0.0056	353.2221
	0.9968	0.0057	335.1079

FIGURE 24.

STEADY STATE COMBUSTION MODEL
MMH AND NTO PROPERTIES

X= 3.015 U= 5323.6 T=5293 TO=5301 P= 98.58 PO= 99.48 O/F= 1.933 MACH=0.115

VAPORIZED FRACTION O 0.426841 F 0.441593 BOTH 0.431758
VAPORIZATION RATE/IN O 0.095488 F 0.056842 BOTH 0.082741

OXIDIZER DROPS	R(MIL)	MASS(LB)	V(IN/SEC)	U-V/A	TEMP	NUMBER		
1	0.0000	0.00000+000	0	0.0000	0.00	0.000+000	1.000+000	0.000+000
2	0.0000	0.00000+000	0	0.0000	0.00	0.000+000	1.000+000	0.000+000
3	0.3700	1.40491-011	3875	0.0313	614.38	2.370+009	9.538-001	-5.523-002
4	0.5968	5.88266-011	3184	0.0467	585.52	1.431+009	8.830-001	-1.283-001
5	0.8339	1.60382-010	2752	0.0563	577.39	9.470+008	7.891-001	-1.244-001
6	1.4413	8.28595-010	2069	0.0715	584.47	1.781+009	5.901-001	-1.735-001
7	2.5015	4.75991-009	1548	0.0832	588.47	4.837+008	3.605-001	-1.308-001
8	4.3867	2.28973-008	1376	0.0870	578.42	1.314+008	1.936-001	-7.838-002
9	8.5108	1.70527-007	1242	0.0900	577.63	1.974+007	6.484-002	-3.407-002

FUEL DROPS									
1	0.0000	0.00000+000	0	0.0000	0.00	0.000+000	1.000+000	0.000+000	0
2	0.0000	0.00000+000	0	0.0000	0.00	0.000+000	1.000+000	0.000+000	0
3	0.0000	0.00000+000	0	0.0000	0.00	0.000+000	1.000+000	0.000+000	0
4	0.4329	2.16156-011	3669	0.0358	818.73	9.042+008	9.456-001	-6.784-002	1
5	0.6047	8.55373-011	3867	0.0493	818.78	5.995+008	8.576-001	-8.960-002	1
6	1.3108	6.00156-010	2222	0.0681	818.98	1.127+009	6.241-001	-1.022-001	1
7	2.4091	3.72636-009	1626	0.0814	819.11	3.042+008	3.661-001	-8.351-002	1
8	4.1437	1.74711-008	1431	0.0858	694.93	8.317+007	1.928-001	-4.948-002	1
9	8.4090	1.34749-007	1298	0.0889	582.74	1.250+007	6.438-002	-1.779-002	1

	R(MIL)	DELV	MED
OXIDIZER			
	0.9869	0.0681	398.1881
	1.7331	0.0745	685.1992
	1.8982	0.0761	747.3142
	1.8581	0.0798	734.6348
FUEL			
	1.1427	0.0631	451.7761
	1.8883	0.0751	746.9833
	1.9914	0.0764	787.3894
	1.7766	0.0738	702.4188
TOTAL			
	1.0888	0.0647	400.9003
	1.7881	0.0748	704.9063
	[illegible]	[illegible]	787.[illegible]
	[illegible]	[illegible]	[illegible]

FIGURE 25

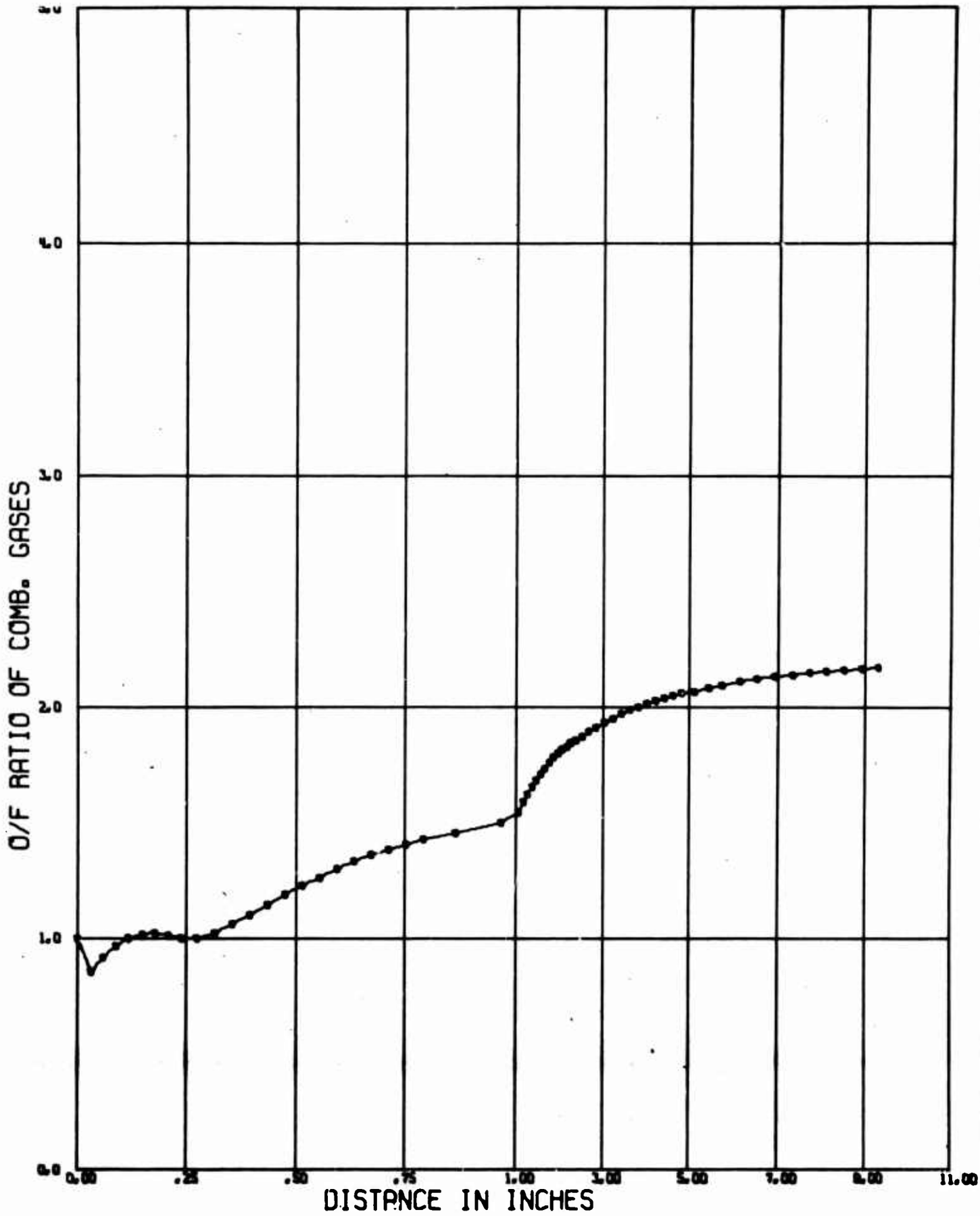
O/F RATIO OF COMB. GASES
DISTANCE IN INCHES
0.0
1.0
2.0
3.0
4.0
0.00
.25
.50
.75
1.00
11.00

FIGURE 26

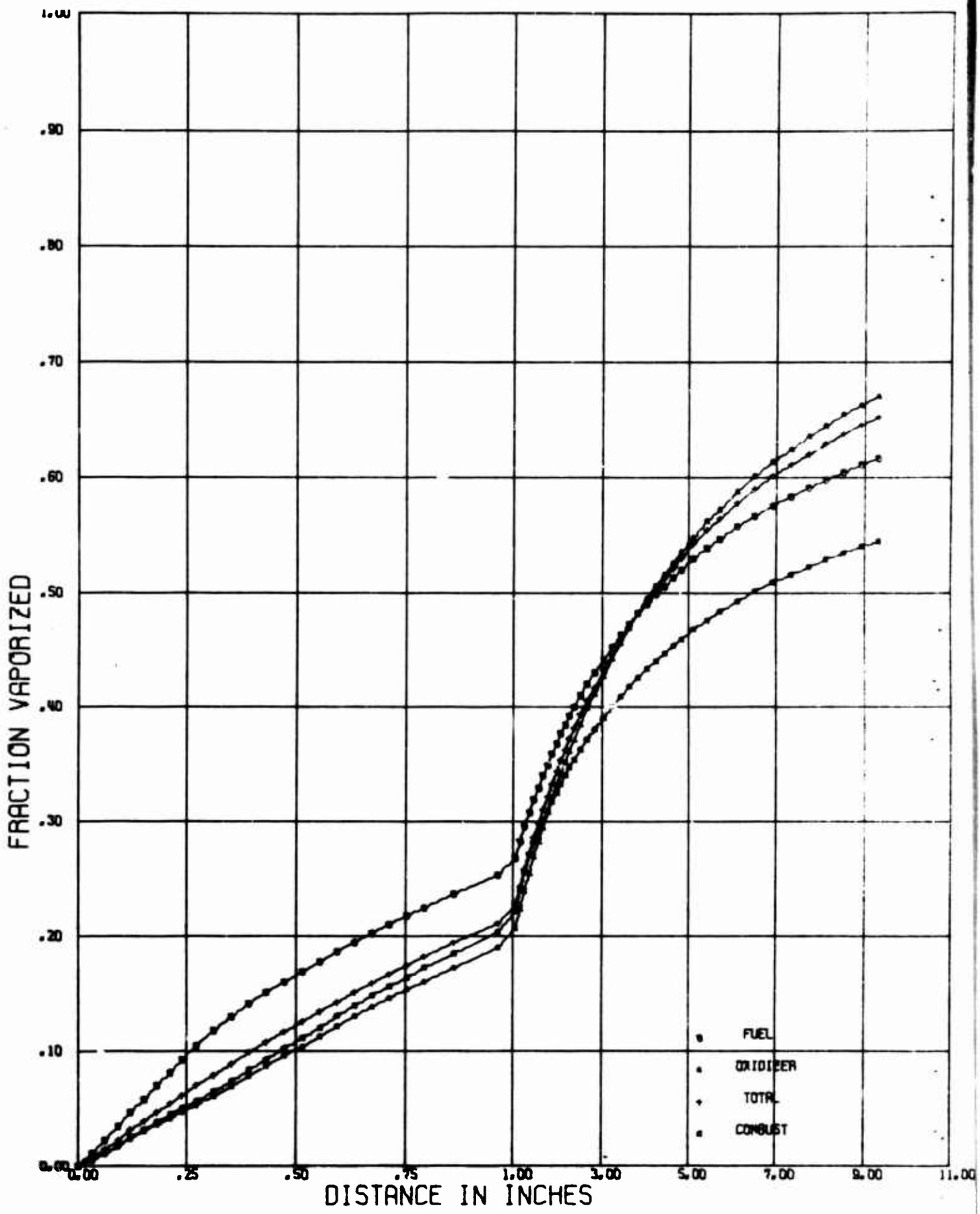
FRACTION VAPORIZED
DISTANCE IN INCHES
1.00
.90
.80
.70
.60
.50
.40
.30
.20
.10
0.00
0.00
.25
.50
.75
1.00
3.00
5.00
7.00
9.00
11.00
FUEL
OXIDIZER
TOTAL
COMBUST

FIGURE 27

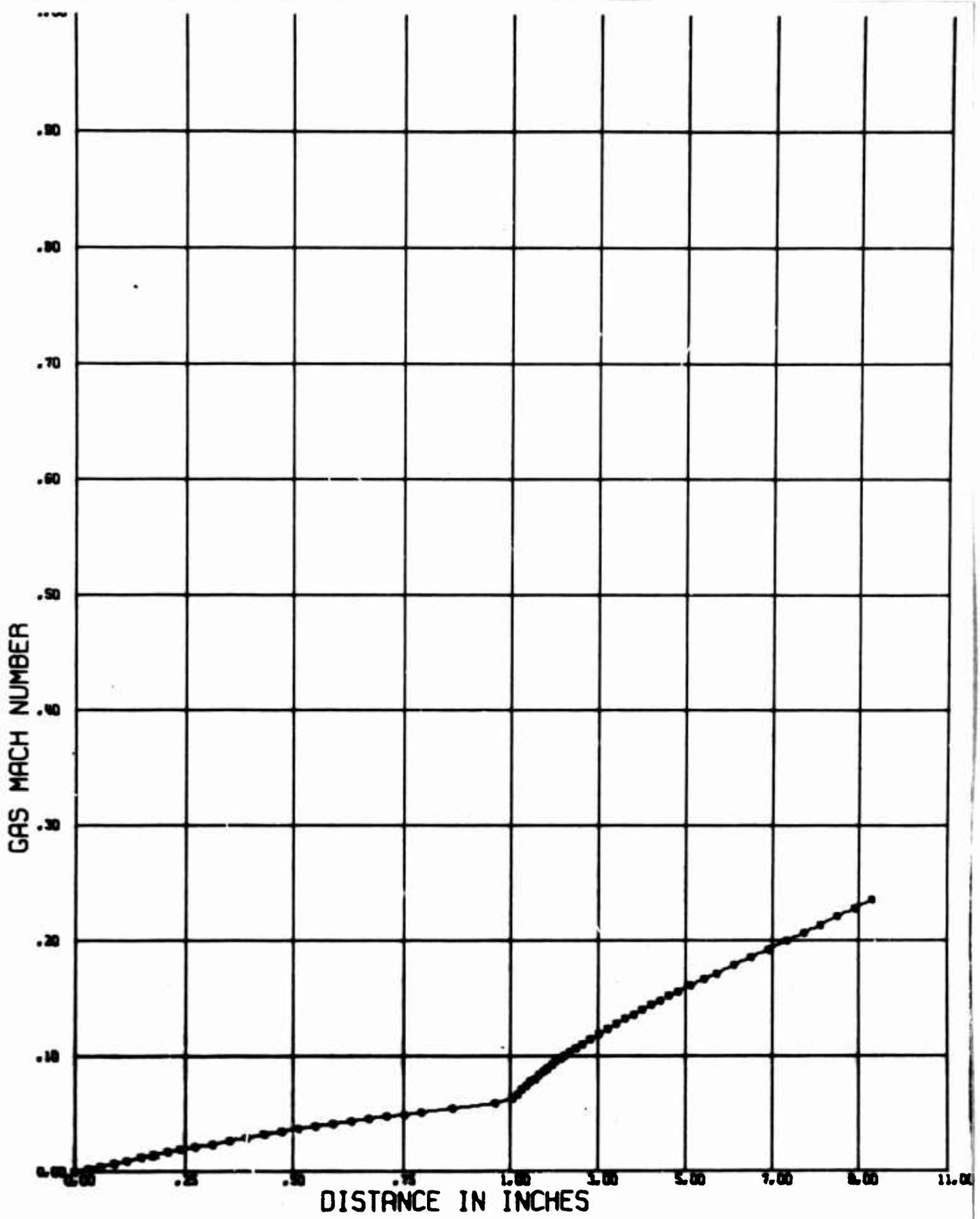
GAS MACH NUMBER
.90
.80
.70
.60
.50
.40
.30
.20
.10
.25
.50
.75
1.00
3.00
5.00
7.00
9.00
11.00
DISTANCE IN INCHES

FIGURE 28

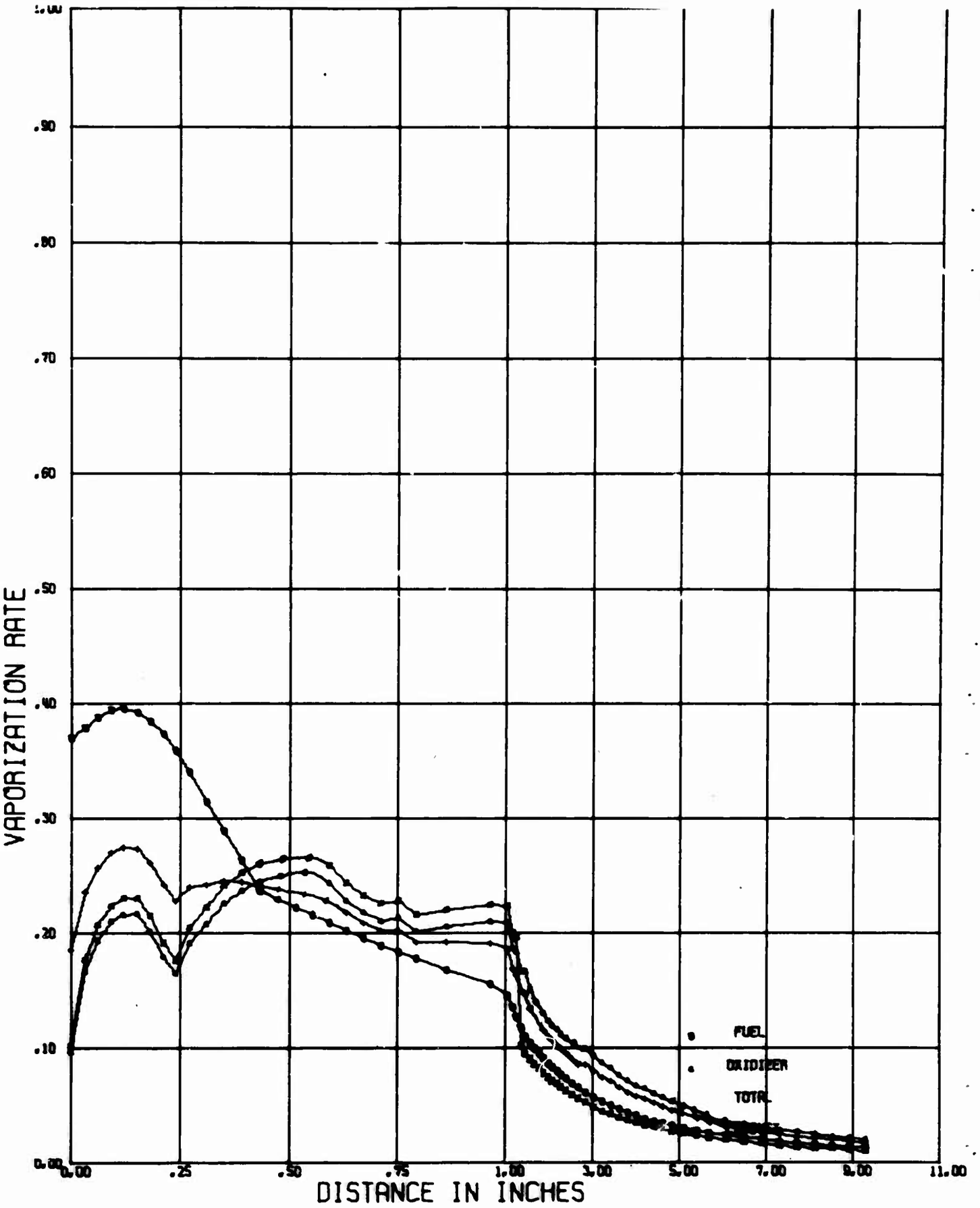
VAPORIZATION RATE
.90
.80
.70
.60
.50
.40
.30
.20
.10
0.00
0.00
.25
.50
.75
1.00
3.00
5.00
7.00
9.00
11.00
DISTANCE IN INCHES
FUEL
OXIDIZER
TOTAL

FIGURE 29

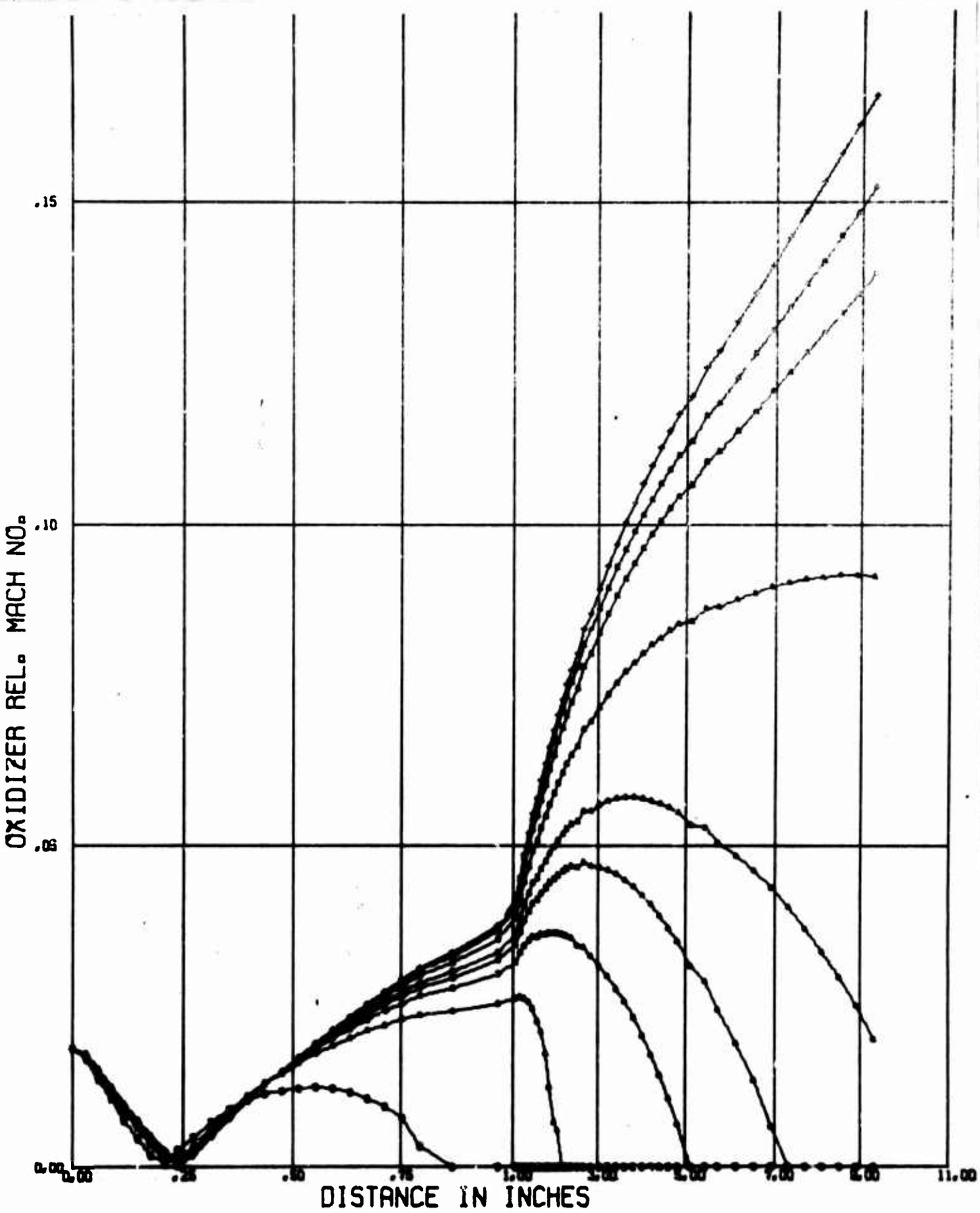

See Figure 32 for Group Drop Size
FIGURE 30

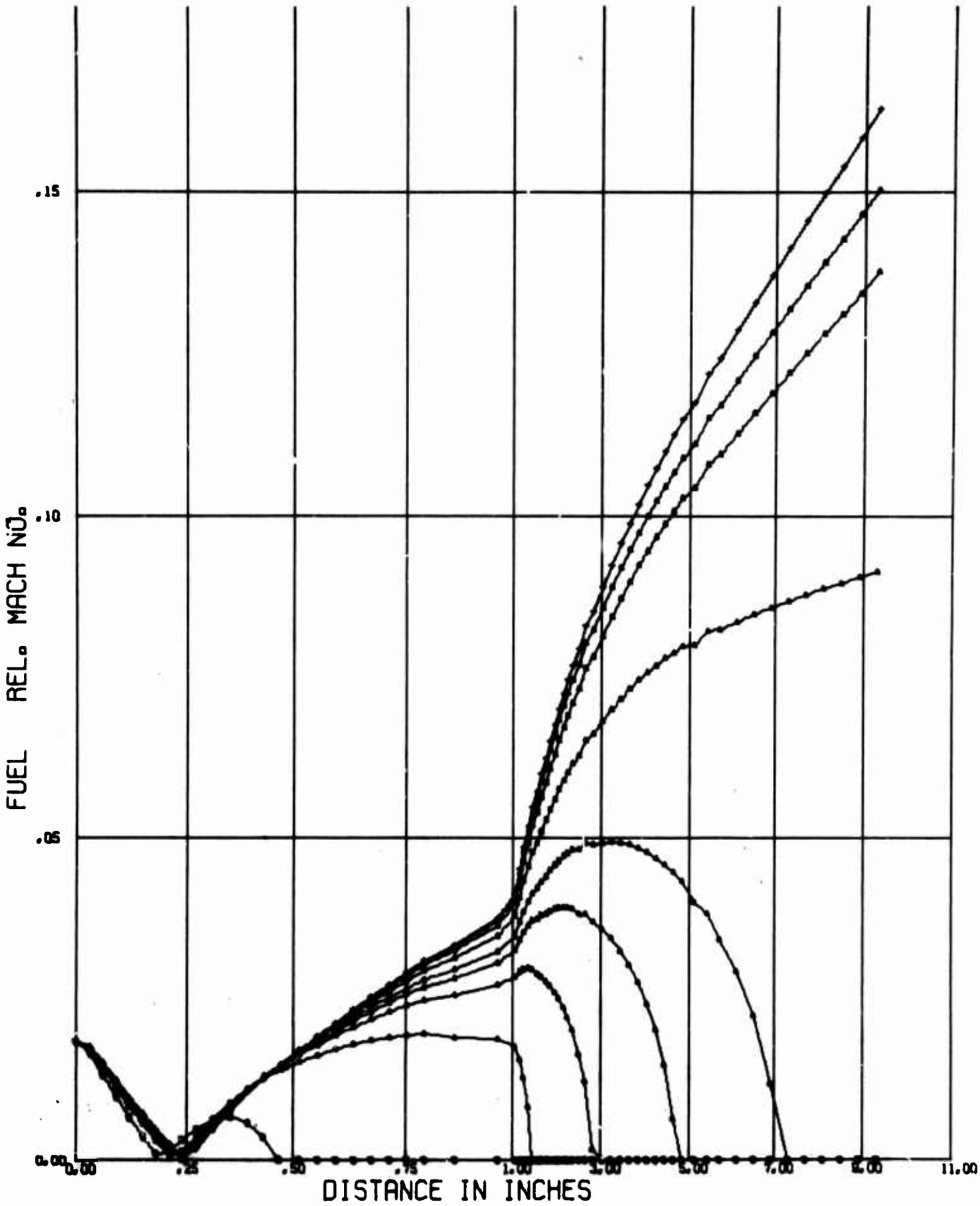

See Figure 33 for Group Drop Size

FIGURE 31

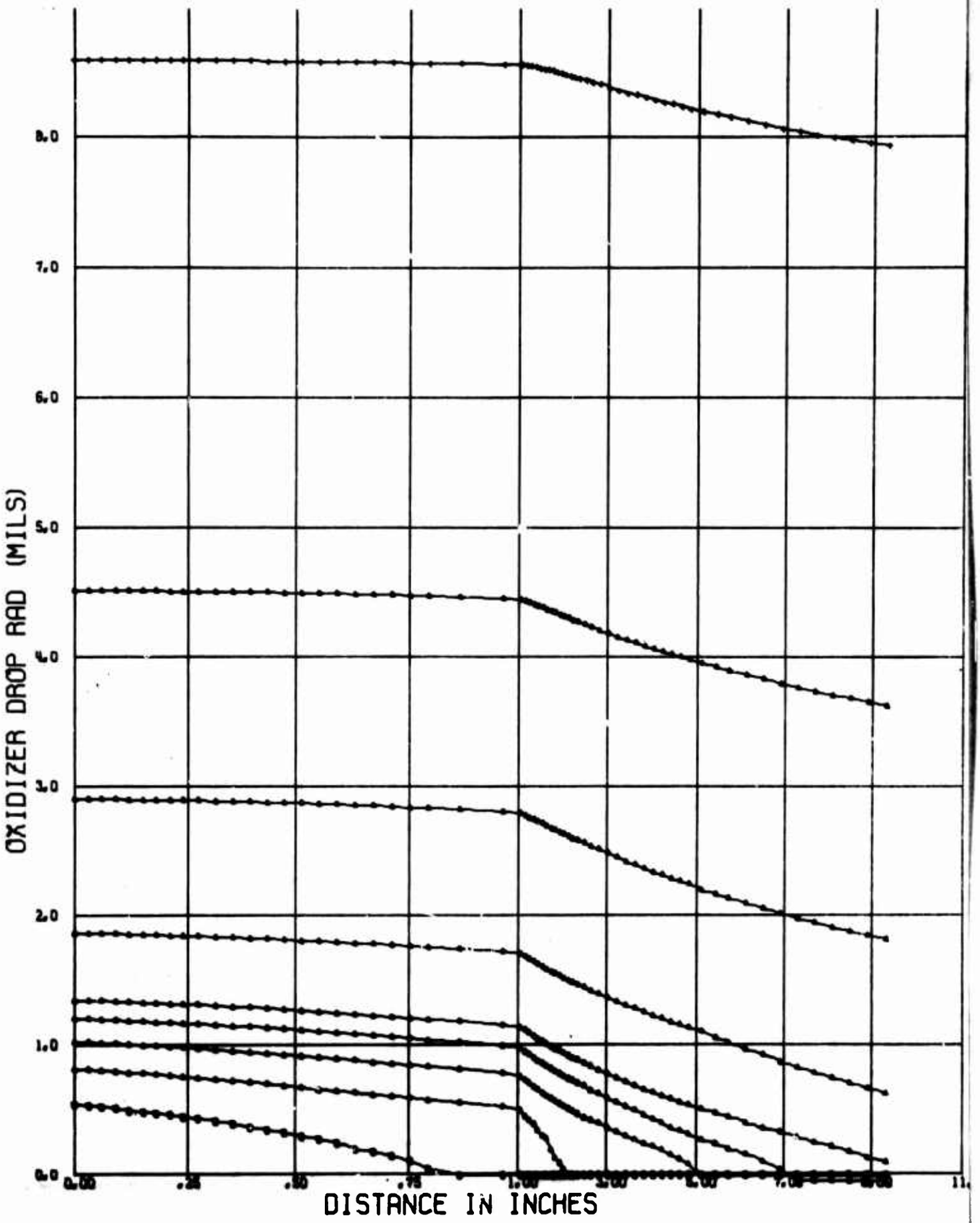
OXIDIZER DROP RAD (MILS)
8.0
7.0
6.0
5.0
4.0
3.0
2.0
1.0
0.0
0.00
.25
.50
.75
1.00
2.00
3.00
4.00
5.00
11.
DISTANCE IN INCHES

FIGURE 32

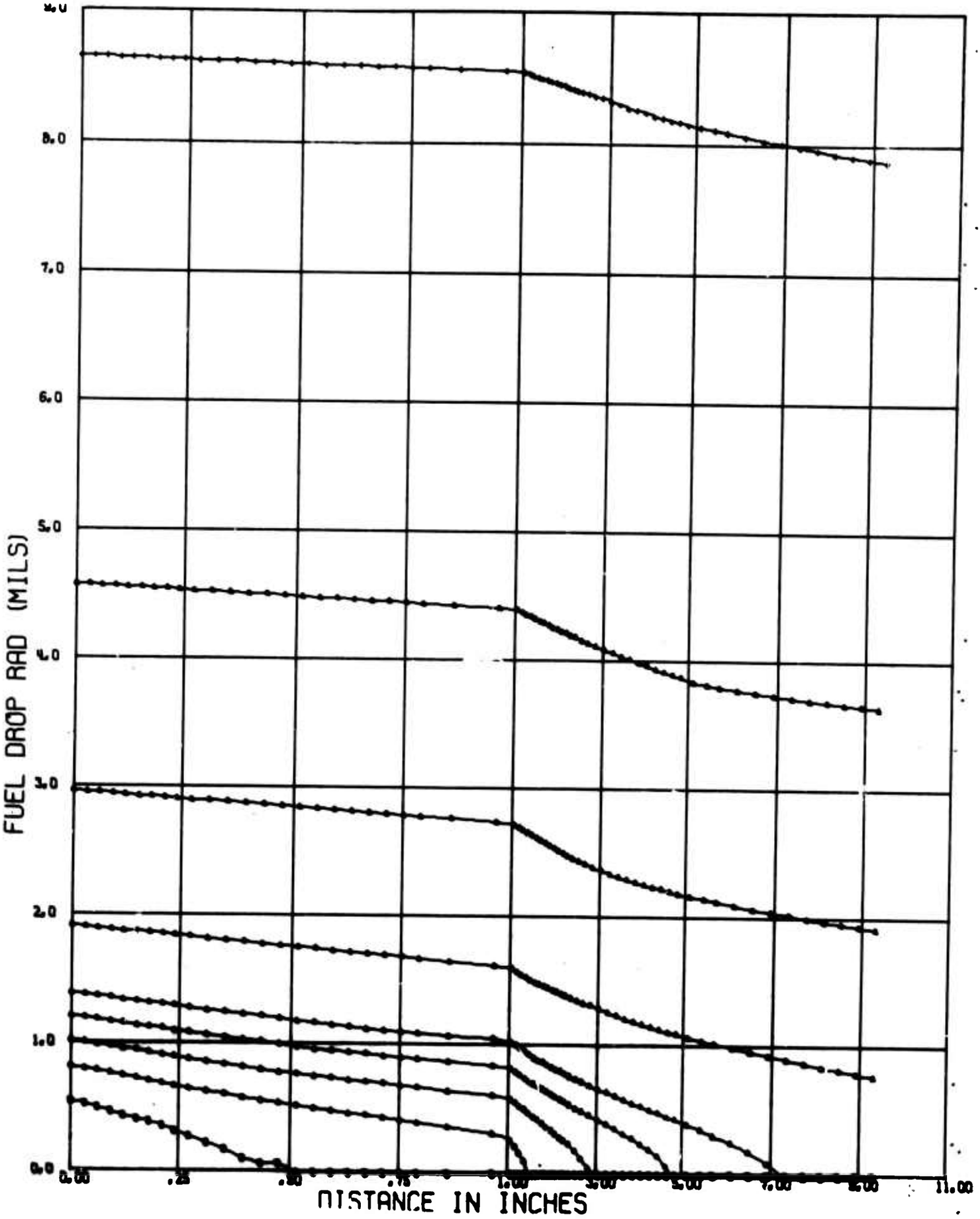
FUEL DROP RAD (MILS)
8.0
7.0
6.0
5.0
4.0
3.0
2.0
1.0
0.0
0.00
.25
.50
.75
1.00
2.00
7.00
11.00
DISTANCE IN INCHES

FIGURE 33

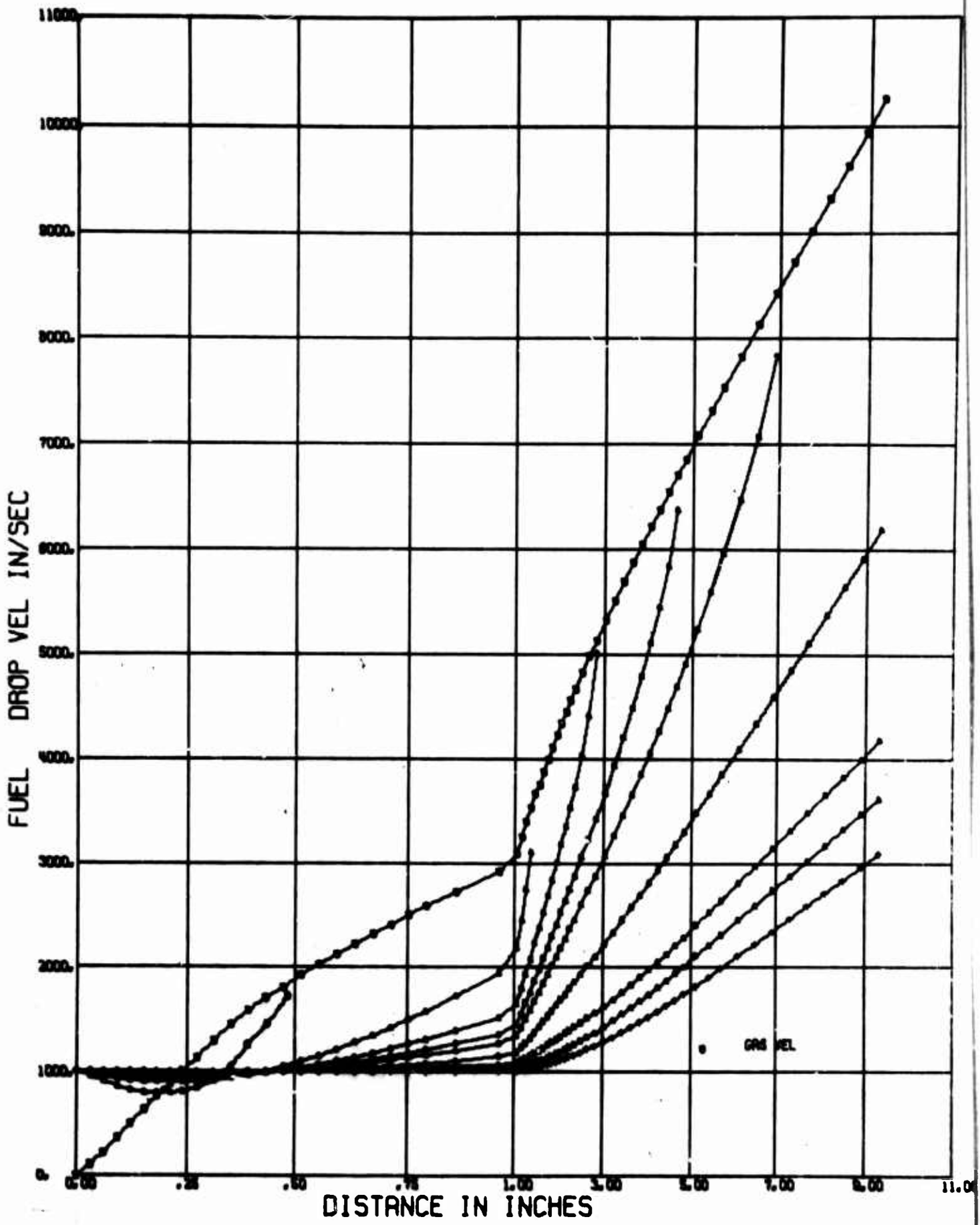
FUEL DROP VEL IN/SEC
DISTANCE IN INCHES
11000
10000
9000
8000
7000
6000
5000
4000
3000
2000
1000
0
0.00
.25
.50
.75
1.00
2.00
5.00
7.00
8.00
11.00

FIGURE 34

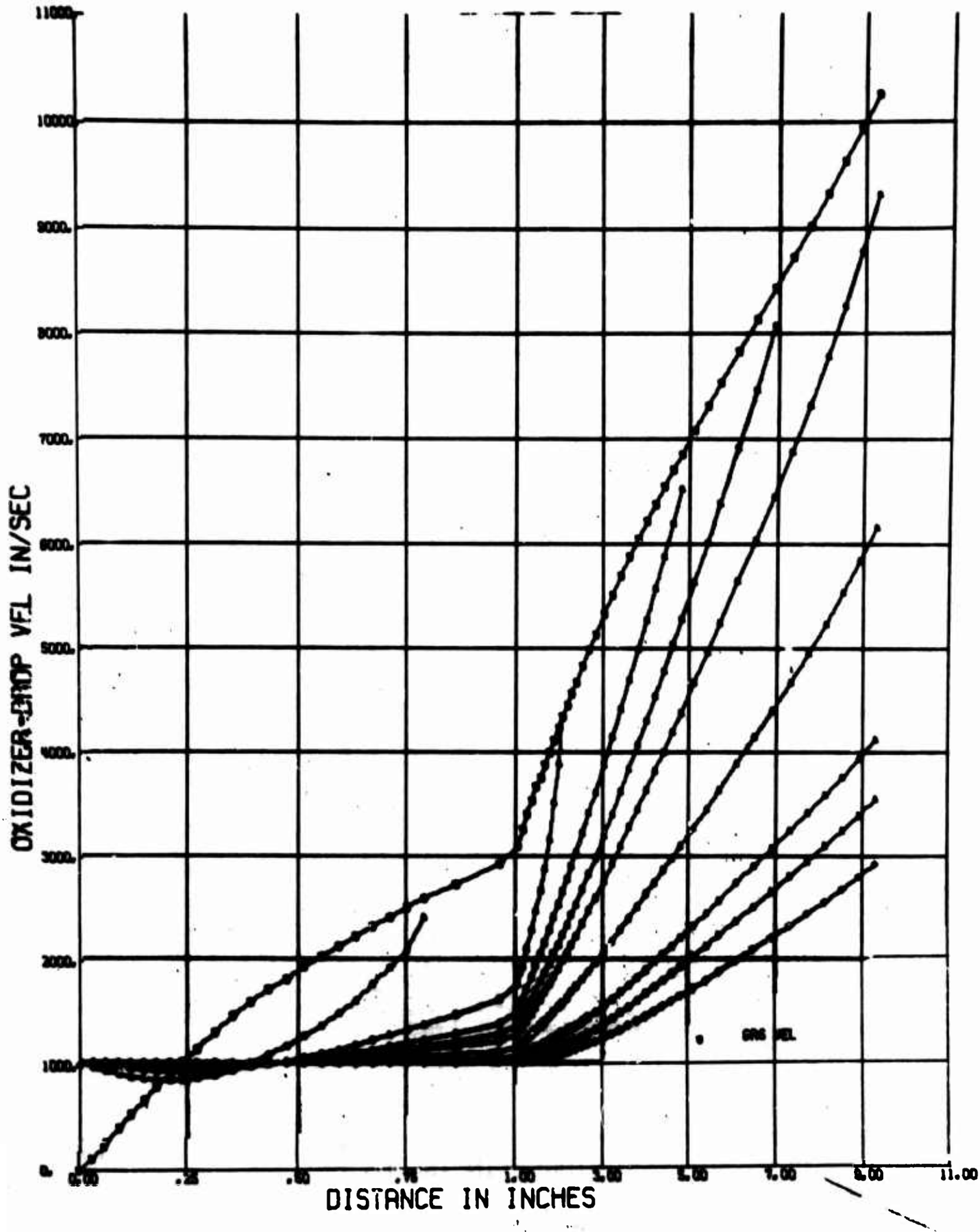
OXIDIZER-DROP VEL IN/SEC
DISTANCE IN INCHES
11000.
10000.
9000.
8000.
7000.
6000.
5000.
4000.
3000.
2000.
1000.
0.
.25
.50
.75
1.00
2.00
5.00
7.00
8.00
11.00

FIGURE 35

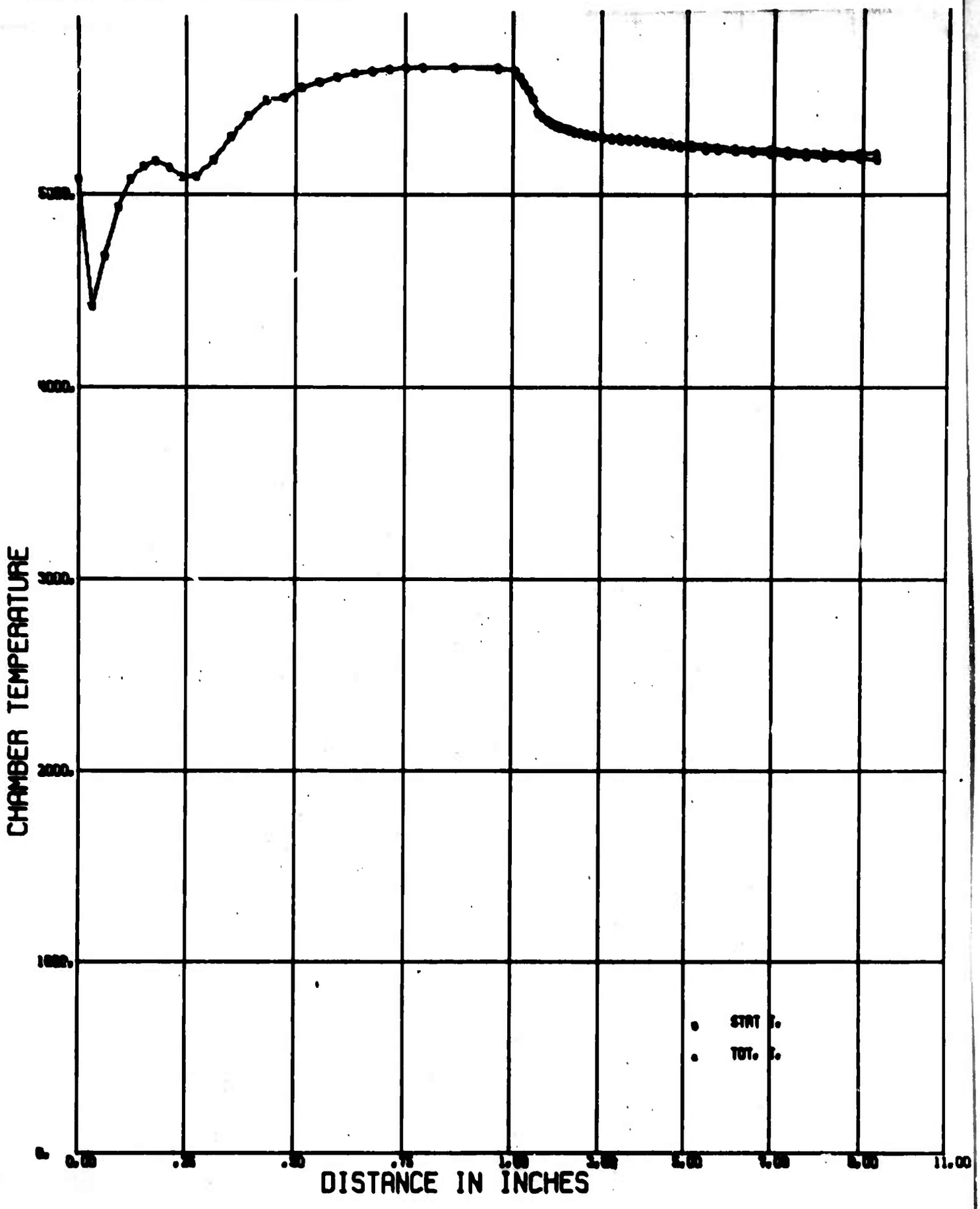

FIGURE 36

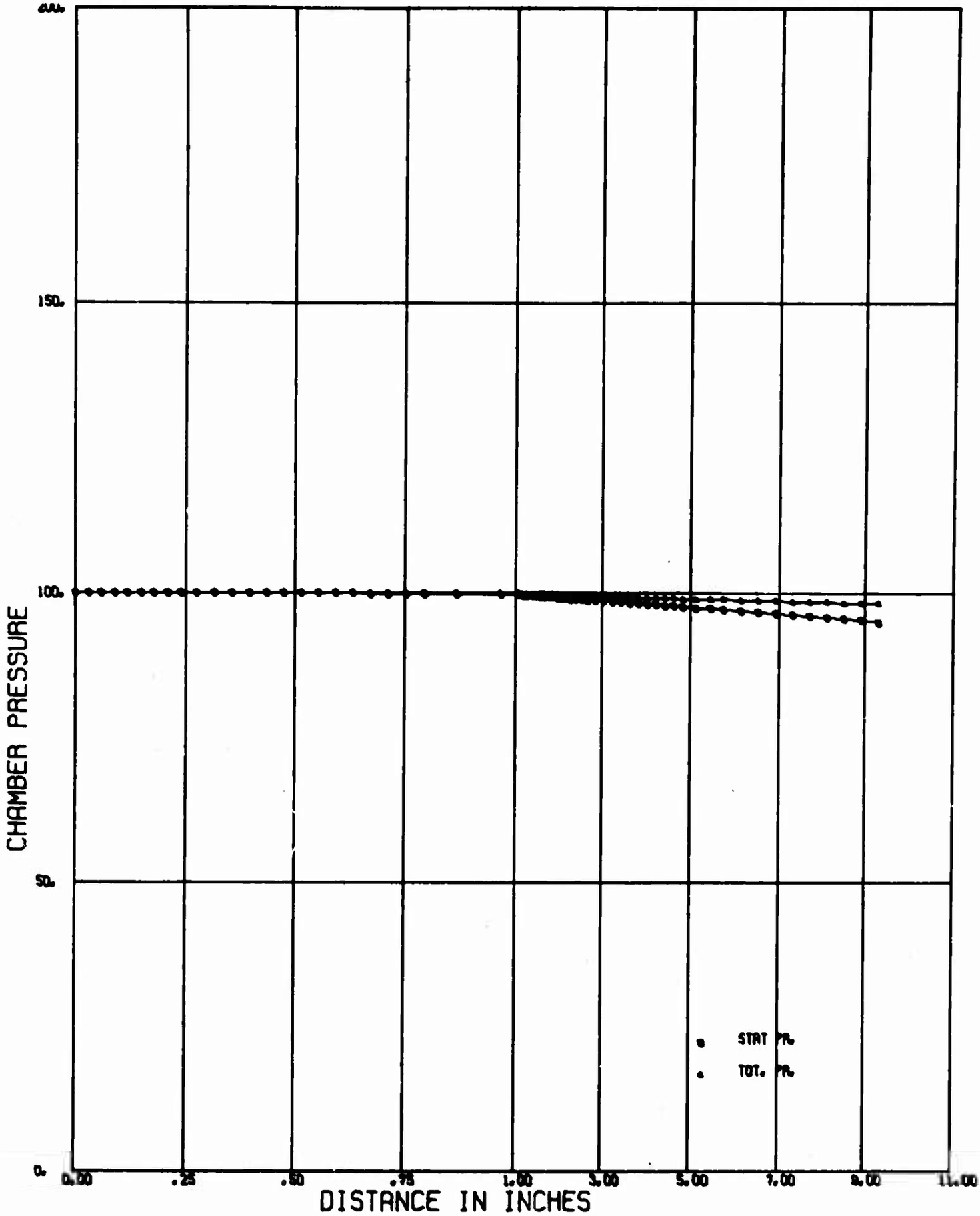
200.
150.
100.
50.
0.
CHAMBER PRESSURE
0.00
.25
.50
.75
1.00
3.00
5.00
7.00
9.00
11.00
DISTANCE IN INCHES
STAT PR.
TOT. PR.

FIGURE 37

APPENDIX II.

COMBUSTION INSTABILITY PROGRAM DESCRIPTION

The Dynamic Science Corporation combustion instability program solves the following set of nonlinear partial differential equations. Cylindrical coordinates are used, in which the z direction corresponds to the axial direction in the chamber. The following dimensionless equations are the result:

Continuity:

$$\frac{\partial \rho'}{\partial t'} + \rho' \left(\frac{\partial v'_\theta}{\partial \theta'} + \frac{\partial v'_z}{\partial z'} \right) + v'_\theta \frac{\partial \rho'}{\partial \theta'} + v'_z \frac{\partial \rho'}{\partial z'} = L\omega' f(\gamma) \qquad \text{(II-1)}$$

Momentum (in θ-direction):

$$\rho' \frac{\partial v'_\theta}{\partial t'} + \rho' v'_\theta \frac{\partial v'_\theta}{\partial \theta'} + \frac{1}{\gamma} \frac{\partial P'}{\partial \theta'} + L\omega' v'_\theta f(\gamma) = \frac{4}{3} J \frac{\partial^2 v'_\theta}{(\partial \theta')^2} f(\gamma) \qquad \text{(II-2)}$$

Energy:

$$\rho' \left(\frac{\partial T'}{\partial t'} + v'_\theta \frac{\partial T'}{\partial \theta'} + v'_z \frac{\partial T'}{\partial z'} \right) + (\gamma - 1) P' \left(\frac{\partial v'_\theta}{\partial \theta'} + \frac{\partial v'_z}{\partial z'} \right) = J \frac{\partial^2 T'}{(\partial \theta')^2} f(\gamma)$$
$$+ L\omega' \left\{ (\gamma - T') + \frac{\gamma - 1}{2} \gamma \left[(\Delta v')^2 + v'^2_\theta \right] \right\} f(\gamma)$$
$$+ \frac{4}{3} \gamma(\gamma - 1) J \left[\left(\frac{\partial v'_\theta}{\partial \theta} \right)^2 + \left(\frac{\partial v'_z}{\partial z'} \right)^2 - \frac{\partial v'_\theta}{\partial \theta'} \frac{\partial v'_z}{\partial z'} \right] f(\gamma) \qquad \text{(II-3)}$$

Ideal Gas:

$$\frac{\partial P'}{\partial \theta'} = T' \frac{\partial \rho'}{\partial \theta'} + \rho' \frac{\partial T'}{\partial \theta'} \qquad \text{(II-4)}$$

The set of equations (II-1, 2, 3) represents a mathematical model used for the analytical determination of the minimum pressure or velocity perturbation required to develop into a traveling wave within the combustion chamber. The one dimensional model employs an annular section of the combustion chamber of thickness Δr and of length Δz.

Previous solutions to analyze combustion instability employ a first order explicit finite difference scheme in the time direction. The spatial or theta derivatives are approximated with a Stirling first order central difference relation. Initial investigation demonstrated that indications of combustion instability were not entirely valid. That is error propagation during the computer solution was giving false indications of combustion instability.

Since the solution of the system of second order nonlinear equations essentially represents an initial value problem for a system of differential equations, it was decided to use more stable but numerically more cumbersome, higher order difference methods. The Dynamic Science computer program uses a third order Adams Bashforth predictor given by:

$$y_{k+1} = y_k + \frac{h}{24}(55f_k - 59f_{k-1} + 37f_{k-2} - 9f_{k-3}) \qquad \text{(II-5)}$$

and a third order Adams Moulton corrector formula of the form

$$y_{k+1} = y_k + \frac{h}{24}(9f_{k+1} + 19f_k - 5f_{k-1} + f_{k-2}) \qquad \text{(II-6)}$$

to advance the solution at each time step. It should be noted that previous methods of solution to the nonlinear set of equations involve only first order methods to advance the solution to the next time step. The present difference equations require a history of four previous points in order to advance the solutions to the next time step. The first order method sustains an error term of order $(\Delta t)^2$ while the predictor corrector formulae (II-5 and 6) sustain an error of order $(\Delta t)^5$ and hence allow larger step sizes during integration while maintaining numerically stable solutions and minimizing error propagation.

The Dynamic Science Corporation program corrects only once and rather than continuing to iterate to converge to the solution a test is made during the integration cycle to check for four significant figure agreement between the predicted values and the corrected values. If sufficient agreement exists then the solution can continue. If sufficient agreement does not exist then the time step is reduced by a factor of 2 and the solution is continued from the last point which satisfied the four significant figure agreement. If sufficient agreement is maintained for eight or more points provisions are made for doubling the independent step. At the present time the step control is based on the absolute difference between predicted and corrected ordinates of the integrated functions ρ, v, and T.

In the spatial or theta direction the accuracy of the theta derivative has been improved by employing higher order central difference formulae. The first order program uses the following equations:

$$\left(\frac{\partial T}{\partial \theta}\right)_{m,n} = \frac{T_{m+1,n} - T_{m-1,n}}{2\Delta\theta} \qquad \text{(II-7)}$$

While the Dynamic Science Corporation computer solution employs the following fourth order central difference relation.

$$\left(\frac{\partial T}{\partial \theta}\right)_{m,n} = \frac{1}{12.\Delta\theta}\left\{T_{m-2,n} - 8.0(T_{m-1,n} - T_{m+1,n}) - T_{m+2,n}\right\} \qquad \text{(II-8)}$$

where $T_{m,n} = T_{(m\Delta\theta, n\Delta t)}$.

The derivatives in the axial direction are determined with the assumption that the total mass, momentum, and energy in the annulus are constant. Furthermore, it is assumed that these derivatives are independent of r and θ. These assumptions result in the following equations, which permit evaluation of the derivatives taken with respect to z:

<u>Continuity</u>:

$$\frac{\partial v'_z}{\partial z'} \int_0^{2\pi} \rho' \, d\theta' + 2\pi v'_z \frac{\partial \rho'}{\partial z'} = Lf(\gamma) \int_0^{2\pi} \omega' \, d\theta' \qquad \text{(II-9)}$$

<u>Momentum:</u>

$$v'_z \frac{\partial v'_z}{\partial z'} \int_0^{2\pi} \rho' \, d\theta' + \frac{1}{\gamma}\left(\frac{\partial \rho'}{\partial z'} \int_0^{2\pi} T' \, d\theta' + \frac{\partial T'}{\partial z'} \int_0^{2\pi} \rho' \, d\theta'\right)$$

$$= -L\Delta v' f(\gamma) \int_0^{2\pi} \omega' \, d\theta' \qquad \text{(II-10)}$$

Energy:

$$v'_z \frac{\partial T'}{\partial z'} \int_0^{2\pi} \rho' \, d\theta' + (\gamma-1) \frac{\partial v'_z}{\partial z'} \int_0^{2\pi} P' \, d\theta' = \frac{8\pi\gamma}{3}(\gamma-1) \, Jf(\gamma) \left(\frac{\partial v'_z}{\partial z'}\right)^2$$

$$+ Lf(\gamma) \int_0^{2\pi} \omega' \left[(\gamma - T') + \gamma \frac{\gamma-1}{2} (\Delta v')^2\right] d\theta' \qquad \text{(II-11)}$$

Ideal Gas:

$$2\pi \frac{\partial P'}{\partial z'} = \frac{\partial \rho'}{\partial z'} \int_0^{2\pi} T' \, d\theta' + \frac{\partial T'}{\partial z'} \int_0^{2\pi} \rho' \, d\theta' \qquad \text{(II-12)}$$

Equation (II-10 - 12) lead to the following system of algebraic equations to be solved at each step in time.

$$\begin{aligned}
a_1 x_1 + a_2 x_2 &= c_1 \\
a_3 x_1 + a_4 x_3 &= c_2 + a_5 x_1^2 \qquad \text{(II-13)} \\
a_6 x_1 + \frac{a_7}{\gamma} x2 + \frac{a_8}{\gamma} x_3 &= c_3 \\
a_7 x_2 + a_8 x_3 + 2\pi x_4 &= 0,
\end{aligned}$$

where (x_1, x_2, x_3, x_4) represents $\left(\frac{\partial v}{\partial z}, \frac{\partial \rho}{\partial z}, \frac{\partial T}{\partial z}, \frac{\partial P}{\partial z}\right)$ respectively and $a_1, \ldots, a_8$ are obtained from (II-9,10,11,12). It might be noted that the z derivatives are permitted to change with time but remain constant around the annulus at each time step. (i.e. only gross property changes are permitted in the solution of this mathematical model.)

The integration cycle consists of six subroutines defined as follows:

(1) Subroutine ASET determines the coefficients of system of equations II-13 to obtain the axial derivatives based on the assumptions that the total mass, energy, and momentum remain constant in the annulus and the axial derivatives are

independent of r and θ.

(2) Subroutine ZDIR solves a fourth order nonlinear system of equations for the axial derivatives using a second order Taylor expansion.

(3) Subroutine TDIR computes the t derivatives at each of the theta nodal positions using equations(II-1, 2, and 3).

(4) Subroutine NADM uses a third order multistep procedure, equations (II-5 and 6), to integrate the variables ρ, T, and v, and compute the absolute difference between the predicted and corrected values for automatic step control at each of the theta nodes of the annulus.

(5) Subroutine THPRED determines theta derivatives of the integrated variables for each of the theta positions around the annulus using equation (II-8).

(6) Finally subroutine SHIFT moves the computed points at the current time step to the position of the previous time step in order to begin the integration cycle at step (1) for the succeeding time step.

The remaining subroutines can be described as follows:

(1) REED - reads initial data.

(2) ORG - initializes print and integration counters.

(3) RSET - Initializes pressure velocity, temperature and density around the annulus.

(4) AVGE - Forms (PMAX-PMIN)/PAVGE for plotting.

(5) DRAW - Subroutine to form graphical output.

Figure 38 represents a graphical presentation of the logic involved in the main program. The routines involved in the integration loop are described above. The test on MPTN indicated in the previous diagram is merely a print indicator in order that the print will occur at equal intervals even though the independent step may be changing in magnitude.

Figure 39 represents the input card format for the Dynamic Science Corporation combustion instability program. The graphical display of the indicated input data is shown in Figures 40-49. Finally, Section II contains a complete listing of the Dynamic Science instability program.

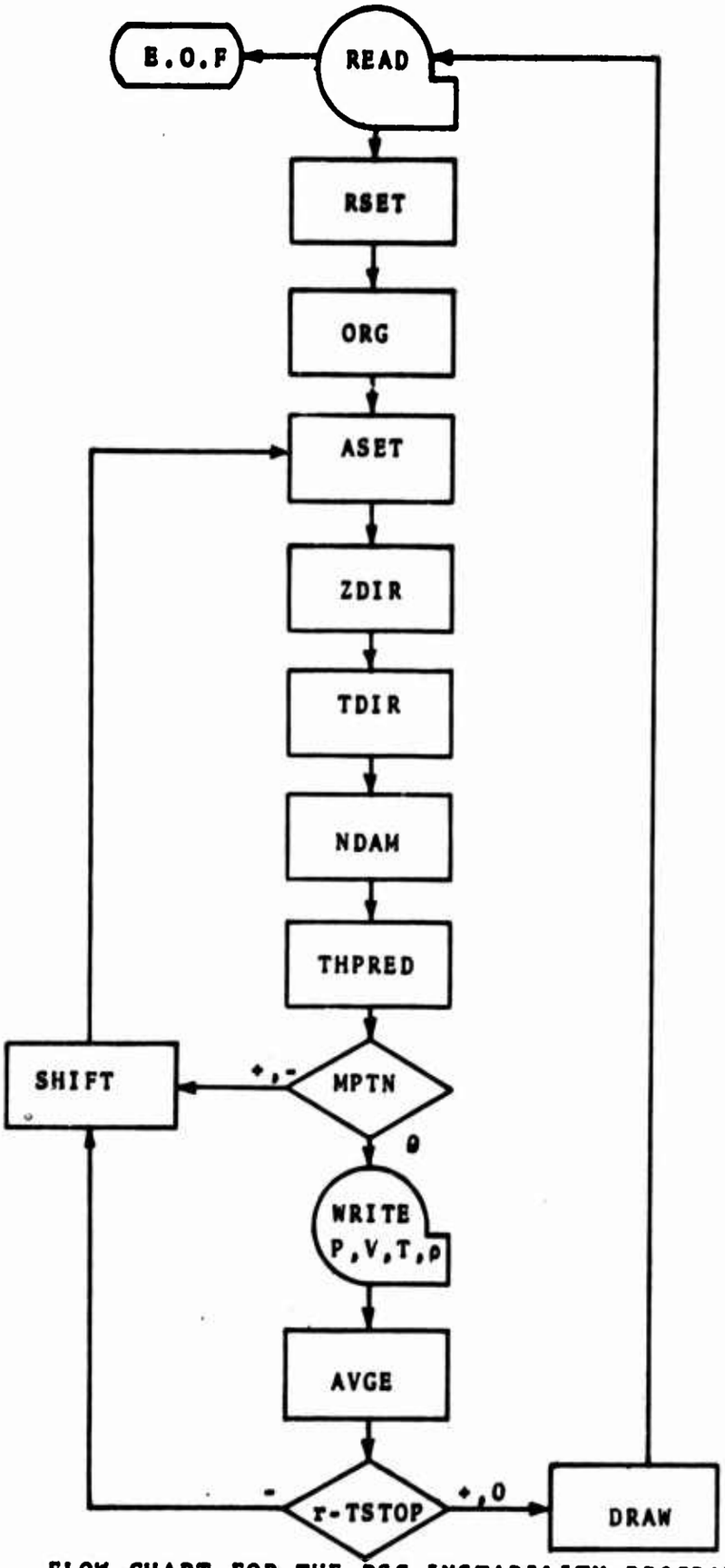

FLOW CHART FOR THE DSC INSTABILITY PROGRAM
FIGURE 38

IBM

Form X28-7327-4
Printed in U.S.A.

FORTRAN CODING FORM

Program		Punching Instructions: Graphic / Punch	Card Form # *
Programmer	Date		Page of / Identification (73–80)

C FOR COMMENT

STATEMENT NUMBER (1–5) | Cont. (6) | FORTRAN STATEMENT (7–72)

CARD NUMBER ONE					
	Maximum	Minimum Error	Maximum Error	Burning Rate	Reynolds Number
Initial Time	Allowable Δt	For P.C. Cycle	For P.C. Cycle	Parameter L	
0.0	.03125	.0001	.01	.028	0.0
CARD NUMBER TWO					
Viscous Dissip.	Delta V	Gamma	One-Half	Schmidt Number	Axial Velocity
Parameter J	ΔV	γ	Initial Press.		
.00000003	.02	1.20	.25	1.0	.05
CARD NUMBER THREE					
	Time Stop				
	18.0				
CARD NUMBER FOUR					
NSW Print Indic.	MP (HMin) = (Max.Step/2.**MP)	No.(Max.Step*No.) = PRT.INT.	ND - No. of Theta Nodes+1		
0	0	1	41		

FIGURE 39

* A standard card form, IBM electro 888157, is available for punching source statements from this form.

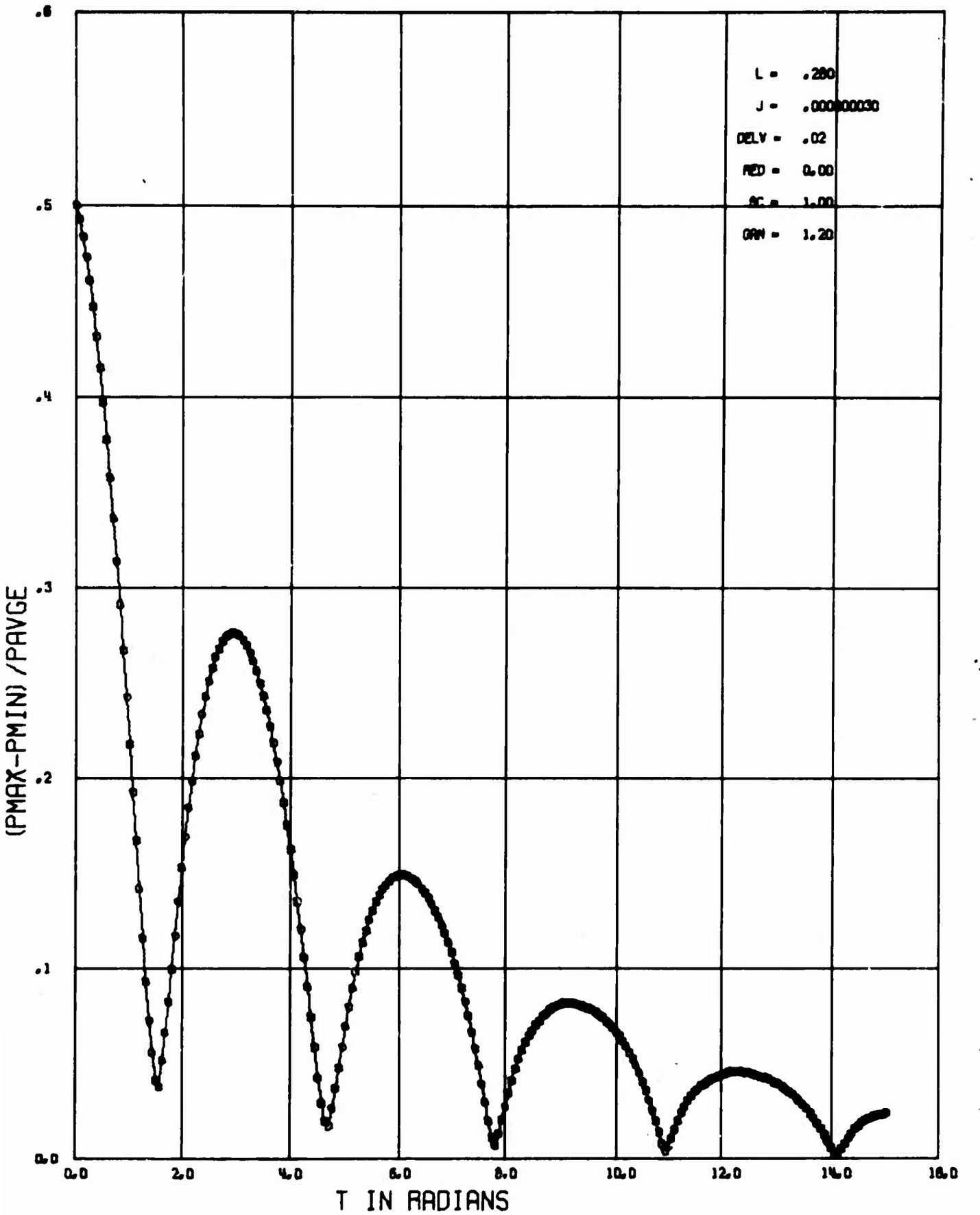
L = .280
J = .000000030
DELV = .02
RED = 0.00
RC = 1.00
GAN = 1.20
(PMAX-PMIN) /PAVGE
T IN RADIANS
.6
.5
.4
.3
.2
.1
0.0
0.0
2.0
4.0
6.0
8.0
10.0
12.0
14.0
16.0

FIGURE 40

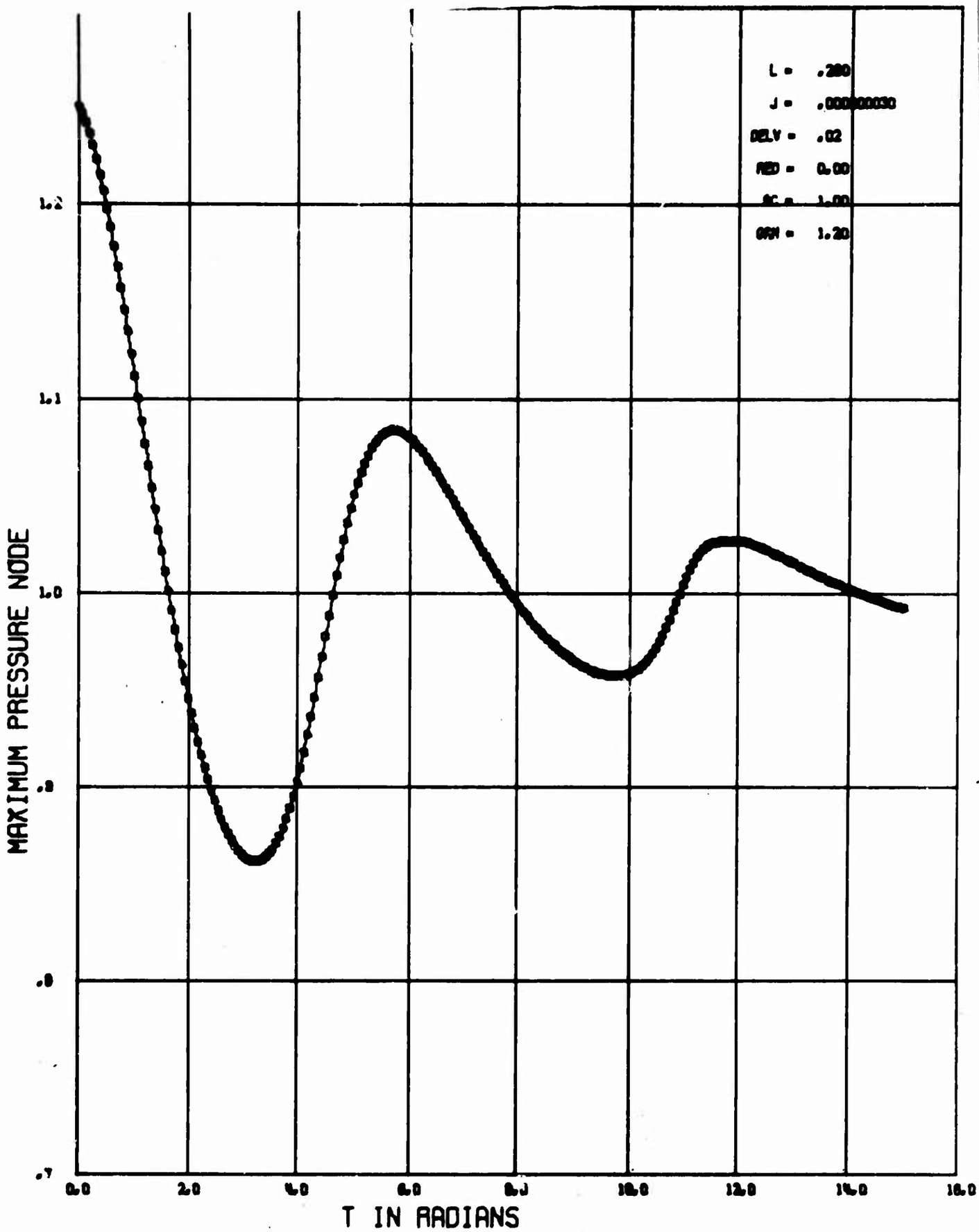
L = .200
J = .000000030
DELV = .02
RED = 0.00
SC = 1.00
GRN = 1.20
MAXIMUM PRESSURE NODE
T IN RADIANS

FIGURE 41

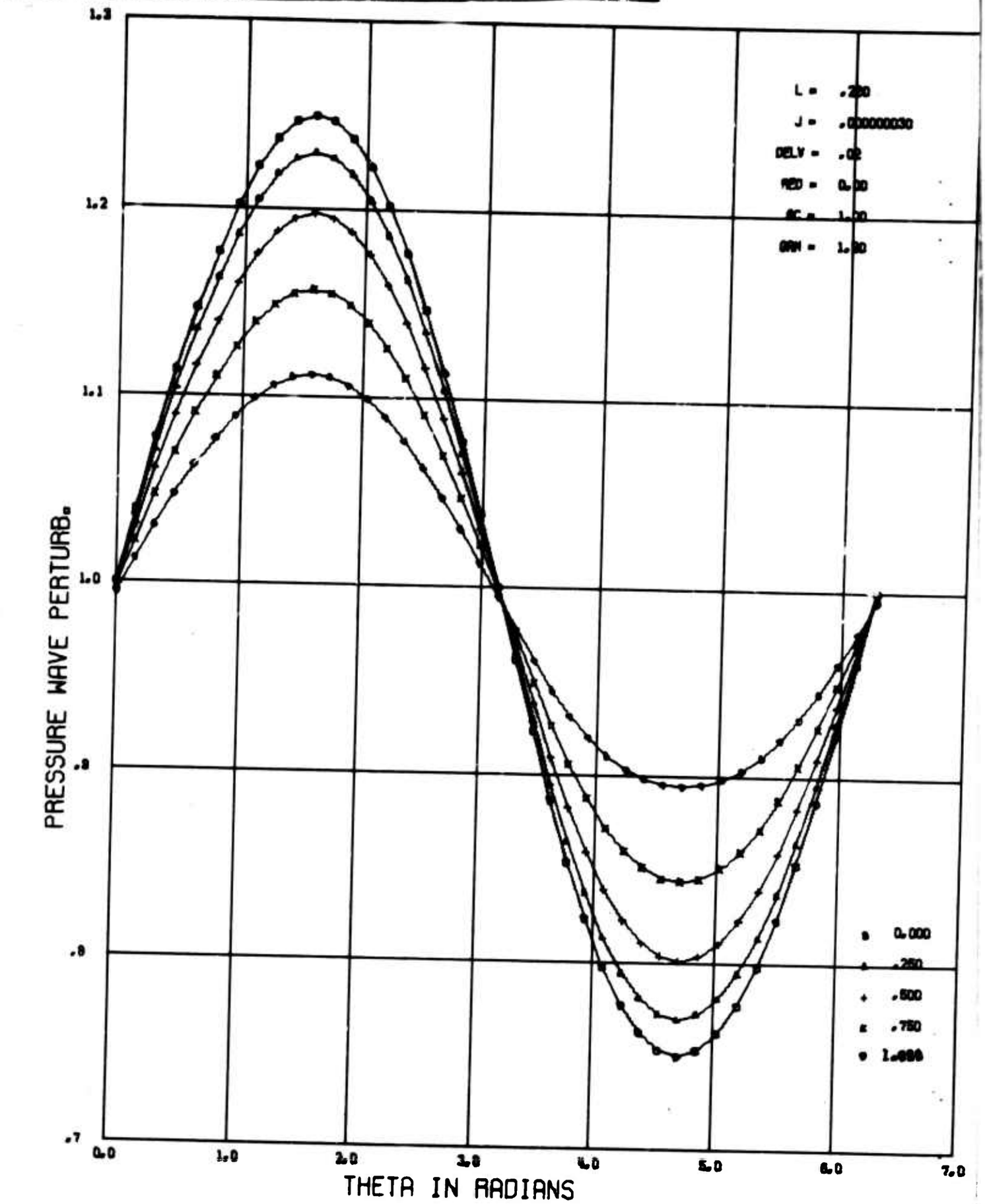
L = .200
J = .000000030
DELV = .02
RED = 0.00
BC = 1.00
GRN = 1.00
0.000
.250
.500
.750
1.000
PRESSURE WAVE PERTURB.
THETA IN RADIANS
1.3
1.2
1.1
1.0
.9
.8
.7
0.0
1.0
2.0
3.0
4.0
5.0
6.0
7.0

FIGURE 42

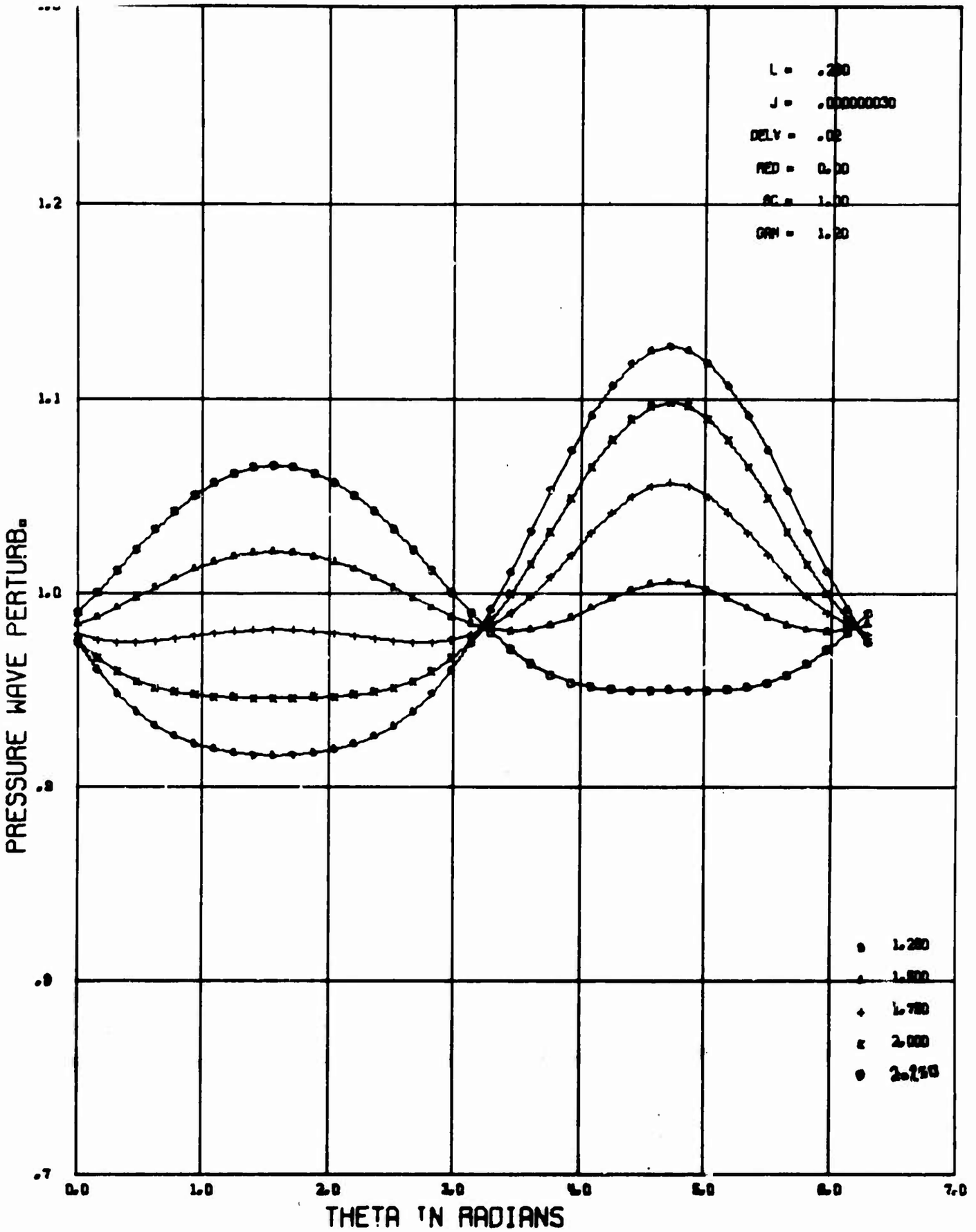
L = .200
J = .000000030
DELV = .02
RED = 0.00
RC = 1.00
GAM = 1.20
1.280
1.800
1.780
2.000
2.250
PRESSURE WAVE PERTURB.
THETA IN RADIANS
1.2
1.1
1.0
.9
.7
0.0
1.0
2.0
3.0
4.0
5.0
6.0
7.0

FIGURE 43

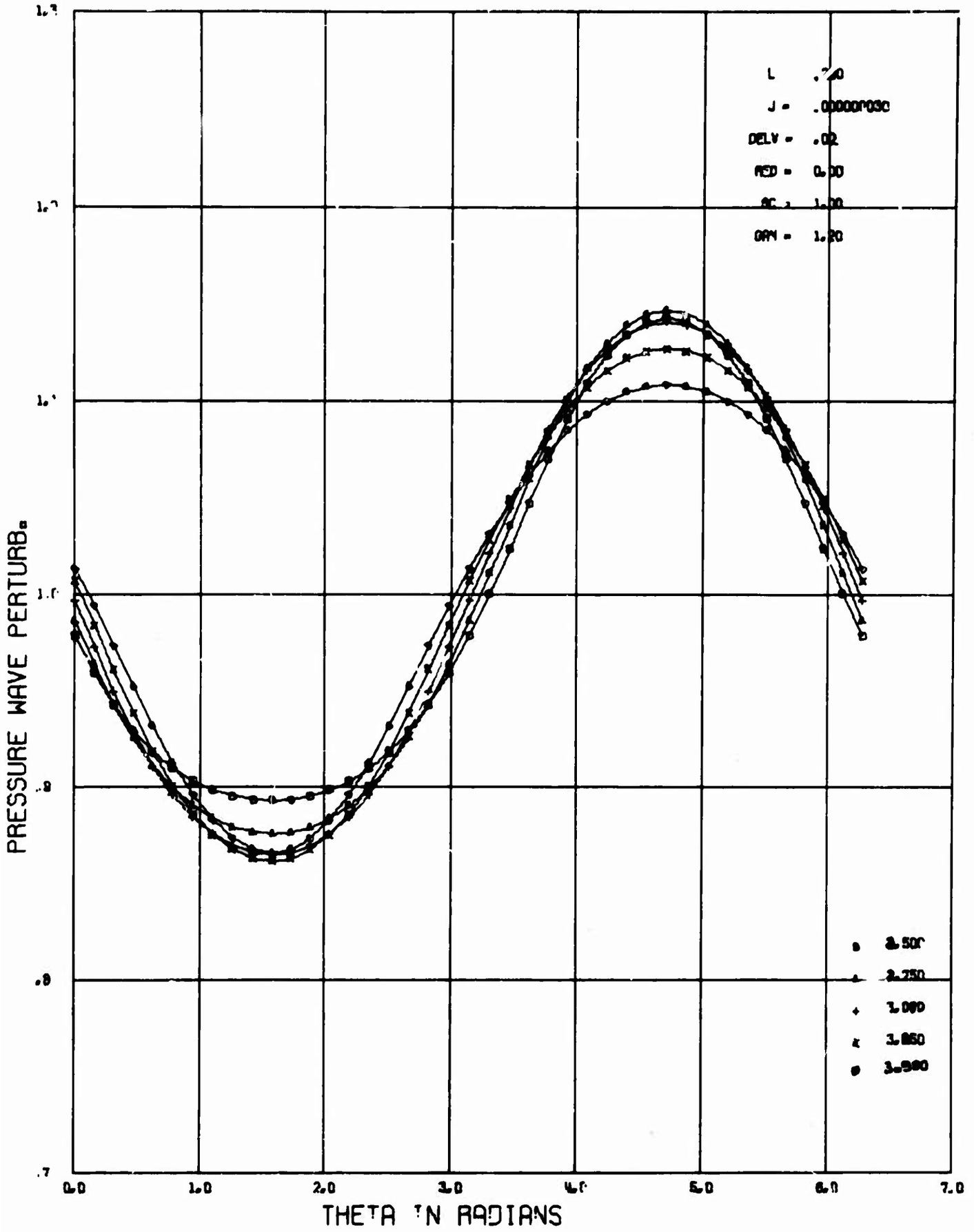

L
J = .000000030
DELV = .02
RED = 0.00
SC = 1.00
GAN = 1.20
PRESSURE WAVE PERTURB.
THETA IN RADIANS
0.0
1.0
2.0
3.0
4.0
5.0
6.0
7.0

FIGURE 44

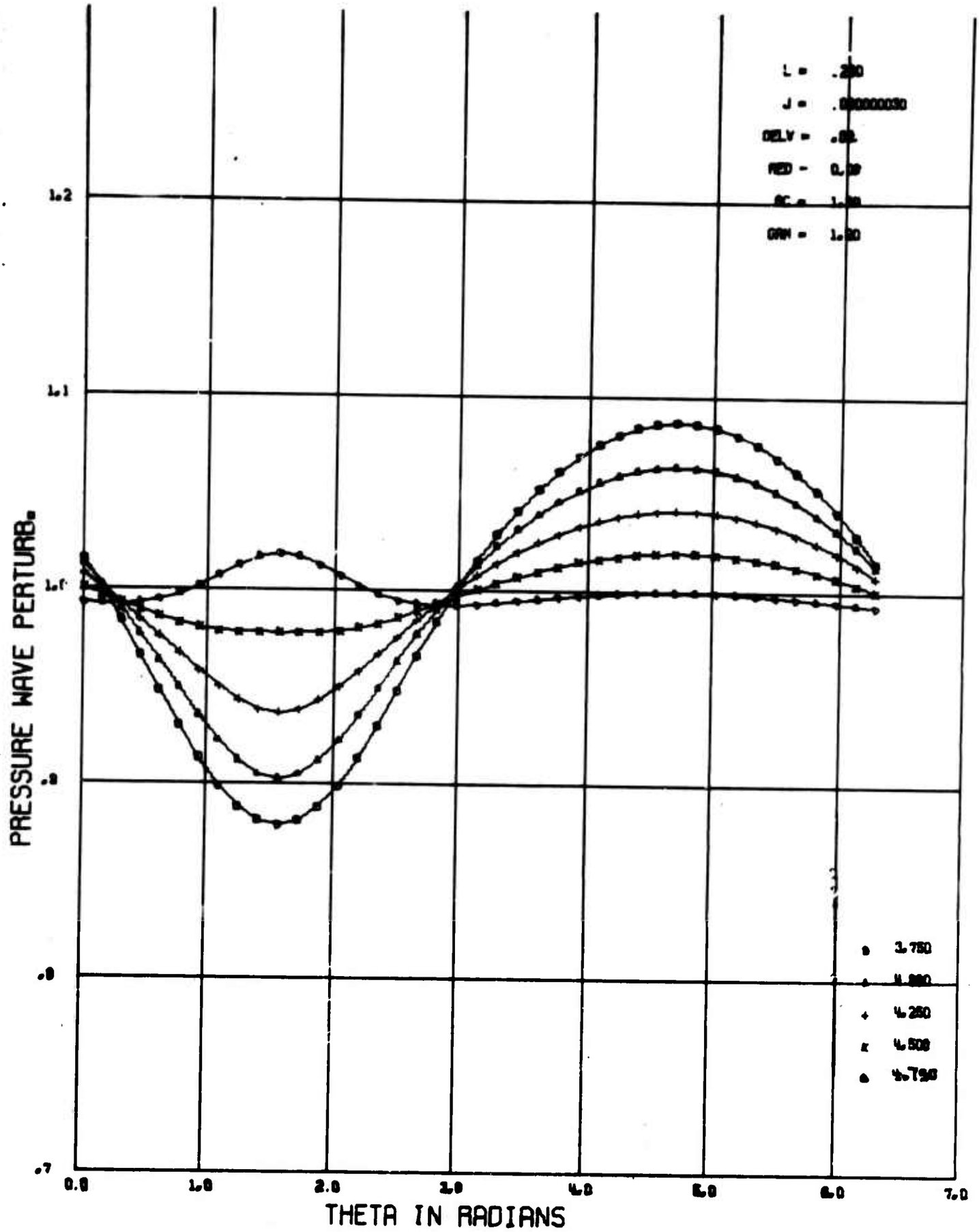

L = .200
J = .000000030
DELV = .02
RED = 0.00
AC = 1.00
GAM = 1.00
1.2
1.1
1.0
.9
.8
.7
PRESSURE WAVE PERTURB.
0.0
1.0
2.0
3.0
4.0
5.0
6.0
7.0
THETA IN RADIANS
3.750
4.250
4.500

FIGURE 45

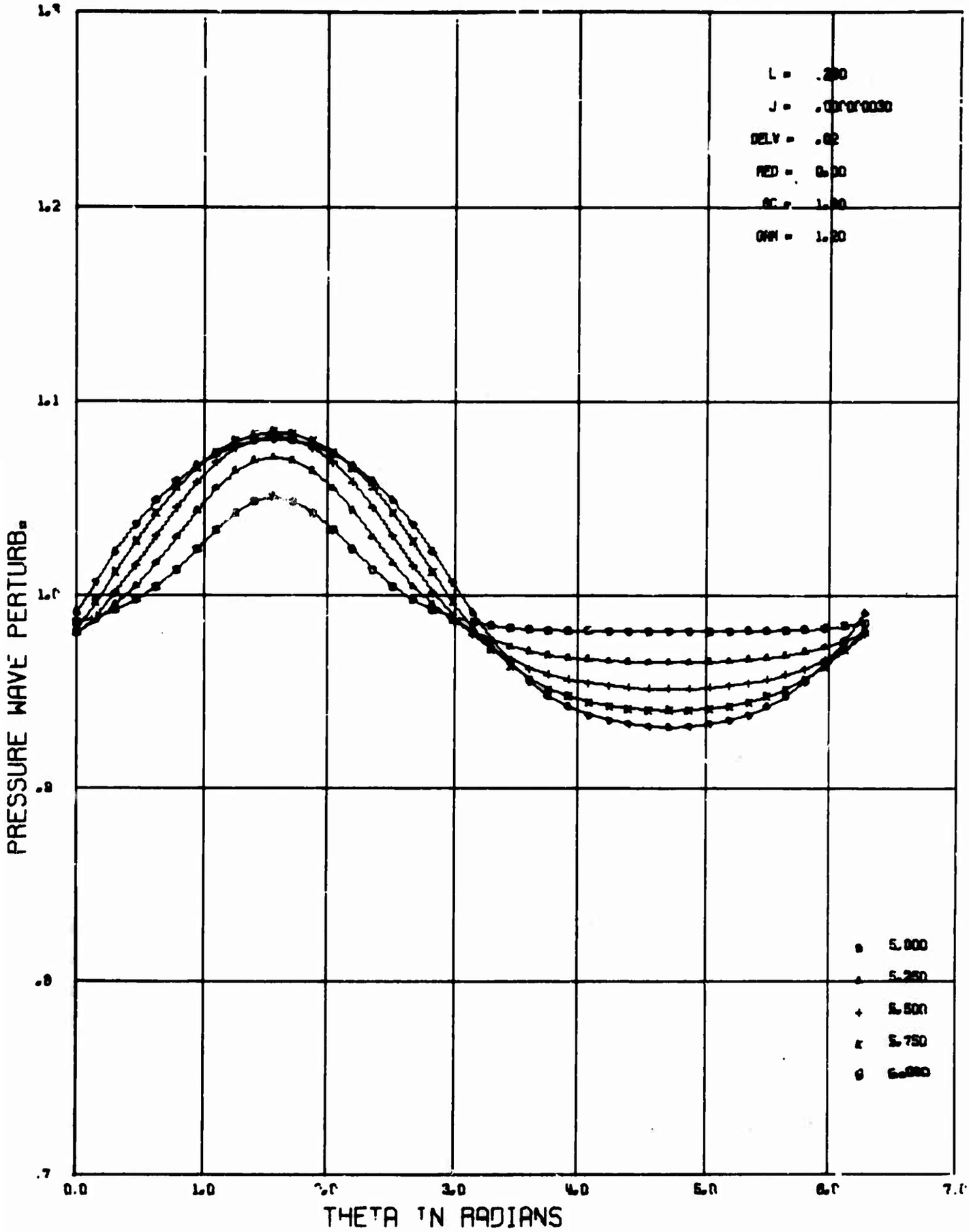
L = .200
J = .00000030
DELV = .02
RED = 0.00
OMN = 1.20
5.000
5.250
5.500
5.750
6.000
PRESSURE WAVE PERTURB.
THETA IN RADIANS
0.0
1.0
3.0
4.0
5.0
1.2
1.1
.8
.7

FIGURE 46

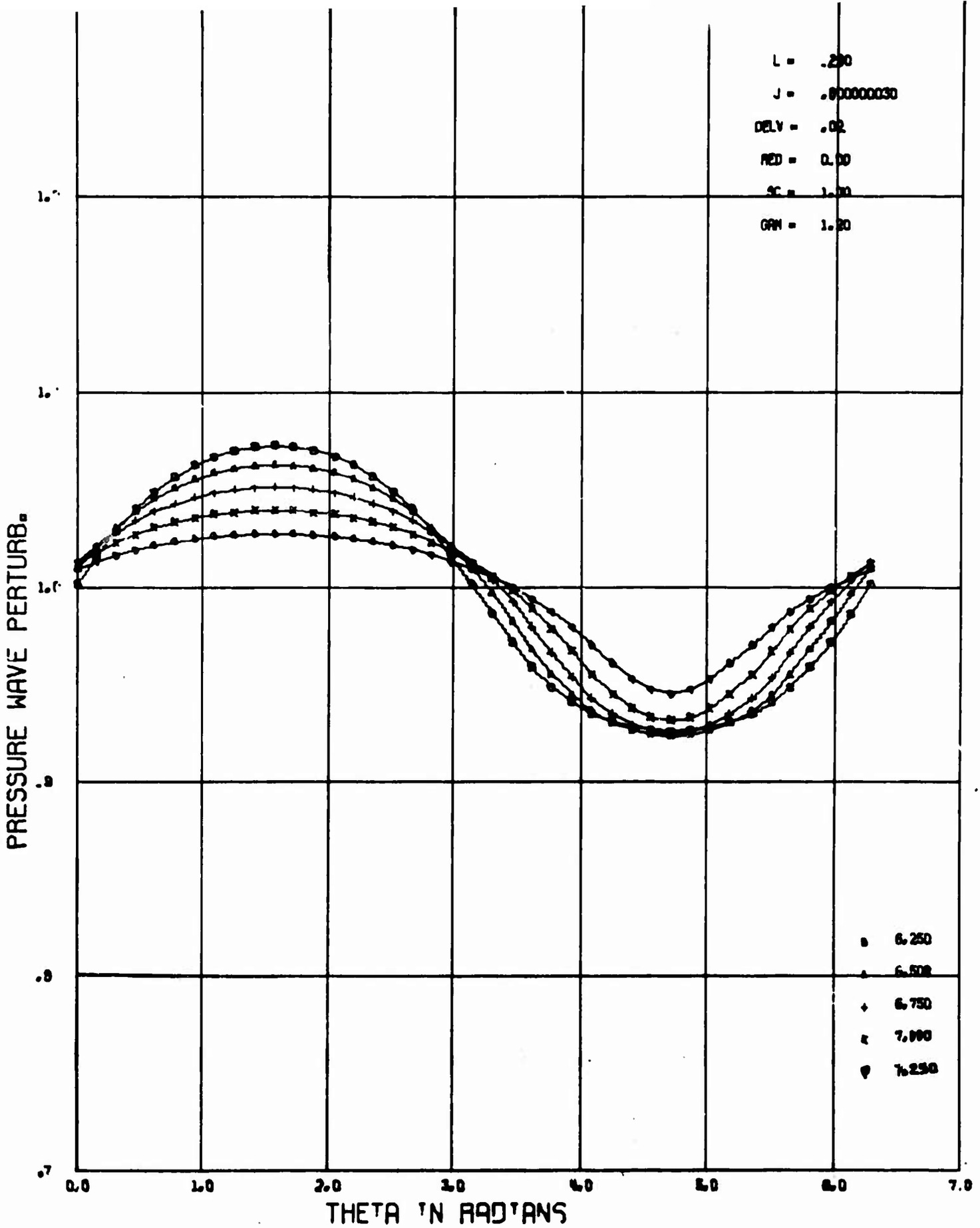
L = .200
J = .000000030
DELV = .02
RED = 0.00
SC = 1.00
GAM = 1.20
6.250
6.500
6.750
7.000
7.250
PRESSURE WAVE PERTURB.
THETA IN RADIANS
0.0
1.0
2.0
3.0
4.0
5.0
6.0
7.0
.7
.8
.9
1.0
1.1
1.2

FIGURE 47

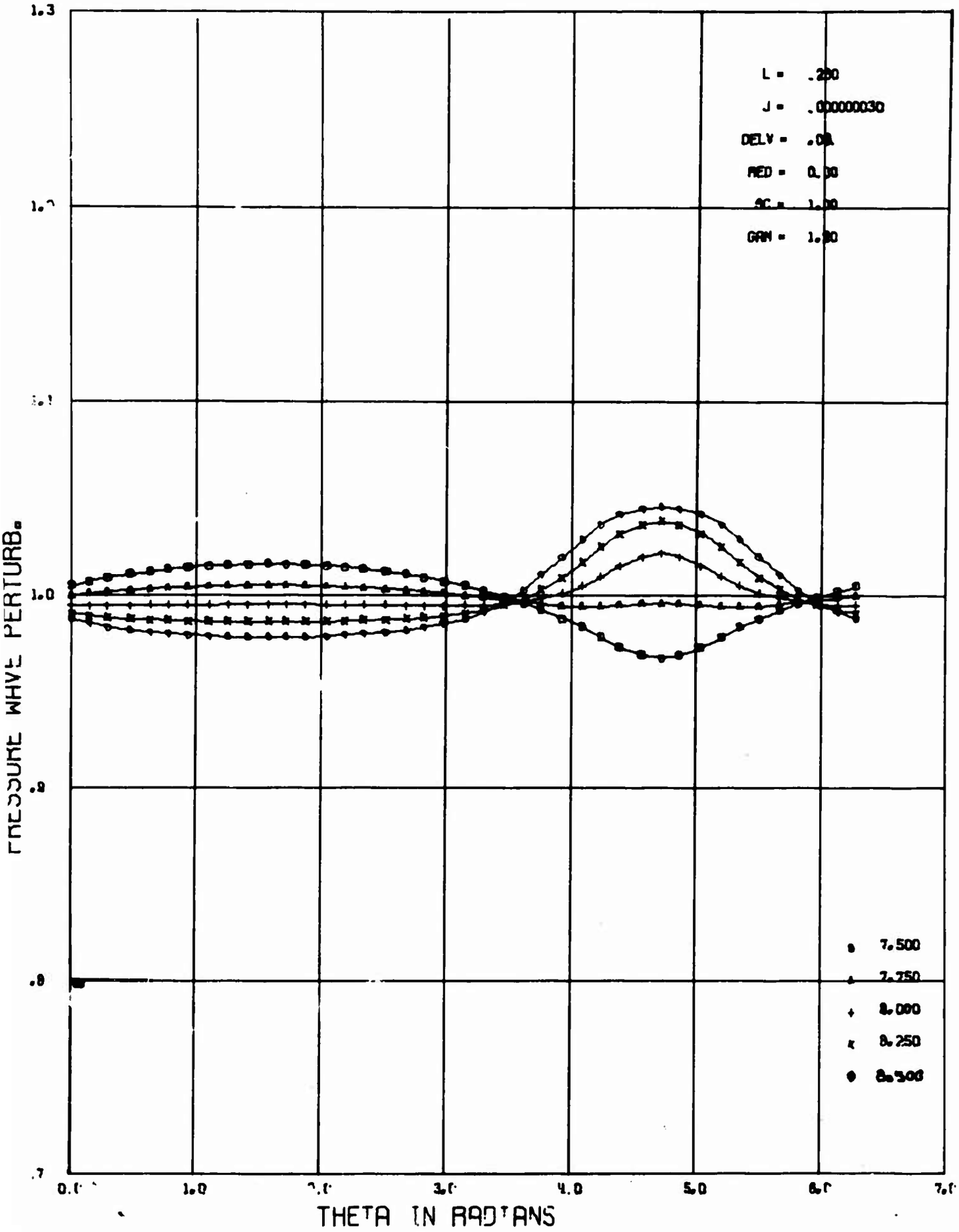
L = .200
J = .00000030
DELV = .001
RED = 0.00
GRN = 1.00
7.500
7.750
8.000
8.250
8.500
1.3
1.0
.9
.8
.7
0.0
1.0
2.0
3.0
4.0
5.0
6.0
7.0
THETA IN RADIANS

FIGURE 48

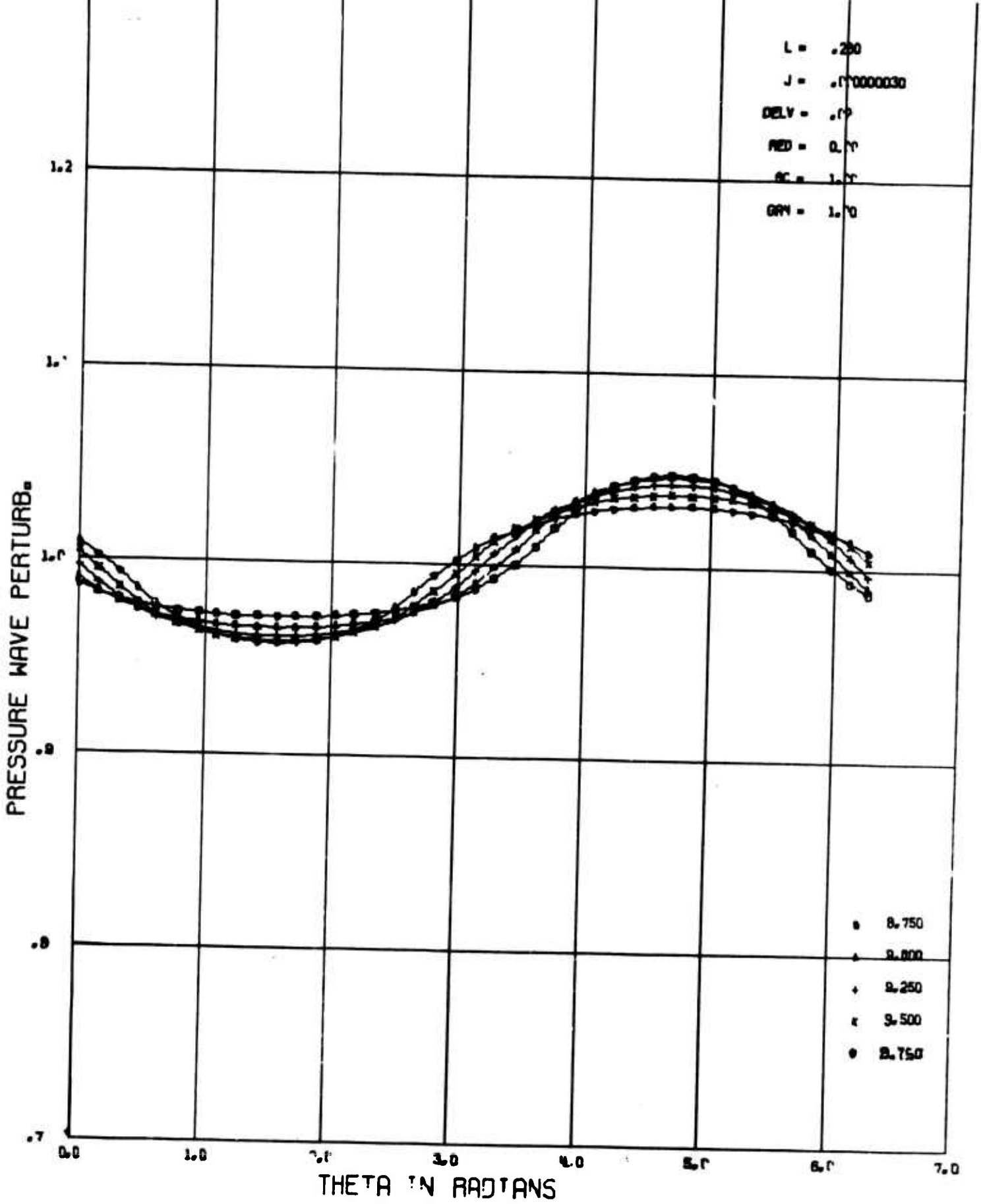

L = .280
J = .000000030
DELV = .0
RED = 0.0
AC = 1.0
GAM = 1.0
1.2
1.0
.9
.8
.7
PRESSURE WAVE PERTURB.
0.0
1.0
3.0
4.0
5.0
6.0
7.0
THETA IN RADIANS
8.750
9.000
9.250
9.500
8.750

FIGURE 49

2. Program Listing.

```
      PROGRAM MAIN
C     MAIN PROGRAM FOR COMBUSTION INSTABILITY MODEL OF DSC
      DIMENSION FC(80), NM(20),  BD(10,21,16), ART(2000,2), V(10,21)
     1 , P(10,21) ,RHO(10,21), T (10, 21)
       DIMENSION DTT(10,21),DTTH(10,21),DRHOTH(10,21),DVT(10,21)
     1 ,DVTH(10,21), DRHOT(10,21)
       DIMENSION W(10,21), WZ(10,21)
      COMMON /E/ FC,NM /B/ BD /C/ ART
      EQUIVALENCE (BD(2941), W), (BD(3151), WZ)
       EQUIVALENCE (BD(1051),DTTH),(BD(1891),DRHOTH), (BD(2521),DVTH)
      EQUIVALENCE  (FC(1), TI), (FC(31), TSTOP), (NM(4), MGAM),
     1 (FC(3), H), (NM(5), MPTN), (NM(3), MALP), (NM(13), I),
     2 (FC(38), ZIP), (FC(32), XL), (FC(34), XJ), (FC(35), DELV),
     3 (FC(36), GAM) ,(NM(7),NSW)
      EQUIVALENCE (BD(631),  T), (BD(841), DTT), (BD(2101), V),
     1 (BD(2311), DVT), (BD(1471), RHO), (BD(1681), DRHOT), (BD(1), P)
C     FORM   INITIALIZES COUNTERS FOR INTEGRATION ROUTINE
C     READ 'N TITLES FOR PLOTTING ROUTINES FIX TITLES
C     EXECUTE  DATA READ FOR BOTH INTEGRATION AND STABILITY INITIALIZAT
    5   I = 1
       CALL REED
      CALL RSET
C     SUBROUTINE  ORG INITIALIZES PRINT COUNTERS AND SETS UP THE NECESS
C     ARY  INTEGRATION TERMS
         CALL ORG
C     SET UP COEFFICIENTS TO SOLVE FOR  Z  DERIVATIVES
   10    CALL ASET
C     SUBROUTINE ZDIR SOLVES FOR Z DERIVATIVES
         CALL  ZDIR
C     NOW SOLVE FOR T DERIVATIVES       P
         CALL TDIR
C     NADM  PERFORMS THE ACTUAL NUMERICAL INTEGRATION
         CALL NADM (DRHOT, RHO, 1)
         CALL NADM (DVT , V, 2)
         CALL NADM (DTT, T,  3)
       CALL THPRED
C     NEXT TEST FOR PRINT POINT
        IF(MPTN) 60,50,60
C     BRANCH TO 50 IMPLIES PRINT POINT OBTAINED
   50    CALL  AVGE
   51 WRITE(6,21) (ART(I,J),J=1,2),H,(P(I,J),RHO(I,J),T(I,J),V(I,J),
     1 W(I,J),WZ(I,J), J=1,21)
   21 FORMAT(1H0,3E20.8/(6E18.8))
       WRITE(6,48)  (DTT(I,J),DTTH(I,J), DRHOT(I,J),DRHOTH(I,J),
     1  DVT(I, J), DVTH(I, J), J=1,21)
   48 FORMAT(1H0, (6E18.8))
   52  I = I+1
C     TEST FOR  TIME STOP.
                IF (TI - TSTOP)  60,  55, 55
C     STORE PRINT POINT FOR  PLOTTING
   55     ZIP  =  ART(1,2)
       I = I-1
C     CALL PLOTTING ROUTINES
      CALL DRAW
         GO  TO 5
C     SUBROUTINE  SHIFT  UPDATES TERMS INVOLVED WITH INTEGRATION
   60    CALL SHIFT
         GO TO 10
                          END
```

```
      SUBROUTINE REED
      DIMENSION FC(80), NM(20), BD(10,81,15), WT(20)
      COMMON /E/ FC,NM /B/BD
      EQUIVALENCE  (FC(1),T), (FC(6),HMAX),(FC(8),EMIN),
     1 (FC(9),EMAX), (FC(11), WT(1)), (FC(31), TSTOP),(FC(32),XL),
     2  (FC(33),RED), (FC(34),XJ), (FC(35),DELV), (FC(36),GAM),
     3 (FC(37),AP), (FC(39),SC), (FC(41), VZ),(FC(54),DTH)
      EQUIVALENCE (NM(7),NSW), (NM(9),MP), (NM(11),NO),(NM(14), ND)
         DO 10 I = 1,20
10     WT(I) = 1.0
      READ( 5,20) T,HMAX, EMIN, EMAX, XL,RED,XJ,DELV,GAM,AP,SC,VZ,DTH
     1 ,TSTOP
         IF( EOF, 60)  90,18
20    FORMAT(6E12.8)
18    READ( 5,21) NSW, MP, NO, ND
21    FORMAT(4I12)
      XND = ND - 1
      DTH = 6.2831853071/XND
      WRITE(6,40) T,HMAX,EMIN,EMAX,XL,RED,XJ,DELV,GAM,AP,SC,VZ,DTH,
     1 TSTOP
40    FORMAT(1H1,21HT,HMAX,EMIN,XL,RED,XJ/1H ,7E15.7/
     1 1H ,26HDELV,GAM,AP,SC,VZ,DTH,TSOP/1H ,7E15.7)
       RETURN
90 END FILE 17
      STOP
      END
```

```
      SUBROUTINE  RSET
      DIMENSION P(10,81), DPTH(10,81), RHO(10,81), DTTH(10,81),
     1 DRHOT(10,81), D2TTH(10,81), BD(10,81,15), T(10,81),
     2 V(10,81), DVTH(10,81), D2VTH(10,81), FC(80), NM(20)
     3  , DRHOTH(10,81), A(8)
      COMMON /E/ FC, NM /B/ BD
      EQUIVALENCE (BD(1), P), (BD(811), DPTH), (BD(1621),T),
     1 (BD(3241), DTTH), (BD(4051), D2TTH), (BD(4861), RHO),
     2 (BD(6481), DRHOTH), (FC(54), DTH), (FC(36), GAM),
     3 (BD(7291), V), (BD(8911), DVTH), (BD(9721), D2VTH), (FC(37), AP)
     4,(FC(59),SRD), (FC(60),SCB), (FC(61),SCR), (FC(35),DELV),
     5 (FC(40),DEL2V), (FC(64),BB), (FC(65),  BC), (FC(66),BZ),
     6 (FC(33), RED), (FC(39), SC), (FC(32), XL), (FC(34), XJ),
     7  (FC(42), FGAM)  ,(FC(62),SIP),(FC(63),SIP2), (FC(38),ZIP)
     8 , (FC(43), A), (FC(41), VZ)
      EQUIVALENCE (NM(14), ND), (NM(15),N1),(NM(20),NOD), (FC(70),D2)
     1, (FC(71), DSQ), (NM(16),NZ),(NM(17),N2),  (NM(18),N3)
     2 , (NM(19), N4), (NM(12),N5)
C
C     SET UP  INITIAL ARRAY
      DEL2V = DELV*DELV
        GAM1  = GAM + 1.0
        FGAM  = SQRTF((2.0/GAM1)**(GAM1/(GAM-1.0)))
              BB = XL*FGAM
              BC = XJ*FGAM
              BZ = 1.3333333333*BC
        SIP2=  GAM*(GAM - 1.0)
       SIP = SIP2/2.0
        ZIP =  GAM +  SIP*DEL2V
        SRD = SQRTF( RED)
        SCB = .6                *SC**.33333333333
        SCR = SCB*SQRTF(DELV)*SRD + 2.0
         A(2) = 6.2831853071*VZ
         A(5) =  8.37758040*GAM*(GAM-1.0)*XJ* FGAM
      D2 = 12.0*DTH
      DSQ = D2*DTH
      NOD = 10*ND
      N1 = ND - 1
       NZ = ND + 3
       N2 = NZ + 1
      N3 = N2 + 1
        N4 = N1 - 1
      N5 = N4 - 1
              CON1 =  1.0/GAM
              CON2 =  1.0 - CON1
        DO 20  I = 1,ND
        XI = I -1
        ZIG  = XI*DTH
        P(1,I) =  AP*SINF(ZIG) + 1.0
        DPTH(1,I) = AP*COSF(ZIG)
        T(1,I) = P(1,I)**CON2
        RHO(1,I)= P(1,I)**CON1
        V(1,I) = 0.0
        DTTH(1,I) =  CON2/RHO(1,I)*DPTH(1,I)
        DVTH(1,I) =  0.0
        DRHOTH(1,I) = CON1/T(1,I)*DPTH(1,I)
        D2VTH(1,I)  = 0.0
20      D2TTH(1,I)  = CON2/RHO(1,I)*(-CON1/P(1,I)* DPTH(1,I)*DPTH(1,I
     1  + 1.0 - P(1,I))
                RETURN
                END
```

```
      SUBROUTINE ORG
      DIMENSION FC(80), NM(20), W(20)
       COMMON /E/ FC, NM
       EQUIVALENCE (FC(1),T), (FC(2),RKT), (FC(3),H), (FC(4),HO),
     1 (FC(5), HMIN), (FC(6),HMAX), (FC(7),HZD2), (FC(8),EMIN),
     2(FC(9),EMAX), (FC(11),W), (FC(10),E1),
     3 (NM(1),IM), (NM(2),INDR), (NM(3),MALP), (NM(4),MGAM),
     4 (NM(5),MPTN), (NM(6),MPTS), (NM(7),NSW), (NM(8),NCOU),
     5 (NM(9),MP), (NM(10),NV) , (NM(11), NO)
C     ****************************************************************
C          DESCRIPTION OF THE LISTED VARIABLES
C     T - THIS CELL CONTAINS CURRENT INTEGRATION TIME
C     RKT - START TIME OR PREVIOUS RUNGE-KUTTA TIME
C     H - CURRENTLY USED STEP SIZE IN COMPUTING
C     HO - STORED STEP SIZE
C     HZD2 - HALF OF STORED STEP SIZE
C     HMIN - MINIMUM STEP SIZE
C     HMAX - MAXIMUM ALLOWABLE STEP
C     EMIN-WMAX MIN OR MAX ALLOWABLE ERROR
C      W - ARRAY OF WEIGHTS TO WEIGH ERROR CONSIDERATION
C     IM - NO OF GOOD POINTS FROM R.K START
C     INDR - INDICATOR FOR ERROR OUTSIDE OR WITHIN MIN MAX TOLERANCE
C     MALP - COUNTER FOR RUNGE KUTTA INTERMEDIATE POINTS
C     MGAM - PHASE INDICATOR -1,PREDICTOR0,R.K  1, CORRECTOR
C     MPTN - PRINT COUNTER, CURRENT
C     MPTS - TOTAL NO OF POINTS IN PRINT INTERVAL
C     NSW - PRINT INDICATOR IN NADM ROUTINE
C     NCOU - TOTAL NO OF COMPUTED POINTS DURING INTEGRATION CYCLE
C     MP - POWER OF 2 VARIATION FROM HMIN TO HMAX
C     HMAX, MP, NO, NSW, NV AND W(I) MUST EITHER BE READ INTO CORE OR
C     INITIAIZED BY AN ADDITIONAL ROUTINE
C     ****************************************************************
      HMIN = HMAX/2.**MP
      HO = HMIN
      HZD2 = HO/2.0
      H = HZD2
      RKT = T
       E1 = 0.0
C     ****************************************************************
C      FIXED POINT INITIALIZATIONS
C     ****************************************************************
       IM = 0
       MALP = 4
       MGAM = 0
         MPTN = 0
       MPTS  = NO*2**MP
       INDR = 0
       NCOU = 0
C     ****************************************************************
C      MPTN SET TO ZERO TO PRINT INITIAL CONDITIONS
C     ****************************************************************
       RETURN
       END
```

```
      SUBROUTINE ASET
C     THIS SUBROUTINE CALCULATES THE COEFFICIENTS FOR THE AXIAL
C     DERIVATIVE PACKAGE AND ALSO INITIATES THE W ARRAY AND THE WZ
C     ARRAY.
      DIMENSION FC(80), NM(20), BD(10,81,15),                A(11),
     1 C(3), RHO(10,81),V(10,81), T(10,81),W(10,81),WZ(10,81),P(10,81)
     2 ,AZ(81),DD(81), PVD(81),BVD(81), BZD(81)
      DIMENSION DVTH(10,81) , DTTH(10,81)  ,D2TTH(10,81)
       COMMON /E/ FC, NM  /B/ BD
      EQUIVALENCE (BD(1), P), (BD(1621),T), (BD(4861), RHO),
     1 (BD(7291), V), (BD(10531),W), (BD(11341),WZ)
     2,(BD(8911),DVTH), (BD(3241),DTTH), (BD(4051),D2TTH)
      EQUIVALENCE (FC(33), RED), (FC(39), SC), (FC(35), DELV),
     1 (FC(32), XL), (FC(34), XJ),  (FC(40), DEL2V), (FC(41), VZ),
     2  (FC(42), FGAM),  (FC(36),  GAM),  (FC(43),  A), (FC(51), C)
     3 ,(FC(59), SRD), (FC(60),SCB),(FC(61),SCR),(FC(62),SIP),
     4 (FC(38), ZIP) ,(FC(64),BB),(NM(14), ND)
     5,(FC(63),SIP2), (FC(65),BC), (FC(66),BZ)
          DO  40   I = 1,ND
          BVD(I) = RHO(1,I)*  V(1,I)
         PVD(I) = P(1,I)*DVTH(1,I)
         DD(I) = DVTH(1,I)**2
         BZD(I) = BVD(I)*DTTH(1,I)
         IF(RHO(1,I)) 60,20,20
   20 W(1,I) = (2.0+SCB*SQRTF(RHO(1,I))*(V(1,I)**2+DEL2V)**.250*SRD)
     1  /SCR
         AZ(I) = W(1,I)*V(1,I)**2
   40     WZ(1,I)  =  W(1,I)*(ZIP -  T(1,I))
C     INITIALIZATION OF  A- ARRAY  EMPLOYING  W- ARRAYS
          A(1) =  WEDD(RHO)
          WINT = WEDD (W)
          C(1) = BB      *WINT
                A(3) = (GAM - 1.0)* WEDD(P)
                A(4) =  VZ* A(1)
         BAB = WEDS(AZ)
         BAD = WEDS(DD)
          BAE = WEDS(PVD)
        BABE = -WEDS(BZD)
         FINK = BZ*SIP*BAD
         FINK2 = SIP2*BB*BAB
         FINK4 = -(GAM - 1.0)*BAE
         FINK5 = BC*WEDD(D2TTH)
       A(6) = A(4) + WEDD(DVTH)*SIP*BZ
        C(2) = BB*WEDD(WZ) + FINK +FINK2 + FINK4 + BABE+FINK5
          A(7) = WEDD(T)
          A(8) =  A(1)
                C(3) = -C(1)*DELV
          RETURN
   60   CALL DRAW
       STOP
          END
```

```
      FUNCTION  WEDS(B)
C     THIS FUNCTION EMPLOYS WEDDLES RULE TO EVALUATE THE INTEGRAL(0,2PI
      DIMENSION          B(81), FC(80), NM(20)
      COMMON /E/ FC,NM
      EQUIVALENCE (NM(15), N1),(FC(54),DTH)
      SUM = 0.0
          DO 30   I = 1,N1,5
   30     SUM =  SUM +  38.*B(I) +75.*(B(I+1) + B(I+4)) + 50.*(B(I+2) +
     I    B(I+3))
      WEDS = 5.0*DTH/288.*SUM
                    RETURN
                    END
```

```
      FUNCTION  WEDD(A)
C     THIS FUNCTION EMPLOYS WEDDLES RULE TO EVALUATE THE INTEGRAL(0,2PI)
      DIMENSION A(10,81), B(81), FC(80), NM(20)
      COMMON /E/ FC,NM
      EQUIVALENCE (NM(15), N1),(FC(54),DTH)
      DO 10 I = 1,N1
10    B(I) =  A(1,I)
      SUM = 0.0
      DO 30   I = 1,N1,5
30    SUM =  SUM +  38.*B(I) +75.*(B(I+1) + B(I+4)) + 50.*(B(I+2) +
     1 B(I+3))
      WEDD = 5.0*DTH/288.*SUM
                    RETURN
                    END
```

```
      [illegible] C(3), X(4), FC(80), NN(20)
      [illegible] FC, NN
      [illegible] (FC(36), GAM), (FC(43), A), (FC(51), C),
     1 (FC(55), X) , (FC(41), VZ)
            I = 0
            A5 = 2.0* A(5)
            ZIP1 = C(2) +(A(7)/A(2)*C(1) -  GAM*C(3))*VZ
            ZIP2 = -A(3) +(A(6)/GAM - A(7)*A(1)/A(2))*VZ
      QZ =  -ZIP1/ZIP2
      QZZ = A5*QZ/ZIP2
        X(1) = QZ*(1.0 + QZZ/2.0*(1.0 + QZZ))
200     X(2) =  (C(1) - A(1)*X(1))/A(2)
      X(3)=(GAM*C(3)+(-GAM*A(6)+A(7)*A(1)/A(2))*X(1) -A(7)*C(1) /A(2))
     1  /A(8)
210                 RETURN
                    END
```

```
      SUBROUTINE  TDER
C     THIS ROUTINE COMPUTES THE PARTIAL DERIVATIVES WITH RESPECT TO T
      DIMENSION X(4), BD(10,81,15), DRHOT(10,81), DTT(10,81),
     1 DVT(10,81), RHO(10,81), DVTH(10,81),DRHOTH(10,81), W(10,81),
     2 DPTH(10,81), D2VTH(10,81), DTTH(10,81), P(10,81), D2TTH(10,81),
     3 WZ(10,81) , V(10,81), T(10,81), FC(80), NM(20)
      COMMON /E/ FC,NM /B/ BD
      EQUIVALENCE (BD(1), P),                          (BD(811), DPTH),
     1 (BD(1621),T), (BD(2431),DTT), (BD(3241), DTTH), (BD(4051), D2TTH)
     2,(BD(4861), RHO), (BD(5671), DRHOT), (BD(6481), DRHOTH),
     3 (BD(7291), V), (BD(8101), DVT), (BD(8911), DVTH),
     4 (BD(9721), D2VTH), (BD(10531),W), (BD(11341),WZ)
      EQUIVALENCE (FC(32), XL),(FC(34), XJ), (FC(33), RED),
     1 (FC(41),  VZ),  (FC(42), FGAM), (FC(36), GAM), (FC(55), X)
     2,(FC(64),BB),(FC(65),BC), (FC(66),BZ), (FC(62),SIP),(FC(63),SIP2)
     3  ,(NM(14), ND)
              BA = VZ*X(2)
              BE = VZ*X(3)
C     THE DERIVATIVE OR RHO WITH RESPECT TO T -  THE CONTINUITY EQUATION
C     THE MOMENTUM EQ. - THE ENERGY EQUATION
      DO 40  I= 1, ND
      DRHOT(1,I) = -RHO(1,I)*(DVTH(1,I) + X(1))  - V(1,I)*DRHOTH(1,I
     1)  - BA  + W(1,I)*BB
      DVT(1,I) = (-(RHO(1,I)*DVTH(1,I) + BB*W(1,I))*V(1,I) -
     2  DPTH(1,I)/GAM +BZ*D2VTH(1,I))/RHO(1,I)
   40 DTT(1,I) =  -V(1,I)*DTTH(1,I) -BE + ((1. -GAM)*P(1,I)*(DVTH(1,
     1I)+ X(1))+ BC*D2TTH(1,I) + BB*WZ(1,I) + BZ*SIP2          *(DVTH(1,I
     2)**2  + X(1)*(X(1) - DVTH(1,I))) +  BB*W(1,I)*SIP              *
     3  V(1,I)**2) /RHO(1,I)
                        RETURN
                        END
```

```
      SUBROUTINE NADM(YP,Y,KK)
      DIMENSION YP(810), Y(810), FC(80), NM(20), WT(20)
      COMMON /E/  FC,NM
      EQUIVALENCE (FC(3),H), (FC(11),WT), (FC(10), E1), (FC(9), EMAX),
     1 (FC(8), EMIN), (NM(2), INDR), (NM(7), NSW), (NM(4), MGAM),
     2 (NM(3), MALP)  ,(NM(20), NOD)
C     ******************************
C     MGAM=-1,0,1 INDICATES PREDICTOR-RUNGE-KUTTA OR CORRECTORPHASE
C     MALP-INDICATES PERT OF RUNGE KUTTA PHASE
C     NSW- PRINT SWITCH FOR ERROR INDICATION
C     E1 - CONTAINS MAXIMUM ERROR FOR EACH CYCLE
C     YP - ADDRESS OF DERIVATIVE ARRAY
C     Y - ADDRESS  OF THE ORDINATE ARRAY
C     ******************************
      IF (MGAM) 40, 10,  60
C     ****************************
C     THIS ROUTINE EMPLOYS A FOURTH ORDER RUNGE-KUTTA STARTER
C     ********************************
   10 IF(MALP - 2) 20, 15 ,15
   15    K = 4 - MALP
         DO 18 I = 1,NOD,10
         J = I + K
   18    Y(I+9) = Y(J) + H*YP(I)
      GO TO 99
   20    DO 22 I = 1,NOD,10
   22    Y(I+9) = Y(I+3) + H/6.*(YP(I)+2.*(YP(I+1)+YP(I+2)) + YP(I+3))
      GO TO 99
C     ***************************
C     ADAMS BASHFORTH THIRD ORDER PREDICTOR FORMULA
C     ******************************
   40    DO 42 I = 1,NOD,10
   42 Y(I+9) = Y(I) + H/12.0*(23.0*YP(I) -16.0*YP(I+1) +5.0*YP(I+2))
      GO TO 99
C     ***************************
C        ADAMS MOULTON THIRD ORDER CORRECTOR FORMULA
C     ********************************
   60    DO 98 I = 1,NOD,10
       Y(I) = Y(I+1) + H/12.0*(5.0*YP(I) + 8.0*YP(I+1) - YP(I+2))
      E = ABSF(Y(I) - Y(I+9))*WT(KK)
         IF(Y(I))  70, 80, 70
   70    E = E/ABSF(Y(I))
   80  IF( E - EMAX) 85, 95, 95
   85  IF(E - EMIN) 98, 87, 87
C     ********************************
C     RELATIVE ERROR CHECK-BRANCH TO 99 INDICATES ERROR SMALLER THAN
C     ALLOWABLE ERROR-ADDING ONE TO INDR INDICATES VARIABLE WITHIN
C     ERROR ALLOWED
C     ********************************
   87 INDR = INDR  + 1
      IF(NSW) 88, 98, 88
   88  WRITE ( 6,2)  KK
    2  FORMAT(1H0, 8HVARIABLE, I3, 13HWITHIN LIMITS)
         GO TO 98
C     ****************************
C     ONE HUNDRED IS SUBTRACTED FOR EACH VARIABLE LARGER THAN THE
C     ERROR LIMITS
C     ********************************
   95  INDR =  INDR - 100
      IF(NSW) 97, 98, 97
   97  WRITE( 6,3)  KK
    3 FORMAT(1H0, 8HVARIABLE, I4, 20HOUTSIDE ERROR LIMITS)
```

```
C     ***********************************
C     E1 CONTAINS MAXIMUM ERROR OCCURING DURING THE CYCLE
C     ***********************************
   98 E1 = MAX1F(E, E1)
   99 RETURN
      END
```

```
      SUBROUTINE AVGE
      DIMENSION P(10,81),FC(80), NM(20),BD(10,81,15), ART( 800,3)
      COMMON ART
      COMMON /E/FC,NM/B/BD
      EQUIVALENCE (FC(1),T), (BD(1), P), (NM(13), IU)
     1 , (NM(14), ND), (NM(15),N1)
      XMA = P(1,1)
      XMI =  XMA
      SUM =  XMI
      DO 10 I = 2,N1
      SUM = SUM + P(1,I)
      IF(P(1,I) -  XMA) 5,10,3
    3  XMA = P(1,I)
      GO TO 10
    5 IF(P(1,I)  - XMI)  7, 10, 10
    7 XMI = P(1,I)
   10 CONTINUE
      XN = N1
      SUM = SUM/XN
      ART(IU,2) =  (XMA - XMI)/SUM
      ART(IU,1)  =  T
      NN = N1/4 + 1
      ART(IU,3) = P(1,NN)
      RETURN
      END
```

```
      SUBROUTINE  THPRED
C     EMPLOYING THE RESULTS OF THE INTEGRATION THIS ROUTINE ATTEMPTS TO
C     COMPUTE THE THETA  DERIVATIVES OF  THE  N+1   ANNULUS
      DIMENSION FC(80), NM(20), BD(10,81,15), DRHOTH(10,81),
     1 DVTH(10,81), D2VTH(10,81), DTTH(10,81),  D2TTH(10,81),
     2 DPTH(10,81),                P(10,81), RHO(10,81), V(10,81),
     3 T(10,81), AA(90), AB(90), AC(90)
      COMMON /E/ FC,NM /B/BD
       EQUIVALENCE (BD(1), P), (BD(811), DPTH), (BD(1621), T),
     1 (BD(3241), DTTH), (BD(4051), D2TTH), (BD(4861), RHO),
     3 (BD(6481), DRHOTH), (BD(7291), V), (BD(8911), DVTH),
     3 (BD(9721), D2VTH), (FC(54), DTH), (NM(4), MGA )
     4 ,(NM(14),ND), (NM(15), N1),(FC(70),D2), (FC(71),DSQ)
     5 ,(NM(16),NZ),(NM(17),N2), (NM(18),N3), (NM(19),N4),(NM(12),N5)
          IF  (MGAM)  10, 10, 12
10    J = 10
        K = 1
        GO TO   13
12      J= 1
    K = 2
13            AA(1) = RHO(J,N5)
              AA(2) = RHO(J,N4)
              AA(3) =  RHO(J,N1)
              AB(1) =  V(J,N5)
              AB(2) =  V(J,N4)
              AB(3) =  V(J,N1)
              AC(1) =  T(J,N5)
              AC(2) =  T(J,N4)
              AC(3) =  T(J,N1)
        DO 20  I=  4,NZ
        AA(I) =  RHO(J,I-3)
        AB(I) =    V(J,I-3)
20      AC(I) =    T(J,I-3)
              AA(N2) = RHO(J,2)
              AA(N3) = RHO(J,3)
              AB(N2) = V(J,2)
              AB(N3) = V(J,3)
              AC(N2) =  T(J,2)
              AC(N3) =  T(J,3)
C     ********************************
C     FOURTH ORDER STIRLING  CENTRAL DIFFERENCE FORMULA
C      ****************************************
        DO 25  I = 1,N1
      DRHOTH(J,I) = (AA(I+1)-8.0*(AA(I+2) - AA(I+4)) - AA(I+5))/D2
      DVTH(J,I) = (AB(I+1) - 8.0*(AB(I+2)-AB(I+4))-AB(I+5))/D2
     DTTH(J,I) = (AC(I+1)-8.0*(AC(I+2)-AC(I+4)) - AC(I+5))/D2
     D2VTH(J,I) = (-AB(I+1)+ 16.0*(AB(I+2) + AB(I+4)) - 30.*AB(I+3)
     1  -AB(I+5))/DSQ
25 D2TTH(J,I) = (-AC(I+1)+ 16.0*(AC(I+2) + AC(I+4)) - 30.*AC(I+3)
     1  -AC(I+5))/DSQ
35    DRHOTH(J,ND) = DRHOTH(J,1)
              DVTH  (J,ND) = DVTH (J,1)
              D2VTH (J,ND) = D2VTH(J,1)
              DTTH (J,ND)  = DTTH(J,1)
              D2TTH(J,ND)  = D2TTH(J,1)
                   DO  50  I =  1,ND
              P(J,I) =  RHO(J,I) * T(J,I)
50            DPTH(J,I) = RHO(J,I)*DTTH(J,I)  +  T(J,I)* DRHOTH(J,I)
      RETURN
      END
```

```
      SUBROUTINE SHIFT
         DIMENSION  FC(80), NM(20),  BD(12150)
       COMMON /E/ FC, NM /B/ BD
      EQUIVALENCE (NM(5),MPTN),(NM(4),MGAM), (NM(3),MALP),
     1 (NM(1),IM), (FC(3),H), (FC(7),HZD2), (NM(10),NV), (FC(4),HO),
     2 (FC(1),T), (NM(2), INDR), (FC(10), E1), (NM(8),NCOU),
     3 (FC(6), HMAX), (NM(6),MPTS), (FC(5),HMIN), (FC(9), EMAX),
     4  (FC(2),RKT), (NM(20), NOD)
C     ******************************************************************
C     SHIFT UPDATES THE VARIABLES SO THAT PROPER POSITIONING
C     OCCURS DURING THE PROPER CYCLE
C     ******************************************************************
      IF ( MPTN) 15, 10, 15
   10  MPTN = MPTS
   15  MGAM = -MGAM
      IF( MGAM ) 80, 20, 60
   20  IF( MALP - 2) 25, 48, 48
   25  IM = IM + 1
      MPTN = MPTN - 1
      NCOU =  NCOU + 1
      IF( 3 - IM)  35, 30, 30
   30  MALP = 4
      H = HZD2
      GO TO 40
   35  MGAM = -1
   40 DO  42 J = 1,15
        NZ = (J-1) * 810 + 1
       NZZ = NZ + NOD - 1
      DO  42 I = NZ,NZZ,10
              BD(I+1) = BD(I+3)
              BD(I+2) = BD(I+4)
              BD(I+3) = BD(I+5)
              BD(I+4) = BD(I+6)
              BD(I+5) = BD(I+7)
   42         BD(I  ) = BD(I+9)
      RETURN
C     ******************************************************************
C     SHIFTING OCCURS AFTER PREDICTOR CYCLE IS COMPLETE
C     ******************************************************************
   48 MALP = MALP - 1
      IF( MALP - 2) 55, 50, 55
   50 H = HO
      GO TO 65
   55 T = T + HZD2
      GO TO 65
   60  T  = T + H
   65 DO  75 J = 1,15
        NZ = (J-1) * 810 + 1
       NZZ = NZ + NOD - 1
      DO  75 I = NZ,NZZ,10
       BD(I+8) = BD(I+7)
       BD(I+7) = BD(I+6)
       BD(I+6) = BD(I+5)
       BD(I+5) = BD(I+4)
       BD(I+4) = BD(I+3)
       BD(I+3) = BD(I+2)
       BD(I+2) = BD(I+1)
       BD(I+1) = BD(I  )
   75  BD(I  ) = BD(I+9)
      RETURN
C     ******************************************************************
```

```
C     THE FOLLOWING STATEMENTS EXIST FOR CHANGING THE STEP SIZE
C     ***************************************************************
   80 IF(INDR) 175, 135, 125
  125 MPTN = MPTN - 1
  130  IM = IM + 1
      INDR = 0
      E1 = 0.0
      NCOU = NCOU + 1
      RETURN
C     ***************************************************************
C     DOUBLE THE INTERVAL IF POSSIBLE
C     ***********************************
  135 IF(IM - 8) 125, 140, 140
  140  KZ = MPTN/2
      IF(2*KZ - MPTN) 150, 125, 150
C     ***************************************
C     IF MPTN IS ODD THERE IS AN EVEN NUMBER OF POINTS LEFT TO COMPUTE
C     ***********************************
  150  IF((H-HMAX)/HMAX) 155, 125, 125
  155 IF(MPTS - 1) 125, 125, 160
  160  MPTS = MPTS/2
      MPTN = MPTN/2
       IM = 5
      DO  165J = 1,15
        NZ = (J-1) * 810 + 1
       NZZ = NZ + NOD - 1
      DO 165 I = NZ,NZZ,10
         BD(I+1) = BD(I+2)
         BD(I+2) = BD(I+4)
         BD(I+3) = BD(I+6)
  165    BD(I+4) = BD(I+8)
      H = 2.*H
      GO TO 130
C     ****************************
C     HALF THE STEP SIZE  IF POSSIBLE
C     ***********************************
  175   IF((H-HMIN)/HMIN) 125, 125, 180
  180 N = LOGF(E1/EMAX  + 1.)/.693147180 5
       DO 185 I = 1,N
      K = I
       IF(H/2.**K - HMIN) 195, 190, 185
  185  CONTINUE
  190  N = K
      GO TO 200
  195  N = K -1
  200   MALP = 4
      MGAM = 0
      IF( IM - 4) 210, 215, 210
  210  T = T-H
      RKT = T
      NN = 1
      GO TO 218
  215  T = RKT
       MPTN = MPTN + 4
      NN=5
  218  MPTS=MPTS*2**N
      MPTN=MPTN*2**N
      DO 222 J = 1,15
        NZ = (J-1) * 810 + 1
       NZZ = NZ + NOD - 1
      DO 222 I = NZ,NZZ,10
```

```
      K = I + NN
222   BD(I) = BD(K)
      HO = H/2.**N
      HOD2 = HO/2.
      H = HOD2
      IM = 0
      INDR = 0
      RETURN
      END
```

```
      SUBROUTINE DRAW
       DIMENSION ART(800,3),AB(82,40), FC(80),NM(20),BC( 3),BD(3),
     1 AC(61)
      COMMON ART, AB
      COMMON /E/ FC, NM
       EQUIVALENCE (NM(13), IM), (NM(10),NN) , (NM(14),ND) ,(NM(15),N1)
      TYPE INTEGER  BC, BD
         JZ = IM
      XN1 = N1
       DX = 6.2832/XN1
      AC(1) = 1.000
      DO 42 JM = 2,ND
   42 AC(JM) = AC(JM-1)  + DX
         NZZ = ART(JZ, 1) + 1.0
C        MAXIMUM ABSCISSA VALUE
         XMA = NZZ $ YM = 0.0
       DO 20 I = 1, JZ
        ART(I,1) = 7.0/XMA*ART(I,1) + 1.0
       IF(ART(I,2)  - YM) 20, 20, 10
   10   YM = ART(I,2)
   20  CONTINUE
         YM = 10.0*YM
       NZZ = YM
      YM = NZZ + 1
       YM = YM/10.0
       YMI = 0.0
      BC(1) =8H T IN RA$BC(2)= 8HDIANS   $ BC(3)= 8H
      BD(1)=8H(PMAX-PM$ BD(2)=8HIN)/PAVG $ BD(3) = 8HE
      CALL GRAPH(ART(1,1),ART(1,2),XMA,0.0          ,YM,YMI,JZ,BC,BD, -1)
      YM = 1.0 + YM/2.0
         YMI = 2.0 - YM  +.00000015
      UO = 0.000
      DO 232 I = 1,JZ
      IF (ART(I,3) - UO) 232, 232, 231
  231  UO = ART(I,3)
  232  CONTINUE
      IF(UO - YM) 234, 234, 233
  233  NZZZ = 10.*UO + 1.0
         UO = NZZZ
      YM = UO/10.0
  234  CONTINUE
      BD(1)=8HMAXIMUM $ BD(2)=8HPRESSURE $ BD(3) = 8H NODE
      CALL GRAPH(ART(1,1),ART(1,3),XMA,0.0,YM,YMI,JZ,BC,BD,-1)
      JZ = ND
      BC(1) = 8HTHETA IN $ BC(2) = 8H RADIANS $ BC(3) = 8H
      BD(1) = 8HPRESSURE $ BD(2) =8H WAVE PE $ BD(3) = 8H [illegible]
         DO 62 L = 1,NN,5
         NZN = L
      CALL GRAPH (AC,AB(1,NZN),7.0000,0.0,YM,YMI, JZ,BC,BD,+1)
         DO 60 I = 1,3
          JL = I + 1
       NJN = NZN + I
   60 CALL GRAPH (AC,AB(1,NJN),7.0000,0.0,YM,YMI,-JZ,BC,BD,JL)
         NZN = NZN + 4
   62 CALL GRAPH (AC,AB(1,NZN),7.0000,0.0,YM,YMI,-JZ,BC,BD,-5)
       RETURN
       END
```

```
      SUBROUTINE GRAPH(AB,OR,XM,XMI,YM,YMI,JZ, BCX, BCY, MS)
      DIMENSION  AB(800), OR(800), BCX(3), BCY(3), FC(80),NM(20), G(400)
      COMMON /E/FC,NM
      EQUIVALENCE (FC(32),XL) , (FC(33), RED), (FC(34),XJ),
     1 (FC(36), GAM), (FC(35),DELV), (FC(39),SC), (NM(13), IM)
     2, (NM(10),NJ)
      DATA (MZ=0)
C     UNIT 17 DESIGNATED  FOR PLOTTED OUTPUT (EQUIP,17=**,SV)
          IF(MZ) 9, 8, 9
    8     CALL PLOTS( G, 400, 17)
          MZ = 1
        MZNM = NJ - 1
C     SCALE ORDINATE VALUES OF INCOMING DATA
    9   NPT = XABSF(JZ)
        NCT = XABSF(MS)
        DIF = 9.0/(YM - YMI)
          DO 14 I = 1, NPT
   14     OR(I) = (OR(I) - YMI)*DIF  + .5000
C     DATA SCALED  FOR  NINE INCH ORDINATE FRAME
       IF(JZ) 70, 15, 15
   15   NZ = 0
      ROW = 2.5
          SIGMA = (YM - YMI)
          SIG = 1.0 $ SIG1 = .10
   19     IF(SIGMA - SIG) 21, 21, 20
   20 YB = 2.0*SIG1
      GO TO 25
   21     IF(SIGMA - .50*SIG) 23, 22, 22
   22 YB = SIG1
      GO TO 25
   23     NZ = NZ + 1
          SIG  = 1.0/10.0**NZ
          SIG1 = SIG/10.0
          GO TO 19
   25 YZ = DIF*YB
C     SCALING PARAMETERS HAVE BEEN SET FOR ORDINATE
C     SET PARAMETERS  FOR  ABSCISSA SCALING
                        XLA  =  XMI
                        XAB  =  1.0
                        DIF  = 7.0/(XM - XMI)
          SIG =10.0 $   SIGMA  = XM - XMI  $  ZM = 1.0
   27     IF( SIGMA - 10.0*ZM)  30, 30, 28
   28     ZM = ZM + 1.0
          GO TO 27
   30     XZ = DIF*ZM
   31 X  = XAB -.07
C     BEGIN ABSCISSA  PLOT
          CALL NUMBER ( X, 0.35, .07, XLA, 0.0, 4HF4.1)
          CALL PLOT (XAB, 0.5, 3)
          CALL PLOT (XAB, 9.5, 2)
          XAB = XAB + XZ
          XLA  = XLA + ZM  $ MM = 2
          IF(XAB - 8.0001) 34, 34, 35
   34     CALL PLOT(XAB, 9.5, 3)
          CALL PLOT(XAB, 0.5, 2)
          X = XAB-.07
          CALL NUMBER(X, .35,.07, XLA,0.0, 4HF4.1)
          XAB = XAB + XZ  $ XLA = XLA +ZM  $ MM = 1
          IF (XAB -8.0001) 31, 31, 35
   35   X = 8.0 + XZ - XAB
          ZETA = XZ/2.0   $ ZEB = XAB - ZETA $XLA = XLA-ZM/2.0+.000001
```

```
      SUBROUTINE GRAPH(AB,OR,XM,XMI,YM,YMI,JZ, BCX, BCY, MS)
      DIMENSION  AB(300), OR(800), BCX(3), BCY(3), FC(80),NM(20), G(400)
      COMMON /E/FC,NM
      EQUIVALENCE (FC(32),XL) , (FC(33), RED), (FC(34),XJ),
     1 (FC(36), GAM), (FC(35),DELV), (FC(39),SC), (NM(13), IM)
     2, (NM(10),NJ)
      DATA (MZ=0)
      UNIT 17 DESIGNATED  FOR PLOTTED OUTPUT (EQUIP,17=**,SV)
          IF(MZ) 9, 8, 9
    8     CALL PLOTS( G, 400, 17)
          MZ = 1
        MZNM = NJ - 1
      SCALE ORDINATE VALUES OF INCOMING DATA
    9   NPT = XABSF(JZ)
        NCT = XABSF(MS)
        DIF = 9.0/(YM - YMI)
          DO 14 I = 1, NPT
   14     OR(I) = (OR(I) - YMI)*DIF  + .5000
      DATA SCALED  FOR  NINE INCH ORDINATE FRAME
       IF(JZ) 70, 15, 15
   15   NZ = 0
      ROW = 2.5
          SIGMA = (YM - YMI)
          SIG = 1.0 $ SIG1 = .10
   19     IF(SIGMA - SIG) 21, 21, 20
   20 YB = 2.0*SIG1
      GO TO 25
   21     IF(SIGMA - .50*SIG) 23, 22, 22
   22 YB = SIG1
      GO TO 25
   23     NZ = NZ + 1
          SIG  = 1.0/10.0**NZ
          SIG1 = SIG/10.0
          GO TO 19
   25 YZ = DIF*YB
      SCALING PARAMETERS HAVE BEEN SET FOR ORDINATE
      SET PARAMETERS  FOR  ABSCISSA SCALING
                     XLA  =  XMI
                     XAB  =  1.0
                     DIF  = 7.0/(XM - XMI)
          SIG =10.0 $   SIGMA  = XM - XMI  $  ZM = 1.0
   27     IF( SIGMA - 10.0*ZM)  30, 30, 28
   28     ZM = ZM + 1.0
          GO TO 27
   30     XZ = DIF*ZM
   31 X  =  $ -.07
      BEGIN ABSCISSA  PLOT
          CALL NUMBER ( X, 0.35, .07, XLA, 0.0, 4HF4.1)
          CALL PLOT (XAB, 0.5, 3)
          CALL PLOT (XAB, 9.5, 2)
          XAB = XAB + XZ
          XLA  = XLA + ZM  $ MM = 2
          IF(XAB - 8.0001) 34, 34, 35
   34     CALL PLOT(XAB, 9.5, 3)
          CALL PLOT(XAB, 0.5, 2)
          X = XAB-.07
          CALL NUMBER(X, .35,.07, XLA,0.0, 4HF4.1)
          XAB = XAB + XZ  $ XLA = XLA +ZM  $ MM = 1
          IF (XAB -8.0001) 31, 31, 35
   35   X = 8.0 + XZ - XAB
          ZETA = XZ/2.0   $ ZEB = XAB - ZETA $XLA = XLA-ZM/2.0+.000001
```

```
      IF(ZEB - 8.0001) 37, 37, 38
37       XAB = ZEB
     GO TO (31, 34) MM
38    ZEB = ZEB - XZ/6.0  $XLA =XLA -ZM/6.0 +.00000015
       IF( ZEB - 8.0001) 37, 37, 40
  WRITE  OUT  PARAMETERS  PERTINENT TO THIS SOLUTION
40     CALL SYMBOL( 6.5, 9.0, .07, 3HL =, 0, 3)
      CALL NUMBER(6.875,9.0, .07, XL, 0.0, 4HF6.3)
       CALL SYMBOL( 6.5, 8.75, .07, 3HJ =, 0, 3)
       CALL NUMBER( 6.875,8.75, .07, XJ, 0, 5HF11.9)
       CALL SYMBOL( 6.35, 8.5, .07, 6HDELV =,0, 6)
       CALL NUMBER( 6.875,8.5, .07  DELV, 0.0, 4HF5.2)
       CALL SYMBOL( 6.4, 8.25, .07, 5HRED =, 0.0, 5)
       CALL NUMBER( 6.875, 8.25,.07, RED, 0.0,  4HF6.2)
       CALL SYMBOL( 6.45, 8.00 , .07, 4HSC =, 0.0, 4)
       CALL NUMBER( 6.875, 8.0,  .07, SC,  0.0, 4HF6.2)
       CALL SYMBOL( 6,4,7.75, .07, 5HGAM =, 0.0, 5)
       CALL NUMBER( 6.875,7.75, .07, GAM, 0.0, 4HF6.2)
       CALL SYMBOL( 3.0, 0.1, .14, BCX , 0.0, 24)
  ABSCISSA HAS NOW BEEN  LABELED  , BEGIN ORDINATE LABEL
48     YLA = YMI   $  YAB = 0.5  $  MM = 3
50   MM = 3
       CALL PLOT ( 8.0, YAB,  3)  $  CALL PLOT (1.0, YAB, 2)
       Y = YAB -.035
54   IF(NZ - 1) 103, 104, 105
03     CALL NUMBER(0.7, Y, .07, YLA, 0.0, 4HF8.1)
       GO TO 108
04     CALL NUMBER(0.7,Y, .07, YLA,  0.0, 4HF5.2)
       GO TO 108
05   IF(NZ - 2) 106, 106, 107
06     CALL NUMBER(0.7, Y, .07, YLA, 0.0, 4HF6.3)
       GO TO 108
07     CALL NUMBER(0.7, Y, .07, YLA, 0.0, 4HF7.4)
08   MM = MM - 1
     IF(MM - 1) 58, 58, 56
56   YAB = YAB + YZ
       IF(YAB  -  9.50001)  109, 109, 60
09   Y = YAB -.035  $ YLA = YLA + YB
     GO TO 54
58  CALL PLOT(1.0, YAB, 3)  $ CALL PLOT(8.0, YAB, 2)
    YAB = YAB +YZ $ YLA = YLA + YB
       IF (YAB - 9.50001)  50, 50, 60
60   YAB  =  YAB - YZ/2.0
       IF(YAB - 9.50001)  62, 62, 65
62   YLA  = YLA - YB/2.0
       GO TO 50
  LABEL ORDINATE
65   CALL SYMBOL(0.6,3.0, .14, BCY, 90.0, 24)
  NEXT PLOT CURVES
70     CALL  PLOT ( AB(1) , OR(1), 3)
         DO 72 I = 1, NPT
72     CALL SYMBOL (AB(I), OR(I) , .05, NCT, 0.0, -2)
     IF ( MS ) 80, 82, 82
80   CALL PLOT(10.0, 0.0, -3)
    RETURN
82     ROW = ROW - .25
    MZNM = MZNM + 1
   CALL SYMBOL(7.25, ROW,.05, NCT, 0.0,-1)
    CALL NUMBER( 7.5, ROW, .07, OR(82), 0.0,4HF7.3)
    RETURN
      END
```

REFERENCES

(1) Priem, R. J. and Heidmann, M. F. "Propellant Vaporization as a Design Criterion for Rocket Engine Combustion Chambers," NASA TR R-67, 1960.

(2) Final Technical Report on Combustion Instability, AFOSR Contract AF 49(638)-1552, Dynamic Science Corporation, Report SN-1800, March 1965.

(3) Beltran, M. R., and Frankel, N. A. "Prediction of Instability Zones in Liquid Rocket Engines." AIAA Journal, Vol. 3, No. 3, pp 516-158, March 1965.

(4) Priem, R. J. and Guentert, D. C. "Combustion Instability Limits Determined by a Nonlinear Theory and a One-Dimensional Model," NASA TND-1409, 1962.

(5) Beltran, M. R., Frankel, N. A., and Wright, R. O. "Prediction of Combustion Instability Zones in the Apollo Service Propulsion System Engine," North American Aviation SID64-1475, 1964.

(6) Beltran, M. R., Wright, R. O., "A Nonlinear Model for Prediction of Liquid Rocket Engine Instability," 2nd Chemical Propulsion Information Agency. Combustion Conference, Los Angeles, California, 1-5 November 1965.

(7) Hersch, M., "An Experimental Method of Measuring Intensity of Turbulence in a Rocket Chamber," ARS Journal 31, 39-46 1961.

(8) Peoples and Baker, "Stability Rating Techniques," paper presented at the Spring Meeting of the Western States Section of the Combustion Institute at Stanford University, 27-28 April 1964.

(9) Levine, R. S., "Experimental Status of High Frequency Liquid Rocket Combustion Instability," paper presented at the Tenth Symposium (International) on Combustion, Cambridge, England, 1964.

(10) Lambiris, S., Combs, L. P., and Levine, R. S. "Stable Combustion Processes in Liquid Propellant Rocket Engines," Fifth Colloquium of the Combustion and Propulsion Panel, AGARD, 1962.

(11) Ranz, W. E. and Marshall, W. R., Jr., "Evaporization from Drops, pt. I., Chemical Engineering Progress, Vol. 48, No. 3., March 1952, pp 141-146. (See, also, pt. II, Vol. 48, No. 4, April 1952, pp 173-180.)

(12) Beltran, M. R., Breen, B. P., and Gerstein, M. "Liquid Rocket Engine Combustion Instability Studies," Dynamic Science Corporation Semiannual Report No. SN-68-51, Monrovia, California, 1965.

(13) Tarifa, C. S. and del Notario, P. P., "Combustion of Monopropellant Droplets: Theoretical Results," AFOSR-TN-59-463, AD 215-268, 1958.

(14) Crocco, Harrje, and Reardon, "Transverse Combustion Instability in Liquid Propellant Rocket Motors," ARS Journal, March 1962, pp 366-373.

(15) Bird, R. B., Stewart, W. E., and Lightfoot, E. N. Transport Phenomena, published by John Wiley & Sons, Inc. New York, 1960.

(16) Sherwood, T. K., and Pigford, R. L., Absorption and Extraction, Second ed., McGraw-Hill Book Co., Inc. 1952.

(17) Crocco, L., Harrje, D. T. Sirignano, W. A., and Ashford, D. M., "Nonlinear Aspects of Combustion Instability in Liquid Propellant Rocket Motors," Princeton University Aeronautical Engineering Report No. 553, June 1961.

UNCLASSIFIED

Security Classification

DOCUMENT CONTROL DATA - R&D

(Security classification of title, body of abstract and indexing annotation must be entered when the overall report is classified)

1 ORIGINATING ACTIVITY *(Corporate author)* DYNAMIC SCIENCE CORPORATION 1900 Walker Avenue, Monrovia, Calif.	2a REPORT SECURITY CLASSIFICATION Unclassified 2b GROUP Propulsion

3 REPORT TITLE

ANALYSIS OF LIQUID ROCKET ENGINE COMBUSTION INSTABILITY

4 DESCRIPTIVE NOTES *(Type of report and inclusive dates)*

Special Report

5 AUTHOR(S) *(Last name, first name, initial)*

Beltran, M. R., et al

6 REPORT DATE January 31, 1966	7a TOTAL NO. OF PAGES	7b. NO. OF REFS 16
8a CONTRACT OR GRANT NO. AF 04(611)-10542 b. PROJECT NO. 3058 c. d.	9a ORIGINATOR'S REPORT NUMBER(S) SN-68-S2 9b. OTHER REPORT NO(S) *(Any other numbers that may be assigned this report)* Technical Report AFRPL-TR-65-254	

10 AVAILABILITY/LIMITATION NOTICES

11 SUPPLEMENTARY NOTES	12 SPONSORING MILITARY ACTIVITY United States Air Force Rocket Propulsion Laboratory Edwards Air Force Base, California

13 ABSTRACT

This report develops a nonlinear model which can be used to predict combustion instability zones in liquid rocket engines. The nonlinear model is developed by combining a nonlinear instability model with a steady-state vaporization model. Such an analysis determines the zones of an engine in which a tangential mode of high frequency instability is most easily initiated. A rocket engine can be analyzed by incrementally dividing the combustion chamber into annular nodes in the r and z directions. Steady-state properties at each annular node or position in the chamber are computed from the steady-state vaporization computer program. The steady-state program is capable of computing combustion profiles in thermally unstable propellants of the monomethylhydrazine/nitrogen tetroxide type. This model describes droplet vaporization with vapor phase decomposition. Using the computed steady-state properties and the stability limit curves from the instability computer program, stability at each node is determined. This process is repeated for each node to determine a stability map of the entire engine. Thus stability can be related to hardware design parameters, thereby enabling the influences of system design and stability rating devices to be determined.

DD FORM 1 JAN 64 1473

UNCLASSIFIED

Security Classification

UNCLASSIFIED

Security Classification

14. KEY WORDS	LINK A ROLE	LINK A WT	LINK B ROLE	LINK B WT	LINK C ROLE	LINK C WT

INSTRUCTIONS

1. ORIGINATING ACTIVITY: Enter the name and address of the contractor, subcontractor, grantee, Department of Defense activity or other organization *(corporate author)* issuing the report.

2a. REPORT SECURITY CLASSIFICATION: Enter the overall security classification of the report. Indicate whether "Restricted Data" is included. Marking is to be in accordance with appropriate security regulations.

2b. GROUP: Automatic downgrading is specified in DoD Directive 5200.10 and Armed Forces Industrial Manual. Enter the group number. Also, when applicable, show that optional markings have been used for Group 3 and Group 4 as authorized.

3. REPORT TITLE: Enter the complete report title in all capital letters. Titles in all cases should be unclassified. If a meaningful title cannot be selected without classification, show title classification in all capitals in parenthesis immediately following the title.

4. DESCRIPTIVE NOTES: If appropriate, enter the type of report, e.g., interim, progress, summary, annual, or final. Give the inclusive dates when a specific reporting period is covered.

5. AUTHOR(S): Enter the name(s) of author(s) as shown on or in the report. Enter last name, first name, middle initial. If military, show rank and branch of service. The name of the principal author is an absolute minimum requirement.

6. REPORT DATE: Enter the date of the report as day, month, year; or month, year. If more than one date appears on the report, use date of publication.

7a. TOTAL NUMBER OF PAGES: The total page count should follow normal pagination procedures, i.e., enter the number of pages containing information.

7b. NUMBER OF REFERENCES: Enter the total number of references cited in the report.

8a. CONTRACT OR GRANT NUMBER: If appropriate, enter the applicable number of the contract or grant under which the report was written.

8b, 8c, & 8d. PROJECT NUMBER: Enter the appropriate military department identification, such as project number, subproject number, system numbers, task number, etc.

9a. ORIGINATOR'S REPORT NUMBER(S): Enter the official report number by which the document will be identified and controlled by the originating activity. This number must be unique to this report.

9b. OTHER REPORT NUMBER(S): If the report has been assigned any other report numbers *(either by the originator or by the sponsor)*, also enter this number(s).

10. AVAILABILITY/LIMITATION NOTICES: Enter any limitations on further dissemination of the report, other than those imposed by security classification, using standard statements such as:

(1) "Qualified requesters may obtain copies of this report from DDC."

(2) "Foreign announcement and dissemination of this report by DDC is not authorized."

(3) "U. S. Government agencies may obtain copies of this report directly from DDC. Other qualified DDC users shall request through _____."

(4) "U. S. military agencies may obtain copies of this report directly from DDC. Other qualified users shall request through _____."

(5) "All distribution of this report is controlled. Qualified DDC users shall request through _____."

If the report has been furnished to the Office of Technical Services, Department of Commerce, for sale to the public, indicate this fact and enter the price, if known.

11. SUPPLEMENTARY NOTES: Use for additional explanatory notes.

12. SPONSORING MILITARY ACTIVITY: Enter the name of the departmental project office or laboratory sponsoring *(paying for)* the research and development. Include address.

13. ABSTRACT: Enter an abstract giving a brief and factual summary of the document indicative of the report, even though it may also appear elsewhere in the body of the technical report. If additional space is required, a continuation sheet shall be attached.

It is highly desirable that the abstract of classified reports be unclassified. Each paragraph of the abstract shall end with an indication of the military security classification of the information in the paragraph, represented as *(TS)*, *(S)*, *(C)*, or *(U)*.

There is no limitation on the length of the abstract. However, the suggested length is from 150 to 225 words.

14. KEY WORDS: Key words are technically meaningful terms or short phrases that characterize a report and may be used as index entries for cataloging the report. Key words must be selected so that no security classification is required. Identifiers, such as equipment model designation, trade name, military project code name, geographic location, may be used as key words but will be followed by an indication of technical context. The assignment of links, rules, and weights is optional.

UNCLASSIFIED

Security Classification